CONTRACT NO. NASw-823

TIGRIS (TELEVISED IMAGES OF GASEOUS REGIONS IN INTERPLANETARY SPACE) TELEVISION CAMERA SYSTEM

FINAL ENGINEERING REPORT

Prepared for the

NATIONAL AERONAUTICS AND SPACE ADMINISTRATION
WASHINGTON, D. C.

By the

ASTRO-ELECTRONICS DIVISION
DEFENSE ELECTRONIC PRODUCTS
RADIO CORPORATION OF AMERICA
PRINCETON, NEW JERSEY

AED R-2583

Issued: January 15, 1965

CONTRACT NO. NASw-823

TIGRIS (TELEVISED IMAGES OF GASEOUS REGIONS IN INTERPLANETARY SPACE) TELEVISION CAMERA SYSTEM

FINAL ENGINEERING REPORT

Prepared for the

NATIONAL AERONAUTICS AND SPACE ADMINISTRATION
WASHINGTON, D. C.

By the

ASTRO-ELECTRONICS DIVISION
DEFENSE ELECTRONIC PRODUCTS
RADIO CORPORATION OF AMERICA
PRINCETON, NEW JERSEY

AED R-2583

Issued: January 15, 1965

PREFACE

This is the final engineering report describing the development, testing, and demonstration of a very sensitive preprototype image orthicon television camera system for the TIGRIS program by the Astro-Electronics Division (AED) of the Radio Corporation of America. The work was performed under the technical direction of the Center for Radio Physics and Space Research at Cornell University under Contract No. NASw-823. The report describes the work performed by AED from October 1963 to October 1964 and is supplied in accordance with the requirements of Article V of the aforementioned Contract. The field engineering phase of the work has not been described in the report, but shall be supplied as an addendum.

TABLE OF CONTENTS

Section		Page
I	INTRODUCTION	
	A. DESCRIPTION OF PROGRAM REQUIREMENTS	I-1
	B. REVIEW OF CONTRACTUAL REQUIREMENTS	I-2
	C. BRIEF OUTLINE OF PROGRAM	I-3
II	DESCRIPTION OF FINAL EQUIPMENT	II-1
	A. INTRODUCTION	II-1
	B. PERFORMANCE	II-1
	1. General	II-1
	2. Detailed Performance Specifications	II-1
	3. Orthicon Performance	II-6
	C. MECHANICAL	II-7
	1. General	II-7
	2. Camera Sensor Assembly	II-7
	3. Camera Electronics Assembly	II-10
III	DESCRIPTION OF DEVELOPMENT	
	A. GENERAL	III-1
	B. CAMERA SENSOR DESIGN	III-1
	1. Selection of Image Orthicon Tube	III-1
	2. Selection of Optics	III-2
	3. Design of Deflection, Focus, and Alignment Coils	III-2
	4. Development of Preamplifier	III-5
	C. CAMERA ELECTRONICS DESIGN	III-6
	1. Power Supplies	III-6
	2. Deflection Circuits	III-7
	3. Integration Programmer	III-8
	4. Video Amplifier and Target Blanking	III-9
IV	ENVIRONMENTAL CONSIDERATIONS	
	A. GENERAL	IV-1
	B. ENVIRONMENTAL DESIGN CRITERIA	IV-1
	1. Acceleration	IV-1
	2. Shock	IV-1
	3. Sinusoidal Vibration	IV-2
	4. Random Vibration	IV-2
	5. Thermal Vacuum	IV-2

TABLE OF CONTENTS (Continued)

Section		Page
V	LABORATORY TESTS	
	A. GENERAL	V-1
	B. LABORATORY TEST EQUIPMENT	V-1
	1. General	V-1
	2. Calibrated Light Box	V-1
	3. Monitor	V-3
	C. ENGINEERING SYSTEM TESTS	V-4
	1. System Measurements	V-4
	2. Integration Performance	V-5
	D. ACCEPTANCE TESTS	V-9
	1. Demonstration of the Linear Increase in Information Capability with Increase in Integration Time	V-9
	2. Signal-to-Noise Ratio Measurements	V-10
	3. Horizontal Resolution Measurements	V-11
	4. Grey Step Measurements	V-11

LIST OF ILLUSTRATIONS

Figure	Title	Page
Frontispiece	TIGRIS Television Camera System, Preprototype Model	x
II-1	TIGRIS Television Camera System, Functional Block Diagram	II-3
II-2	Resolution Characteristics of GE Z7806 LHP Image Orthicon Tube	II-8
II-3	Transfer Characteristics of GE Z7806 LHP Image Orthicon Tube	II-8
II-4	Performance of the GE Z7806 LHP Image Orthicon at a 2-Second Frame Rate for Three Levels of Illumination	II-9
II-5	TIGRIS Camera Sensor Assembly Housing	II-10
II-6	TIGRIS Camera Electronics Assembly Housing	II-11
III-1	Magnetic Field Flux Density Distribution of Focus Coil	III-6
III-2	Image Orthicon, Yoke and Alignment Coils, Schematic Diagram	III-11
III-3	Preamplifier, Schematic Diagram	III-13
III-4	+23V Regulated Power Supply, Schematic Diagram	III-15
III-5	DC-DC Converter, Schematic Diagram	III-17
III-6	Bias Bleeder, Schematic Diagram	III-19
III-7	Decoupler No. 1, Schematic Diagram	III-21
III-8	Decoupler No. 2, Schematic Diagram	III-23
III-9	Focus Current Regulator, Schematic Diagram	III-25
III-10	Vertical Rate Generator, Schematic Diagram	III-27
III-11	Vertical Sawtooth Generator and Deflection Amplifier, Schematic Diagram	III-29
III-12	Horizontal Rate Generator, Sawtooth Generator, and Deflection Amplifier, Schematic Diagram	III-31
III-13	Integration Selector Switch, Schematic Diagram	III-33
III-14	Programmer, Schematic Diagram	III-35
III-15	Integration Gate, Schematic Diagram	III-37
III-16	Video Amplifier and Target Blanking, Schematic Diagram	III-39
V-1	Light Box Calibration, Scene Surface Brightness	V-2
V-2	Transfer Characteristics of Camera System	V-6
V-3	Sensitivity of Camera System Versus Integration Time	V-7

LIST OF TABLES

Table	Title	Page
III-1	Comparative Evaluation of Image Orthicon Tubes Available . . .	III-3
III-2	Comparative Evaluation of Optics Available	III-4
IV-1	Sinusoidal Vibration Test Requirements	IV-2
IV-2	Combustion Resonance Dwell Vibration Test Requirements . . .	IV-3
IV-3	Random Vibration Test Requirements	IV-3
V-1	Light Box Calibration	V-4
V-2	Image Retention Phenomena Data	V-8
V-3	Information Capability Versus Integration Time	V-9
V-4	Horizontal Resolution Measurements	V-11

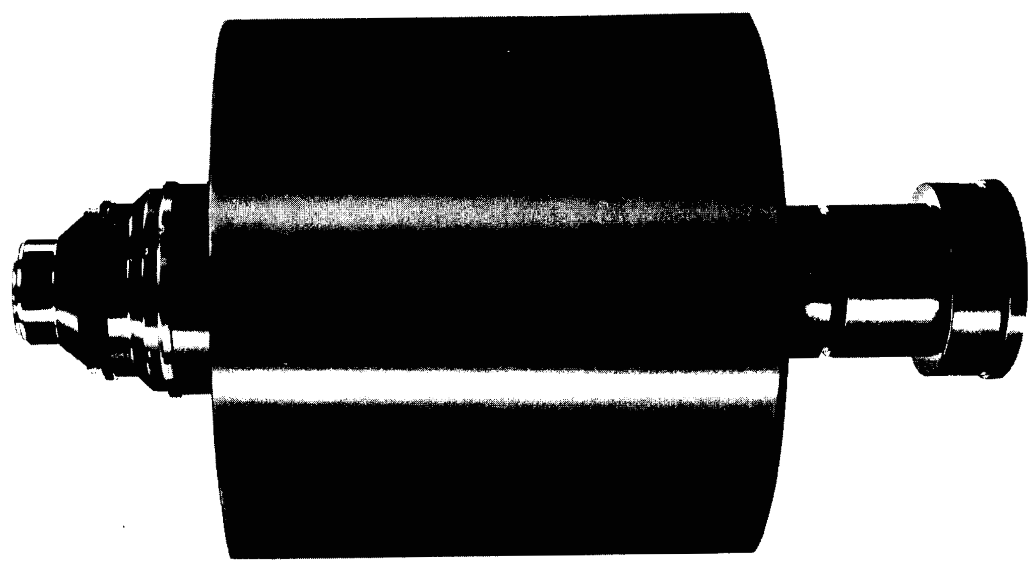

Frontispiece. TIGRIS Television Camera System, Preprototype Model

SECTION I

INTRODUCTION

A. DESCRIPTION OF PROGRAM REQUIREMENTS

The object of the TIGRIS program was to develop and fabricate a preprototype model of a very sensitive television camera system that would have the ability to obtain images of diffuse light-scattering regions in the solar system. Although it has been possible to detect the luminosity of outlaying regions of the solar corona, the zodiacal light, and the Gegenshine from earth-based observations, only the strongest of these sources could be seen due to the limitation of the diffuse luminosity of the ionosphere. The technique to be employed in the TIGRIS program is to obtain pictures above the ionospheric luminescent layers of the weaker sources during a suborbital trajectory for approximately 12 minutes using an extremely sensitive television camera system.

The sensitivity requirement of such a camera system is determined by the available light intensity of the weaker astronomic sources. The brightness expected of these sources above the atmosphere are of the following order.

1. The brightness of the zodiacal light is 2.6×10^{-3} erg/sec cm^2 sterad at 70° elongation and 4.0×10^{-2} erg/sec cm^2 sterad at 20° elongation.
2. The surface brightness of a fully ionized gas cloud is 3×10^{-4} erg/sec cm^2 sterad at 45° elongation assuming a density of 300 particles per cm^3.
3. Integrated starlight in the Milky Way is 4×10^{-3} erg/sec cm^2 sterad and perpendicular to the galactic plane is 2×10^{-4} erg/sec cm^2 sterad.

Based on the brightness of these sources, the sensitivity requirement for the TIGRIS camera system has been set at 3×10^{-4} erg/sec cm^2 sterad (surface brightness of a cloud); this corresponds to 2.8×10^{-8} watts/ft^2 sterad. Since the luminous efficiency for a radiant black body at 6000° K is 95 lumens/watt, the cloud brightness is then 2.66×10^{-6} lumens/ft^2 sterad; this corresponds to 2.66×10^{-6} candles/ft^2. The illuminance produced by the cloud brightness on the photosensitive surface of the image orthicon tube by a lens having an effective aperture of f/2.8 is 2.66×10^{-7} foot-candles.

Since cloud-type formations are to be observed, resolution is not too critical. A 200 line resolution is therefore considered adequate at the lower levels. Tests on the preprototype model have indicated a resolution exceeding 200 lines for comparable levels of light intensity.

B. REVIEW OF CONTRACTUAL REQUIREMENTS

The contract was reviewed upon initiation of work to resolve any technical questions; the following items were clarified.

1. The design of the camera system would be such that a space-qualified system could be produced with a minimum of redesign effort.

2. The environmental and physical design goals would be determined by a review of the Javelin rocket performance.

3. Since the frame rate was to be 2 seconds, the resolution-sensitivity requirements of Section 1.2.3 were modified to provide a resolution-sensitivity requirement of 200 lines at 2.5×10^{-7} foot-candles and 500 lines at 5×10^{-6} foot-candles for a 2-second exposure.

4. The dynamic range (grey scale) of the system (Section 1.2.3) would not be limited by the camera electronics, but would be determined by the image orthicon performance. The peak-white step of the grey scale should correspond to 10^{-5} foot-candles.

5. The integration performance (Section 1.2.3) would be dependent on the image orthicon and not limited by the camera electronics. The statement that "there shall be no departure from a linear increase in information capability" was interpreted to mean that the sensitivity-resolution performance would remain approximately constant for equal products of integration time and illumination level, up to a maximum integration time of ten seconds.

6. The preamplifier (Section 1.2.4) could be solid state, provided that its inclusion would not degrade the system signal-to-noise performance.

7. For the preprototype model, the programmer would be manually adjustable and a preset program would not be provided (Section 1.2.7).

8. The output of the preprototype camera will be a video signal. A subcarrier will not be provided; therefore the reference to the video subcarrier frequency and peak-to-peak deviation reference on page 6 of the Contract is not applicable.

C. BRIEF OUTLINE OF PROGRAM

Work started on the program in October 1963. A brief description of the chronological development of the program is given below.

1. The contract was reviewed to resolve any technical questions; television system requirements to meet the objectives of the program were defined. System concepts and schedules were established based on contractual requirements.

2. Image orthicon tubes were evaluated; and the GE type Z7806 LHP image orthicon selected.

3. The environmental requirements for flight equipment was reviewed to establish design goals.

4. The design and fabrication of an engineering model was initiated using AED-proven camera circuit designs wherever possible; special circuits were developed when required.

5. Optics were evaluated; and the Ziess Distagon lens selected.

6. Special test equipment was designed and fabricated to test the engineering and preprototype model; standard pieces of test equipment were procured.

7. Performance measurements were conducted on the engineering model with manufacturer-supplied sample image orthicon tubes.

8. The mechanical design of the preprototype model was completed and the model fabricated.

9. The preprototype was completed and laboratory acceptance tests were performed. The tests demonstrated that the camera system had successfully met all the contractual requirements.

10. Field tests were conducted at Capella Peak Observatory in New Mexico. Results of these field tests will be reported in an addendum to this report.

SECTION II

DESCRIPTION OF FINAL EQUIPMENT

A. INTRODUCTION

The TIGRIS television camera system consists of two major assemblies- the camera sensor assembly and the camera electronics assembly. The camera sensor assembly consists of a GE type Z7806 LHP image orthicon tube, a 25 mm f/2.8 Zeiss Distagon objective lens, deflection, alignment, and focus coils, and a video preamplifier. The camera electronic assembly consists of power supplies, deflection circuits, a video amplifier and target blanking circuit, and an integration programmer. A detailed functional block diagram of the camera system is shown in Figure II-1.

B. PERFORMANCE

1. General

The TIGRIS television system operating parameters were chosen to be compatible with the TIROS system, insofar as possible, so that existing TIROS ground equipment can be utilized.

The frame time for a readout cycle in the continuous mode of operation is 2 seconds. Since the horizontal line rate is 250 cps, each frame will consist of 500 scanning lines; less blanking. Interlace is not used. About 5 percent to 7 percent of the line time is required for horizontal retrace blanking. A 1/1 aspect ratio is provided (square picture). The video bandwidth of 65 kc allows a horizontal limiting resolution of approximately 530 lines. The direct current component of the video information lost due to a-c coupling is restored by clamping the black level in the picture to a constant voltage. A black reference signal is provided. The following paragraph summarizes the overall performance specifications of the TIGRIS camera system.

2. Detailed Performance Specifications

a. Camera Sensor Assembly

(1) Image Sensor: GE type Z7806 LHP ruggedized image orthicon

(a) Resolution (at 2-second integration time):

500 lines at 5×10^{-6} ft-c
200 lines at 2.5×10^{-7} ft-c

(b) Signal-to-Noise Ratio ($20 \log \frac{S_{p-p}}{N_{rms}}$): 26.3 db

(c) Target Material: Magnesium Oxide

(d) Grey Scale Steps: 9

(2) Optics: Ziess Distagon lens

(a) Focal Length: 25 mm

(b) Numerical Aperture: 2.8

(c) Back Focus: 38.54 mm

(d) Image Size: 1.7 in. diagonal

(e) Resolution: center - 630 lines/mm
off axis - 220 lines/mm

(f) Field of View: 80^{o}

(3) Vertical Deflection Coils

(a) Current: 90 ma, half axis

(b) Resistance: 141Ω, half axis

(c) Inductance: 50 mh

(4) Horizontal Deflection Coils

(a) Current: 220 ma, half axis

(b) Resistance: 41.5Ω, half axis

(c) Inductance: 8.7 mh

(5) Focus Coil

(a) Flux: 75 gauss at center of coil

(b) Current: 860 ma

(c) Resistance: 20.5Ω at $17^{o}C$

(6) Alignment Coils

(a) Flux: 0 to 5 Gauss

(b) Current: 25 ma for 5 Gauss

(c) Resistance: 10.8Ω

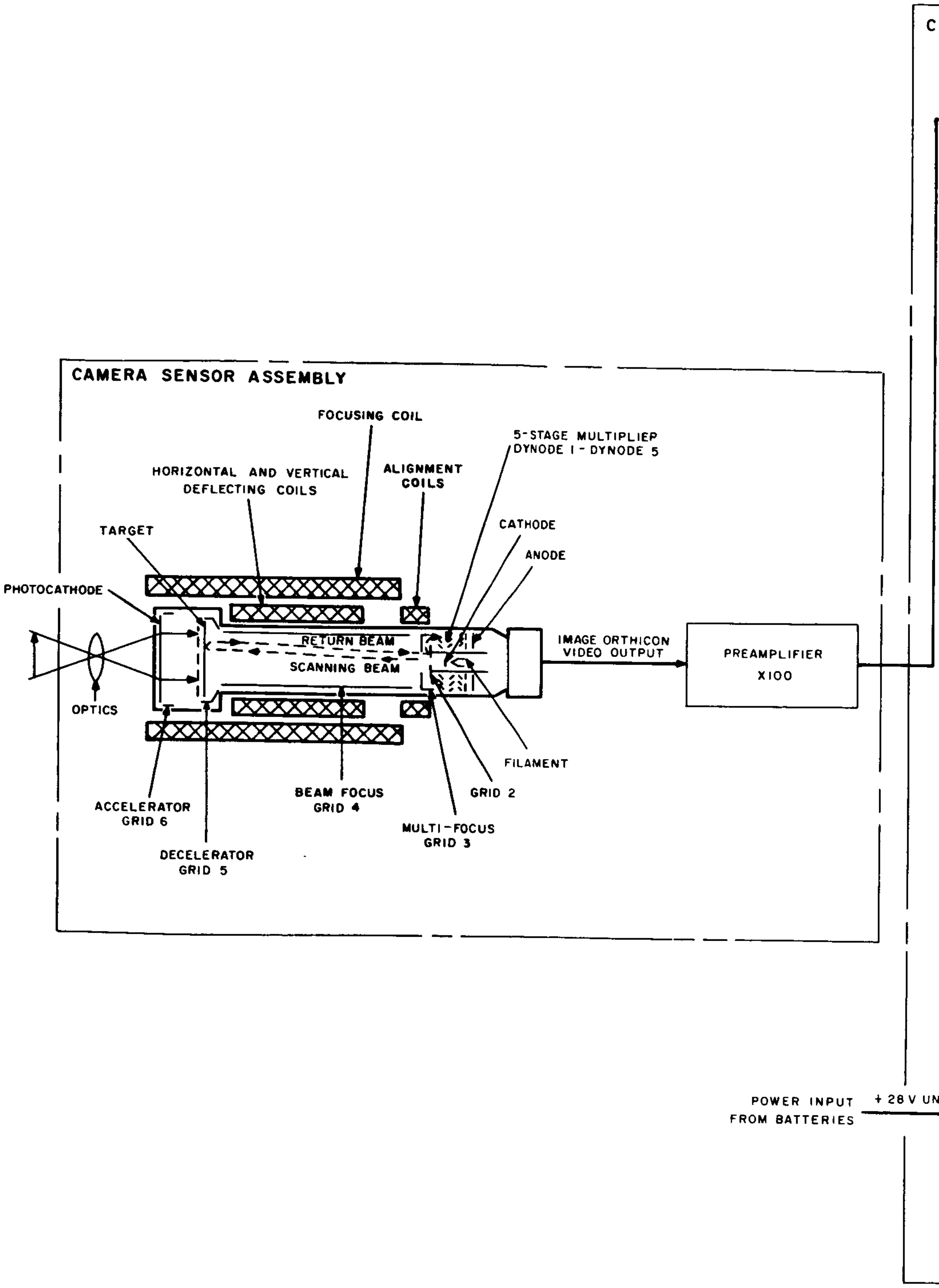
C
CAMERA SENSOR ASSEMBLY
FOCUSING COIL
5-STAGE MULTIPLIEP
DYNODE 1 - DYNODE 5
HORIZONTAL AND VERTICAL
DEFLECTING COILS
ALIGNMENT
COILS
CATHODE
TARGET
ANODE
PHOTOCATHODE
RETURN BEAM
SCANNING BEAM
IMAGE ORTHICON
VIDEO OUTPUT
PREAMPLIFIER
X100
OPTICS
FILAMENT
ACCELERATOR
GRID 6
BEAM FOCUS
GRID 4
GRID 2
MULTI-FOCUS
GRID 3
DECELERATOR
GRID 5
POWER INPUT
FROM BATTERIES
+ 28 V UN

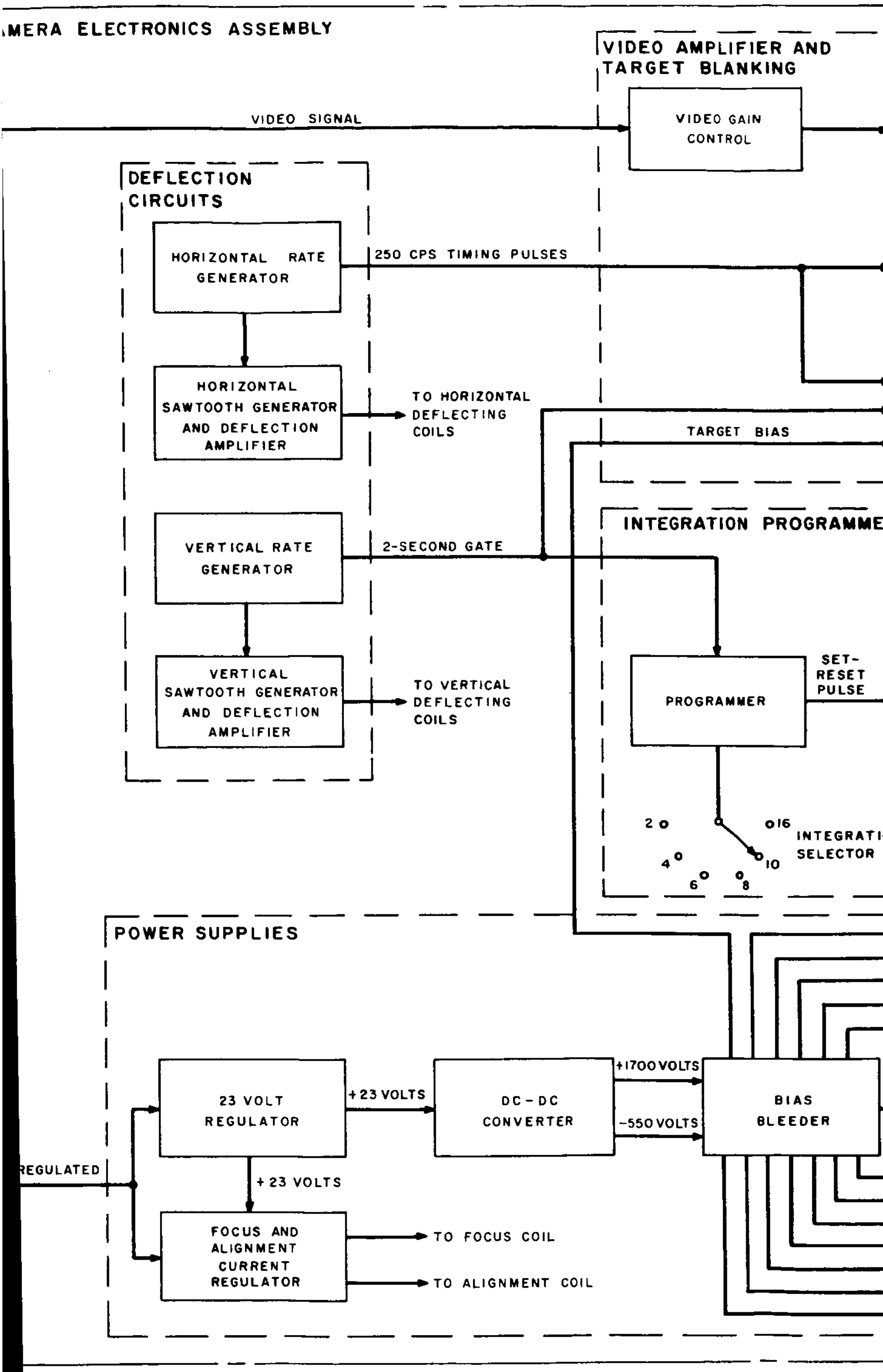
MERA ELECTRONICS ASSEMBLY
VIDEO AMPLIFIER AND TARGET BLANKING
VIDEO SIGNAL
VIDEO GAIN CONTROL
DEFLECTION CIRCUITS
HORIZONTAL RATE GENERATOR
250 CPS TIMING PULSES
HORIZONTAL SAWTOOTH GENERATOR AND DEFLECTION AMPLIFIER
TO HORIZONTAL DEFLECTING COILS
TARGET BIAS
INTEGRATION PROGRAMME
VERTICAL RATE GENERATOR
2-SECOND GATE
VERTICAL SAWTOOTH GENERATOR AND DEFLECTION AMPLIFIER
TO VERTICAL DEFLECTING COILS
PROGRAMMER
SET-RESET PULSE
2 4 6 8 10 16
INTEGRATI
SELECTOR
POWER SUPPLIES
23 VOLT REGULATOR
+23 VOLTS
DC-DC CONVERTER
+1700 VOLTS
-550 VOLTS
BIAS BLEEDER
REGULATED
+23 VOLTS
FOCUS AND ALIGNMENT CURRENT REGULATOR
TO FOCUS COIL
TO ALIGNMENT COIL

2

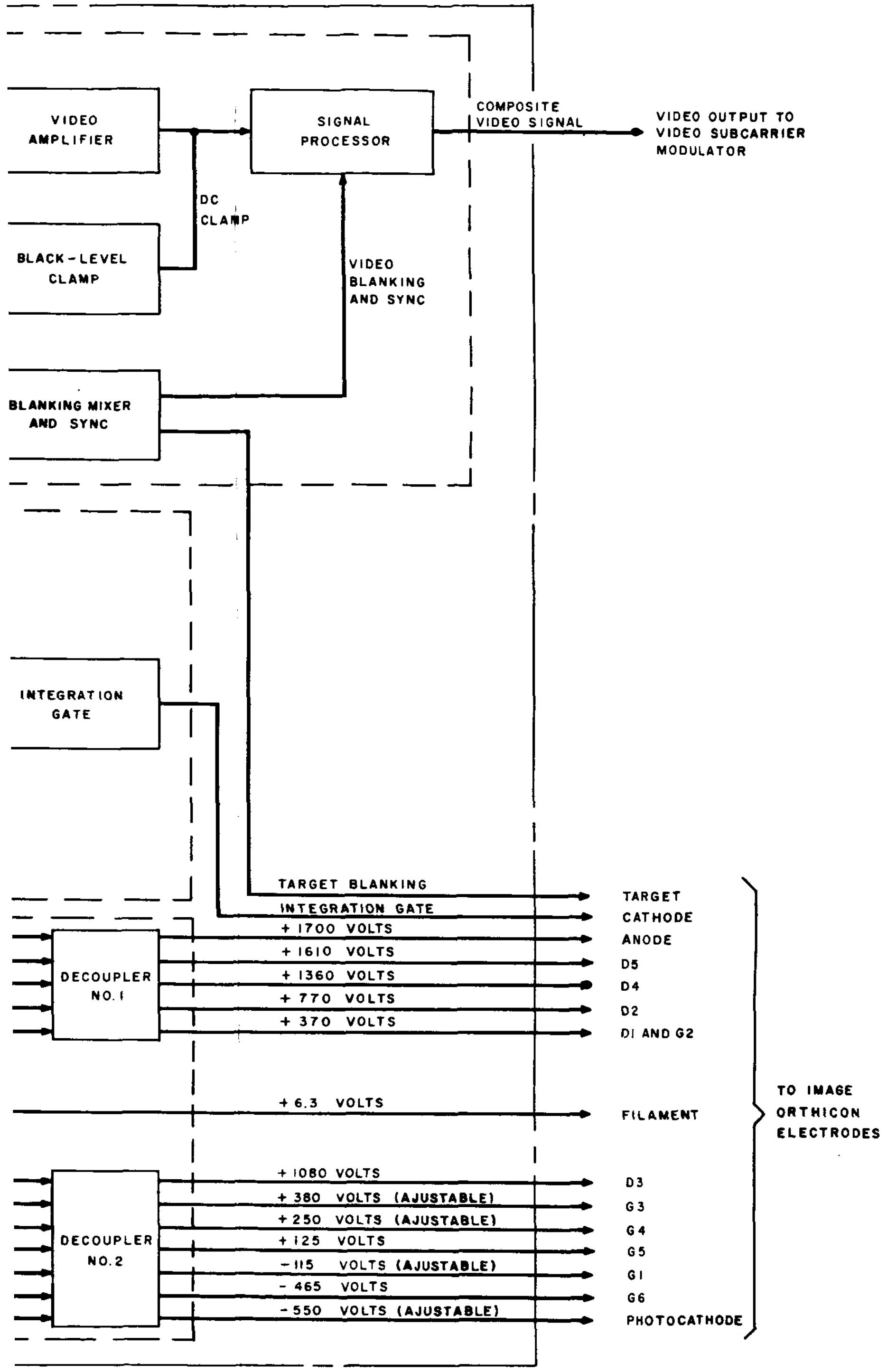

Figure II-1. TIGRIS Television Camera System, Functional Block Diagram

(7) Preamplifier

(a) Voltage Gain: 100

(b) Frequency Response: 12 cps-95 Kc

(c) Noise Figure: 2.3 db

(d) Input Resistance: 200 KΩ

b. Camera Electronics Assembly

(1) 23V Regulator

Input: 28V at 1.8 a (50 watts)
Output: 23V ± 0.2V for changes in line, load and temperature.

(2) DC-DC Converter

Outputs: E_1 = +1700V
E_2 = -552V
E_3 = +6.3V
E_4 = +6.3V

(3) Bias Bleeder (output voltages adjusted for optimum operation of image orthicon tube GE type Z7806 LHP)

Outputs: G1 (Beam) = -99V, adjustable
G2, D1 = +300V
G3 (Multi-Focus) = +285V, adjustable
G4 (Beam Focus) = +180V, adjustable
G5 = +146V
G6 = -300V
Photocathode = -540V, adjustable
Target = 0V, adjustable
D5 = +1300V
D4 = +1050V
D3 = +650V
D2 = +560V
D1 = +300V

(4) Focus and Alignment Current Regulator

(a) Focus Current: 860 ma ± 0.25%

(b) Alignment Current: 25 ma ± 0.25%

(5) Vertical Rate Generator, Sawtooth Generator, and Deflection Amplifier

(a) Repetition Period: 2.0 sec ± 0.1 sec

(b) Retrace: 100 msec ± 5 msec

(6) Horizontal Rate Generator, Sawtooth Generator, and Deflection Amplifier

(a) Repetition Rate: 250 cps ± 12.5 cps

(b) Retrace: 240 μsec ± 12 μsec

(7) Video Amplifier and Target Blanking

(a) Gain: 42, adjustable

(b) Frequency Response: 2 cps - 100 Kc

(c) Black Level: 1.25V, adjustable

(d) Output Impedance: 85Ω

(e) White Level: 4V

(f) Target Blanking: 6V, adjustable

(g) Sync Tip: 0V

(8) Integration Programmer

Manually adjustable integration periods: 2, 4, 6, 8, 10, and 16 seconds

(9) Integration Gate

(a) Duration: derived from programmer

(b) Amplitude: 23V

(10) Video Preamplifier and Video Amplifier

(a) Gain: 4200, adjustable

(b) Frequency Response: 14 cps - 65 Kc from constant current source.

3. Orthicon Performance

The resolution in the picture generated by the camera tube at a constant integration time decreases as the light input decreases. Figure II-2 presents curves that show the limiting resolution in TV lines versus photocathode illumination in foot-candles for a 2-second frame rate is 535 lines at 1×10^{-5} foot-candles and exceeds 200 lines at 2.5×10^{-7} foot-candles. Figure II-3 shows the transfer characteristics of the image orthicon tube for a 2-second and 10-second integration time. Below the knee of the transfer curve the sensitivity resolution curve varies directly with the integration time. Figure II-3 also illustrates an improvement in the signal-to-noise ratio as the integration time is increased.

Monitor pictures are shown in Figure II-4 for illumination levels of 2.5×10^{-4} and 2.5×10^{-7} foot-candles on the image orthicon. As a comparison of the performance of the TV camera and photographic technique, test photographs of the scene were taken with a camera using Polaroid ASA 3000 speed film and with the TIGRIS TV camera. At a scene brightness of 2.8×10^{-4} foot lamberts it required 30,300 seconds (8 hrs. 25 minutes) to record a picture comparable to that obtained in two seconds with the TIGRIS camera. At a scene brightness of 3.125×10^{-6} foot lamberts, no picture was obtained after an exposure of 24 hours, while a useful picture was obtained with the image orthicon at 16 seconds integration. However, it should be noted that the image size on the sensor was not the same as the Polaroid film[1]; also that the Polaroid film may have severe reciprocity loss of sensitivity for long exposures; and that stringent control of all parameters would be required for a more exact comparison.

C. MECHANICAL

1. General

The TIGRIS preprototype television camera has been designed so that flight-type hardware can be produced with a minimum of redesign effort. A stiff structure has been provided to allow the use of a simple isolator in the final payload.

2. Camera Sensor Assembly

The TIGRIS camera sensor assembly housing is shown in Figure II-5. The 3-inch orthicon tube selected (refer to Paragraph III-B1) is of a standard configuration with standard pin connections. The tube mounts inside the ruggedized deflection yoke and focus coil assembly. The video preamplifier is mounted adjacent to the image orthicon tube to minimize effects of stray capacitance. The camera sensor assembly is normally mounted coaxially inside the camera electronics assembly. If desired the camera sensor assembly may be removed and operated separately. The camera sensor assembly is 18-inches long and is 4.75 inches in diameter, less the optics. The weight of the assembly is 13.63 pounds, less optics. The weight of the optics is 1.5 pounds.

[1] The flux at the image plane is proportional to $\frac{1}{(1 + m)^2}$. The factor $(1 + m)^2$ for the TIGRIS camera and the Polaroid-film camera is 1.37 and 3.53 respectively. The ratio of flux at the image plane of the TIGRIS camera to the Polaroid-film camera is 3.53/1.37 = 2.58.

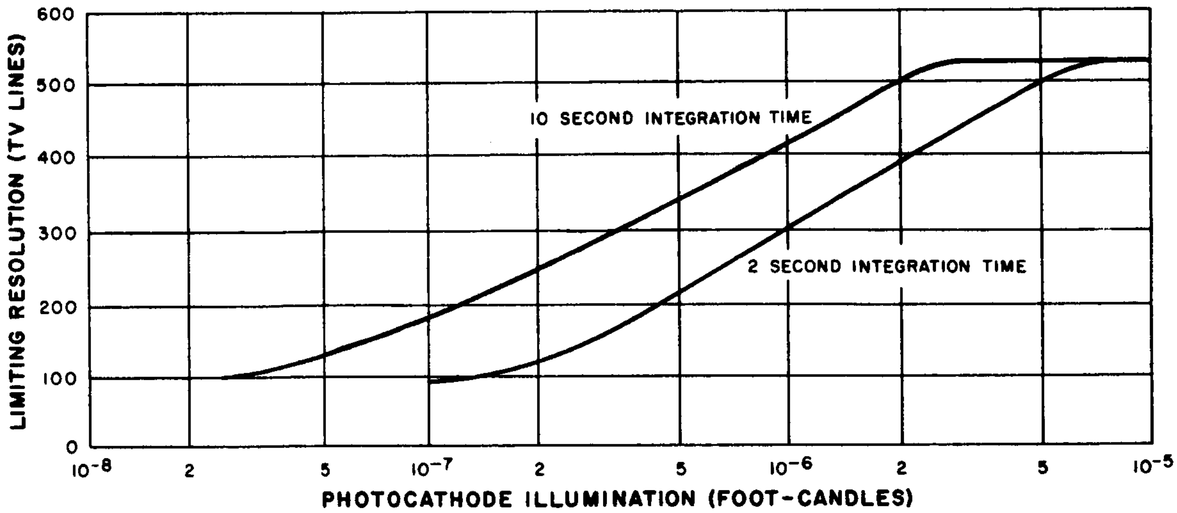

Figure II-2. Resolution Characteristics of GE Z7806 LHP Image Orthicon Tube

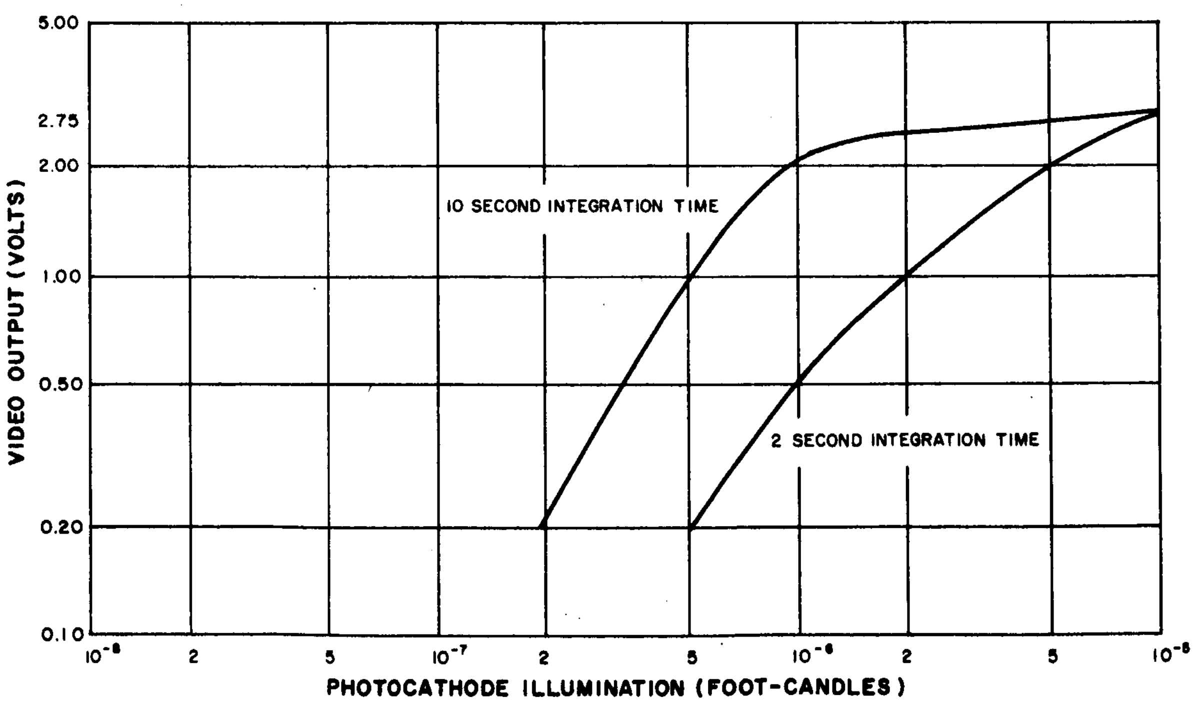

Figure II-3. Transfer Characteristics of GE Z7806 LHP Image Orthicon Tube

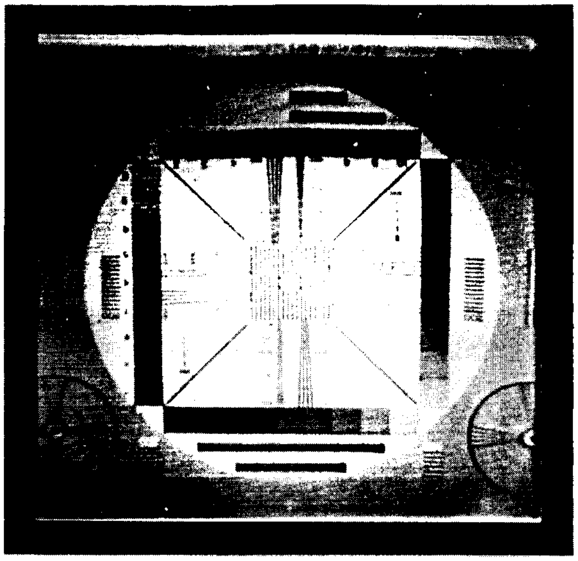

(a) 5.6×10^{-4} ft. -candles

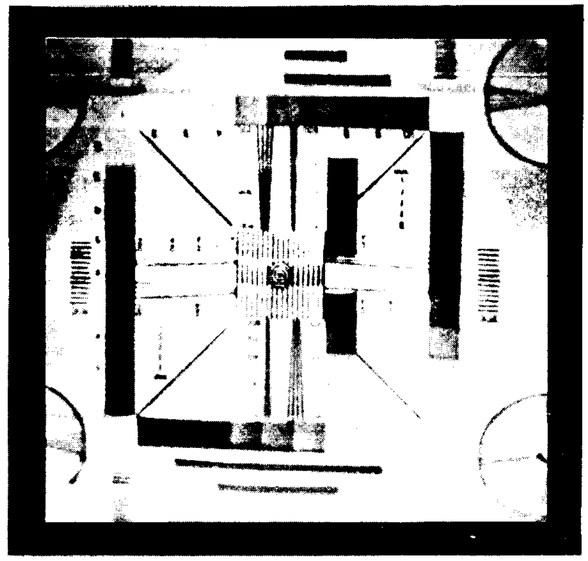

(b) 2.5×10^{-4} ft. -candles

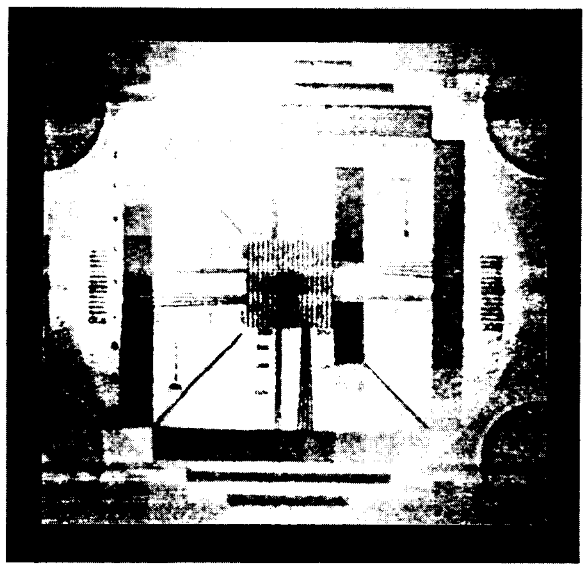

(c) 2.5×10^{-7} ft. -candles

Figure II-4. Performance of the GE Z7806 LHP Image Orthicon at a 2-Second Frame Rate for Three Levels of Illumination

3. Camera Electronics Assembly

The camera electronics assembly (Figure II-6) consists of hollow hexagonal cylinder with six radiating fins which accommodate 12 circuit boards. A metal-backing board is mounted behind each circuit board to provide shielding; and in conjunction with a compressed layer of absorbent material provides a stiff and damped vibration isolator. The assembly is 10.72 inches long and is 11.82 inches in diameter; it weighs 25 pounds.

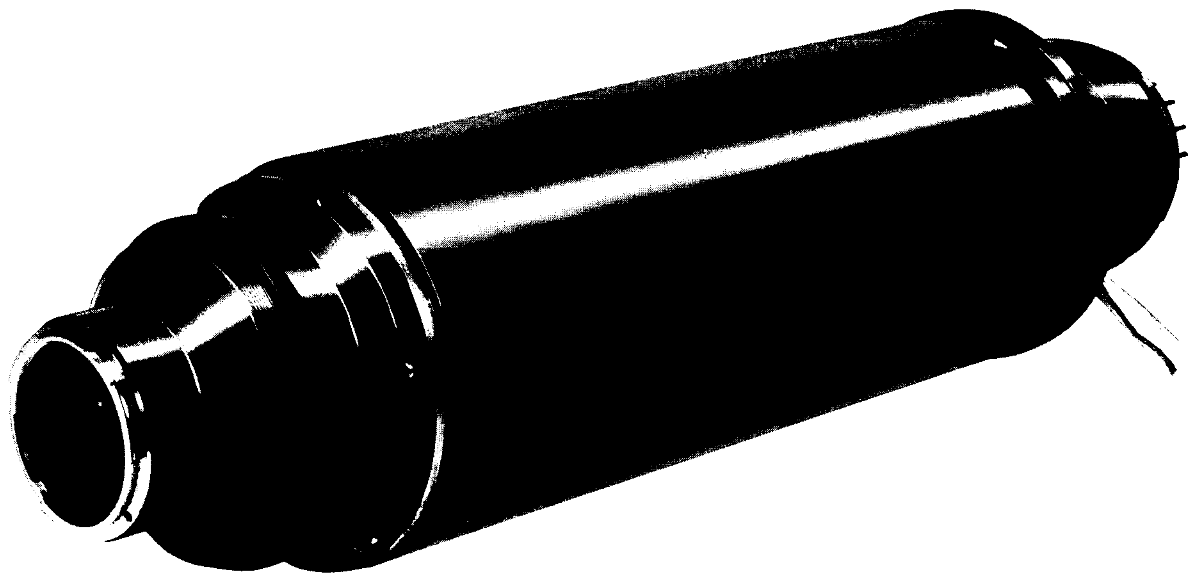

Figure II-5. Camera Sensor Assembly Housing

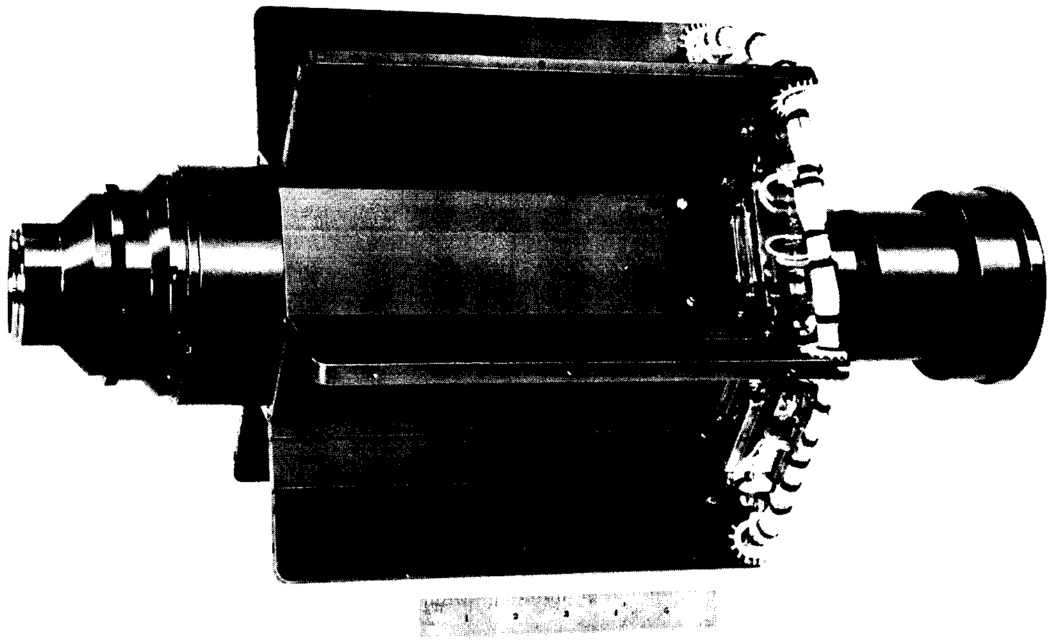

Housing is shown mounted to camera sensor assembly with circuit boards and face cover removed.

Figure II-6. Camera Electronics Assembly Housing

SECTION III

DESCRIPTION OF DEVELOPMENT

A. GENERAL

The engineering model was designed to make optimum use of AED-proven camera designs wherever possible. This permitted rapid fabrication of the engineering model by designing only a few specialized circuits. The engineering model was used to test the overall performance of the image orthicons and to verify that the design concept was satisfactory before beginning the mechanical design of the preprototype model. The following paragraphs describe the development of the camera system, selection of its component parts, and design of its electronic circuitry. Schematic diagrams of the camera sensor and electronics are provided at the end of this section to supplement the circuit descriptions given herein.

B. CAMERA SENSOR DESIGN

1. Selection of Image Orthicon

After careful investigation of the image orthicon tubes available and evaluation of manufacturer's data on their performance, it was concluded that the General Electric type Z7086 LHP was best qualified to meet the requirements of the TIGRIS program. These requirements as defined by the contract are:

a. Select the most appropriate ruggedized image orthicon tube available considering both 2-inch and 3-inch tubes.

b. The tube selected shall have a horizontal limiting resolution of 200 TV lines at a photocathode illumination of 5×10^{-7} foot-candles and 500 TV lines at 10^{-5} foot-candles.

c. At a photocathode illumination of 10^{-5} foot-candles, the tube shall be capable of discerning ten steps of grey.

d. There shall be no departure from a linear increase in information capability over integration times up to 10 seconds.

e. The signal-to-noise ratio shall exceed 20 db.

f. Acceptable operation must be obtained at a frame rate of 2 seconds and a horizontal line rate of 4 milliseconds.

After a review of the available manufacturers of image orthicon tubes it was decided that the tube would be selected from one of the following companies:

a. General Electric Company, Syracuse, New York
b. Radio Corporation of America, Lancaster, Pennsylvania
c. Westinghouse Electric Corporation, Elmera, New York

An evaluation of the tubes listed in Table III-1 was performed to determine the compatibility of each tube with the basic contractual requirements listed above. A comparison was also made of the availability and cost of each item, its photocathode response, resolution, signal-to-noise ratio, target material, grey scale, and mechanical characteristics. An attempt was made to evaluate all the tubes on the same basis; but, since little work has been done by the vendors under slow-scan conditions, the conditions under which the data was taken varies among the several vendors. To insure the intent of the TIGRIS camera system it was decided to limit the choice to ruggedized types only. The choice of ruggedized low-light-level tubes was thus limited to the GE type Z7806 LHP and the Westinghouse type WL-22724. An attempt was made to witness the operation of these two types; but unfortunately Westinghouse did not have one of their tubes available to demonstrate. Based on the demonstration of the GE type Z7806 LHP and its ready availability, it was chosen for the TIGRIS program.

2. Selection of Optics

The TIGRIS mission requirements indicated that the optics for the camera system must have a wide-angle field-of-view of approximately 90 degrees and a low aperture number to obtain optimum sensitivity. Several vendors were contacted to determine the characteristics and availability of suitable optics. Most of the vendors did not have sufficient information on the performance of the optics at the edge of the 1.8-inch diagonal of the image area required for the image orthicon. Consequently, many lenses were obtained on consignment and tests were performed to determine their optical image-area corner resolution, center resolution, and back focus. Table III-2 indicates the test data accumulated for the lenses that were evaluated. The Ziess Distagon lens with a 25 mm focal length, a f/2.8 aperture number, and a field-of-view of 80 degrees was selected as being the best compromise available. Provision was made in the camera design to permit interchanging of the lenses. In addition to Ziess lens, the camera will accept the 75 mm f/0.87 Super Farron lens. This lens would restrict the field-of-view to 26 degrees, but provide an increase in the photocathode illumination by a factor of 10.

3. Design of the Deflection, Focus, and Alignment Coils

The inductance of the deflection yoke was determined by the power supply potential and the maximum desired flyback potential developed during the flyback time of the trace. The yoke potential required for a full target scan is determined by the following equation:

TABLE III-1. COMPARATIVE EVALUATION OF IMAGE ORTHICON TUBES AVAILABLE

Manufacturer & Model No.	Resolution: Horizontal Limiting (lines)	Resolution: Photocathode Illumination (ft. -candles)	S/N (db)	Photocathode Response (RETMA Spectral Response Chart	Target Material	Grey Scale Steps	Mechanical Description
GE Z7962	200 500	7×10^{-7} 1×10^{-5}	16.3	S-20	Magnesium Oxide	<10	3 in. not ruggedized
GE Z7806 LHP	200 500	7×10^{-7} 1×10^{-5}	16.3	S-20	Magnesium Oxide	<10	3 in. ruggedized; shock 30g; vibration 5g; acceleration 70g; low heater power
GE Z7850	Unknown	Unknown	Unknown	S-20	Magnesium Oxide	<10	3 in. ruggedized; shock 30g; vibration 5g; acceleration 70g; low heater power
GE Developmental Model (Nov. '63)	112 327	7×10^{-7} 1×10^{-5}	Unknown	S-20	Magnesium Oxide	<10	2 in. not ruggedized
RCA 7967	200 500 (Scene unknown)	5×10^{-7} 2.8×10^{-6}	9.6	S-20	Magnesium Oxide	<10	3 in. not ruggedized
RCA C74081	200 500	1.7×10^{-6} 4×10^{-5}	2.3	S-20	Magnesium Oxide	<10	2 in. not ruggedized
Westinghouse 22722	200 500	3×10^{-7} 1.2×10^{-6}	Unknown		Aluminum Oxide	Unknown	3 in. not ruggedized
Westinghouse 22724	200 500	3×10^{-7} 1.2×10^{-6}	30 (B. W. unknown, ft. -c level unknown		Aluminum Oxide	Unknown	3 in. ruggedized; shock 15g; vibration 5g; acceleration 5g

Notes:

1. Resolution was determined using a 100 percent contrast chart, standard TV scan rates, and a 1.8-inch diagonal photocathode; unless otherwise indicated.
2. Signal-to-noise ratio (S/N) is given for a video bandwidth of 4.5 Mc and an illumination level of 1×10^{-5} ft.-c. unless otherwise indicated.

TABLE III-2. COMPARATIVE EVALUATION OF OPTICS AVAILABLE

Manufacturer & Type	Numerical Aperture	Focal Length (mm)		Back Focus Measured (mm)	Image Size (in.)	Resolution (lines/mm)		Field of View (deg.)	Remarks
		Rated	Measured			Center	Off Axis		
Ziess:									
Biogon	2.8	35	35.57	16.14	1.9	585	23	70	Field Good
Biogon	4.5	21	21.03	10.28	1.7	390	276	90	Field Good High Contrast
Distagon	2.8	25	26.01	38.54	1.7	630	220	80	Field Good
Kinoptik:									
Apochromat	T2.2	18	18.72	18.49	1.1	782	49	74	Field Small Poor Contrast
Fulgior	1.3	50	54.4	35.52	1.8	537	33	50	Very Poor Contrast
Apochromat	2.0	25	26.11	19.9	1.2	757	39	30	Field Small
Apochromat	2.0	28	29.98	21.9	1.2	764	75	54	Field Small
Apochromat	2.0	50	54.4	43.77	2.2	606	60	54	Low Contrast
Angenieux	2.5	35	35.76	-	1.8	461	183	67	Extreme Field Curvature
B & L:									
Super Baltar	2.0	25	26.17	30.61	1.35	727	99	66	Field Small Astignmatic
FARRON	0.87	76	75	1.5	1.7	-	-	26	Designed for Image Orthicon

$$E_{yoke} = \Delta I \left(R + \frac{L}{\Delta T_{flyback}} + \frac{L}{\Delta T_{scan}}\right)$$

The maximum deflection yoke flyback potential was limited to 20 V peak-to-peak so that the unregulated 28 volt power supply could operate the deflection amplifiers; thus maintaining power efficiency.

Each of the vertical deflection push-pull coils has an inductance of 50 millihenries and a resistance of 141 ohms. A current of 90 milliamperes is required to deflect the beam along the vertical axis. Each of the horizontal push-pull coils has an inductance of 9 millihenries and a resistance of 30 ohms. A current of 220 milliamperes is required to deflect the beam along the horizontal axis. A magnetic field flux density of 75 gausses at the center of the focus coil is required to focus the beam. To permit optimum operation of the image orthicon, alignment fields of 0 to 5 gauss are required. This field is created by 10-ohm alignment coils which are placed in series with the focus coil. Since the focus current is maintained at a constant value, rheostats are connected across the alignment coils to adjust the alignment currents.

The schematic diagram of the image orthicon, yoke and alignment coils is shown in Figure III-2.

4. Development of the Preamplifier

The preamplifier developed for the TIGRIS camera system is a solid-state device utilizing a type 2N2497 field-effect transistor in the input stage. The solid-state preamplifier has the following advantages over a comparable vacuum-tube type: (1) reliability, (2) instant operation, (3) no heater power, (4) less microphonics, and (5) minimal size. The noise performance of the field-effect transistor which is very similar to that of a vacuum tube is negligible in comparison to the scanning-beam noise of the image orthicon.

The preamplifier shown in Figure III-3 consists of a four-stage, non-inverting, feedback amplifier. Since the anode of the image orthicon is at a high d-c level, a-c coupling is used to the preamplifier. When it is operated with the image orthicon, its frequency response is down 3 db at 12 cps and 100 kc. Since the output impedance is low (50 ohms) and the signal level relatively high (voltage gain of 100), the camera electronics can be remotely positioned at a distance of approximately 25 feet from the camera head if desired. The measured noise figure is 2.3 db above the theoretical Johnson noise and well below the image-orthicon beam noise.

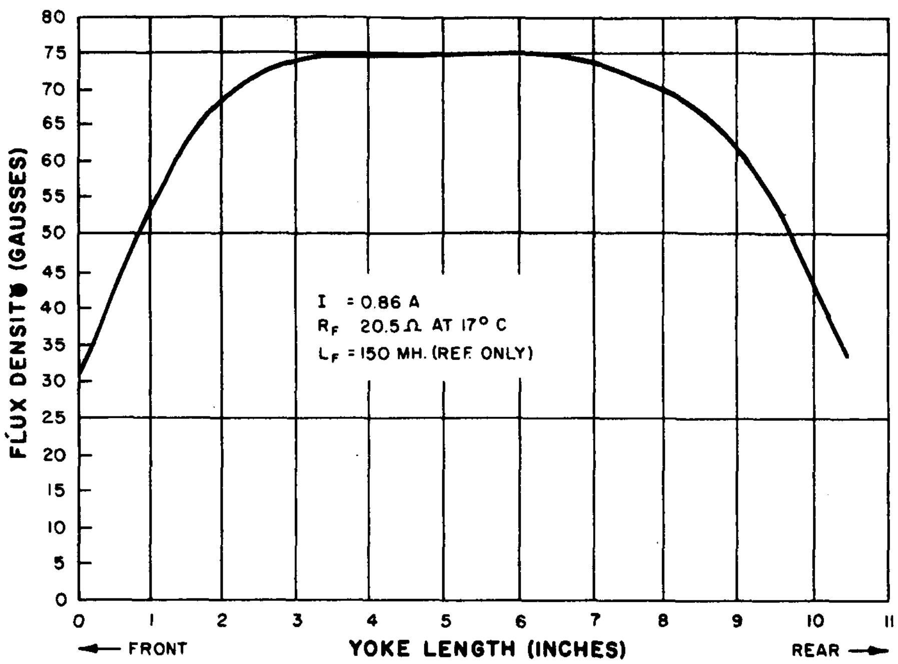

Figure III-1. Magnetic Field Flux Density Distribution of Focus Coil

C. CAMERA ELECTRONICS DESIGN

1. Power Supplies

Several power converters are required to furnish appropriate voltages for the image orthicon and the preamplifier. These include a 23V regulator, a dc-dc converter, a bias bleeder, decoupling circuits, and a focus and alignment current regulator.

a. 23V Regulator

The 23V regulator is provided to regulate the input power level to all of the low-level amplifier stages, critical programmer timing circuits, and dc-dc converter. The schematic diagram of the regulator circuitry is shown in Figure III-4. The unregulated bus input of 28 volts ± 10 percent is applied to zener diode CR1 and transistor Q1 which provide a constant current to the series reference diodes CR2, CR3, and CR4. The differential amplifier, composed of transistors Q4 and Q5, senses the 23-volt output voltage and compares a portion of it to the reference potential. Any difference voltage existing is sensed by a pnp-npn Darlington pair composed of transistors Q2 and Q3 which operates to compensate for the voltage deviation. The regulator circuitry compensates for load, line, and temperature variations to provide better than one percent regulation of the 23-volt bus.

b. DC-DC Converter

The dc-dc converter as shown in Figure III-5 consists of a transistorized chopper, a conventional saturable core transformer, an inverter circuit, a full-wave rectifier bridge and an output filter. The 23-volt regulated level is converted into the four dc output voltage levels of +1700 volts, -550 volts, +6. 3 volts, and +6. 3 volts. The high voltage outputs of the converter are connected to the bias bleeder which provides the required potentials for the image orthicon electrodes. The 6. 3-volt levels are used as image orthicon filament voltages.

c. Bias Bleeder

The bias bleeder shown in Figure III-6 is basically a voltage divider network which provides the required levels of dc voltage to the image orthicon electrodes.

d. Decouplers

The decoupler circuits shown in Figures III-7 and III-8 are resistance-capacitance filters which prevent a-c transients such as power supply spikes or 60-cycle pick up from appearing on the dc voltage levels supplied to the image orthicon electrodes.

e. Focus and Alignment Current Regulator

The current regulator shown in Figure III-9 is employed to maintain constant current in the focusing and alignment coils when changes in temperature or input voltage occur. It is essential that a constant flux of 75 gausses be maintained at the center of the image orthicon focus coil to provide the resolution and shading requirement for the tube operation throughout the flight. The focus current is monitored as a voltage across a 2-ohm resistor and compared with a stabilized reference voltage by differential amplifiers. Any deviation from the preset reference voltage is sensed by an pnp-npn Darlington-pair control stage which operates to compensate for the deviation. The focus current is regulated to ± 0. 25 percent.

2. Deflection Circuits

a. Vertical Rate Generator

The vertical rate generator provides the vertical timing pulses at 2-second intervals to the vertical deflection circuits, image orthicon target blanking mixer, and vertical synchronizing insertion circuit. As shown in Figure III-10, the circuit consists of a complementary symmetrical-type astable multivibrator. This type of multivibrator is characterized by relatively low power requirements and very low output impedance during its "on" time since both transistors of the multivibrator are turned "on" during the short blanking interval and turned off during long sweep period. This circuit is a standard AED design which has been used successfully on many TV camera programs.

b. Vertical Sawtooth Generator and Deflection Amplifier

The vertical sawtooth generator and deflection amplifier provides the vertical current waveform for the image orthicon deflection yoke. As shown in Figure III-11, the vertical sawtooth generator consists of a switch (transistor Q1), and constant current charging networks (transistor Q2, diode CR2, resistor R4, and charging capacitor C1). A balanced amplifier (transistors Q3 and Q4) provides temperature compensation and vertical size control for the sawtooth generator. Transistors Q5 and Q12 provide additional amplification. A push-pull driver (transistors Q6 and Q11) converts the sawtooth signal to push-pull signals. This signal is fed to a push-pull Darlington output stage which is connected to the vertical deflection yoke coils. The final output stages, transistors Q7, Q8, Q9, and Q10, are operated from the unregulated 28-volt power supply. Balanced feedback is derived from a 10-ohm resistor in series with the deflection coils to insure that the deflection yoke current remains stable and linear.

c. Horizontal Rate Generator, Sawtooth Generator, and Deflection Amplifier

The horizontal rate generator provides horizontal timing pulses at a repetition rate of 250 cycles per second to the horizontal deflection circuits, target blanking mixer, horizontal synchornizing circuit, and the video amplifier clamp circuit. The horizontal sawtooth generator and deflection amplifier provide the horizontal current waveform for the image orthicon deflection yoke. As shown in Figure III-12, the horizontal rate generator (transistors Q1 and Q2) is basically a complementary symmetrical type astable multivibrator operating at a repetition rate of 250 cycles per second. The sawtooth generator and switch consists of transistors Q4 and Q3 respectively. The output of the phase splitter (transistor Q5) is connected to a differential amplifier (transistors Q6 and Q7). The push-pull output stage consists of two Darlington pairs (transistors Q8, Q9, and Q10, Q11). As in the operation of the vertical circuitry, the output stage is operated from the unregulated 28-volt power supply. Negative feedback is used to insure deflection current linearity.

3. Integration Programmer

It is desirable that the illumination detected by the photocathode bring the charge level on the target to near its full storage value to provide the best signal-to-noise ratio and resolution. This is accomplished by programming the exposure to provide the optimum integration time period of the image orthicon target. The programmer by means of the integration selector switch shown in Figure III-13 permits adjustment of the integration time for durations of 2, 4, 6, 8, 10 and 16 seconds. The programmer counter as shown in Figure III-14 consists of three bistable multivibrators with manually adjustable feedback. The input trigger to the counter is derived from the vertical rate generator. The multivibrators count the 2-second vertical input pulses for the time duration set on the programmer switch. A set-reset multivibrator is provided to generate a read pulse at the end of the integration period. The output of the counter is fed to the integration gate. The integration gate is provided to cutoff the beam current of the image orthicon for the period of time set on the programmer switch. The integration gate shown in Figure III-15 consists of a two-stage amplifier. Its output is applied to the cathode of the orthicon tube. During the integration period, the output transistor Q2 saturates, applying an output potential of +23 volts to the orthicon cathode. This bias is sufficient to cut off the beam current. During the read period, the output transistor is turned off returning the cathode through resistor R6 to ground potential.

4. Video Amplifier and Target Blanking

The video amplifier elevates the signal level derived from the preamplifier and resets the black level of the a-c coupled amplifier by means of a black level clamp. The horizontal and vertical pulses from the rate generators are mixed and added to the video signal to form the blanking and synchronizing component of the composite video signal. Target blanking is also derived for the target of the image orthicon. The video amplifier presents a low output impedance due to the emitter follower configuration of its output stage.

As shown in Figure III-16, the signal input from the preamplifier in the camera sensor assembly is connected to the video gain control of the video amplifier. The output of the gain control is fed to a two-stage amplifier. Each stage consists of a doublet feedback amplifier having a voltage gain of 6.5. The second stage also provides some aperture correction to compensate for the shape of the image orthicon beam spot. A black-level clamp circuit is provided to restore the d-c component of the video signal. Transistors Q10, Q11, and Q12 provide a delayed pulse, referred to the horizontal retrace and sync period, to turn on clamp-switch transistor Q9 at the start of each horizontal sweep. An opaque mask on the image orthicon faceplate is provided to insure that the clamp operates on a black scene. When clamp switch Q9 is turned on, capacitor C7 is charged to the preset video black level determined by the setting of the variable resistor R22. The output of the clamp circuit is directly coupled to transistor Q7 which provides synchronization insertion and video output. Vertical and horizontal pulses are fed to an OR gate and amplified by transistors Q13 and Q8. The output of transistor Q8 is connected to the emitter follower output stage. An output from transistor Q13 is used to provide negative-going blanking pulses to the image orthicon target.

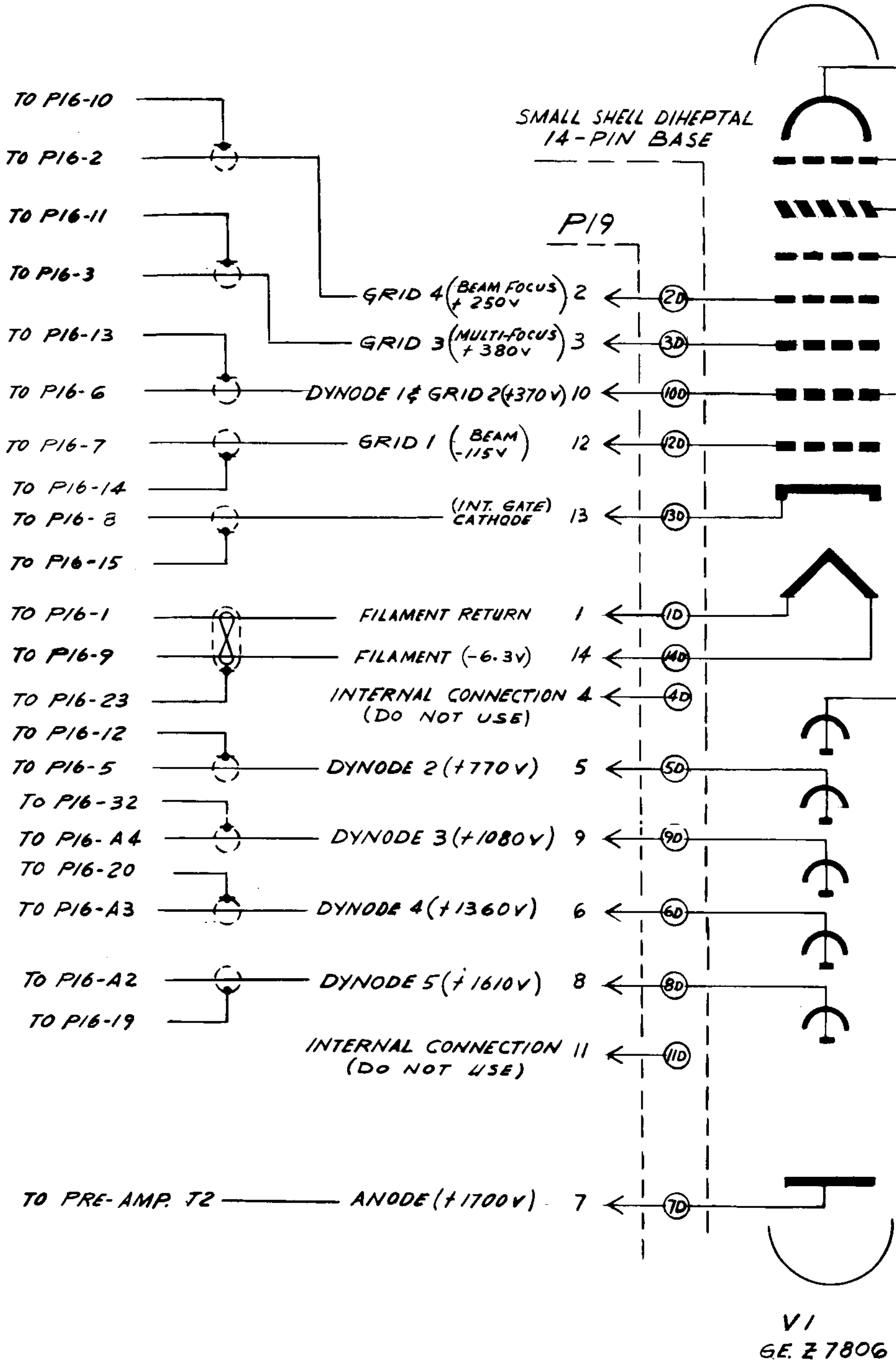

NOTES:

1. VOLTAGES IN PARENTHESES ARE FOR REFERENCE ONLY.

2. KEYED JUMBO ANNULAR 7-PIN BASE SOCKET IS NOT USED. INSTEAD WIRES ARE CONNECTED DIRECTLY TO PINS 1, 2, 5 & 6.

/

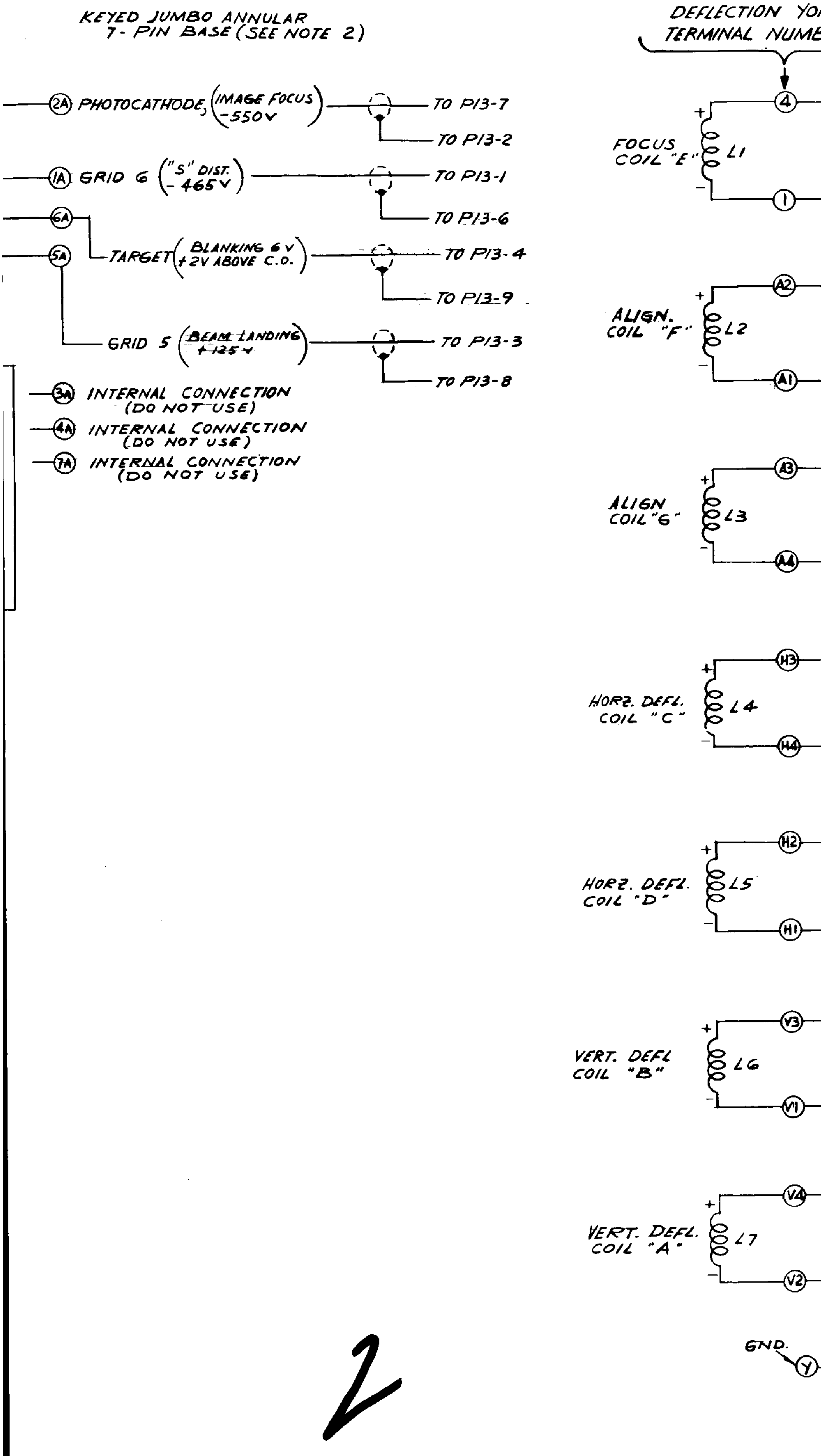
KEYED JUMBO ANNULAR
7-PIN BASE (SEE NOTE 2)
DEFLECTION YO
TERMINAL NUMB
2A PHOTOCATHODE, (IMAGE FOCUS -550V)
TO P13-7
TO P13-2
1A GRID 6 ("S" DIST. -465V)
TO P13-1
TO P13-6
6A
5A
TARGET (BLANKING 6V +2V ABOVE C.O.)
TO P13-4
TO P13-9
GRID 5 (~~BEAM LANDING +125V~~)
TO P13-3
TO P13-8
3A INTERNAL CONNECTION (DO NOT USE)
4A INTERNAL CONNECTION (DO NOT USE)
7A INTERNAL CONNECTION (DO NOT USE)
4
FOCUS COIL "E"
L1
1
A2
ALIGN. COIL "F"
L2
A1
A3
ALIGN COIL "G"
L3
A4
H3
HORZ. DEFL. COIL "C"
L4
H4
H2
HORZ. DEFL. COIL "D"
L5
H1
V3
VERT. DEFL COIL "B"
L6
V1
V4
VERT. DEFL. COIL "A"
L7
V2
GND.
Y
2

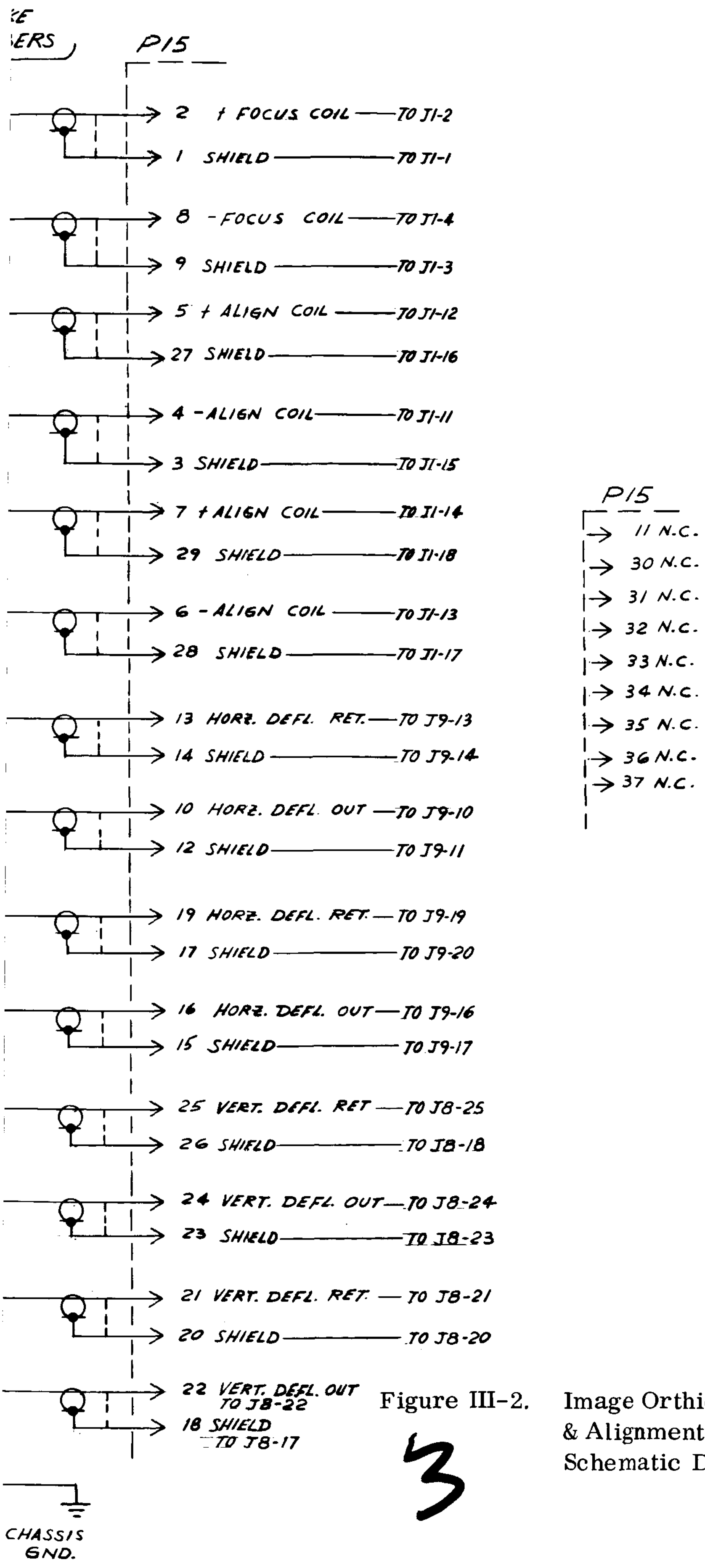

Figure III-2. Image Orthicon, Yoke & Alignment Coils, Schematic Diagram

3

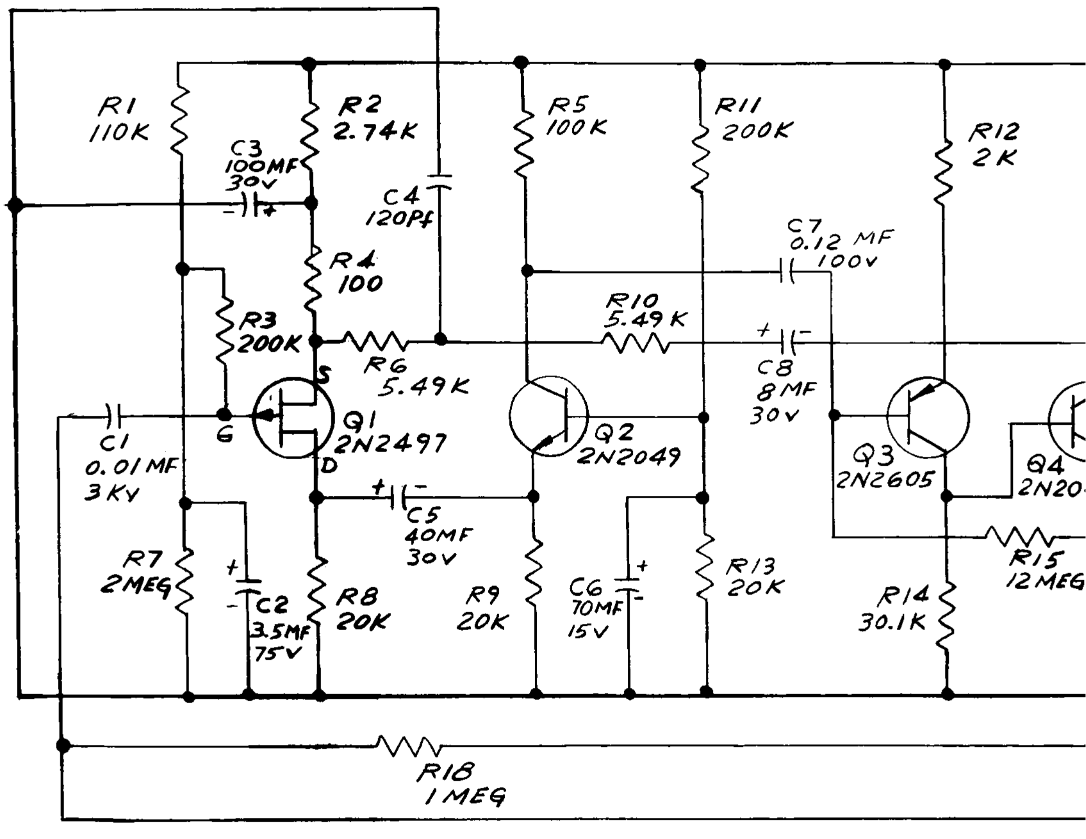
R1
110K
R2
2.74K
C3
100MF
30V
C4
120Pf
R4
100
R3
200K
R6
5.49K
Q1
2N2497
S
G
D
C1
0.01MF
3KV
C5
40MF
30V
R7
2MEG
C2
3.5MF
75V
R8
20K
R5
100K
Q2
2N2049
R9
20K
R10
5.49K
R11
200K
C6
70MF
15V
R13
20K
C7
0.12 MF
100V
C8
8MF
30V
R12
2K
Q3
2N2605
R14
30.1K
Q4
R15
12MEG
R18
1MEG

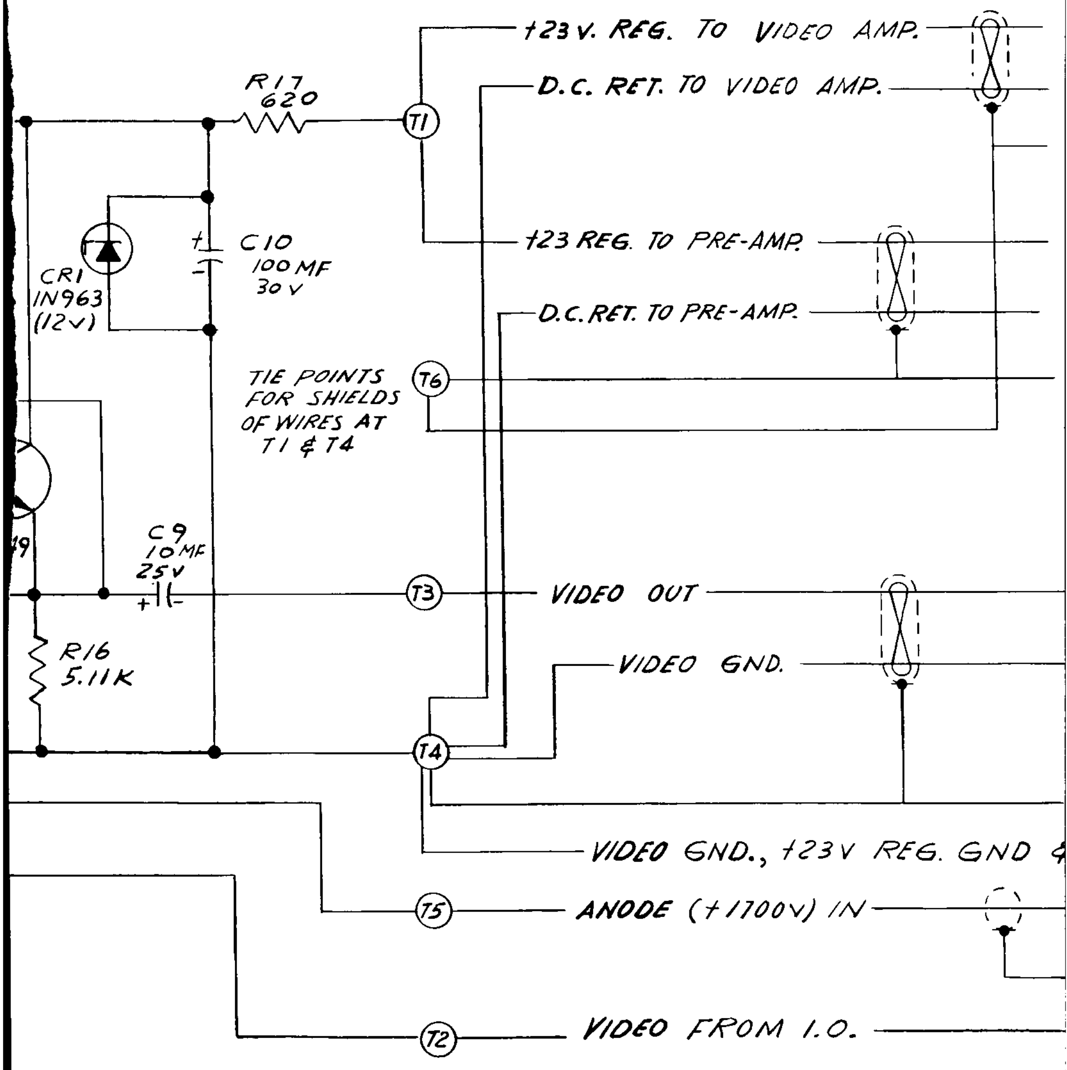

+23 V. REG. TO VIDEO AMP.
D.C. RET. TO VIDEO AMP.
R17
620
T1
CR1
1N963
(12V)
C10
100 MF
30 V
+23 REG. TO PRE-AMP.
D.C. RET. TO PRE-AMP.
TIE POINTS
FOR SHIELDS
OF WIRES AT
T1 & T4
T6
C9
10 MF
25 V
T3
VIDEO OUT
VIDEO GND.
R16
5.11K
T4
VIDEO GND., +23V REG. GND
T5
ANODE (+1700V) IN
T2
VIDEO FROM I.O.

2

TO P16-29 —— TO J4-4

TO P16-30 —— TO J4-3

TO P16-28

TO P16-4 —— TO J12-21

TO P16-31 —— TO J12-14

TO P16-27

-TO P16-21 —— TO J4-A1

TO P16-25 —— TO J4-1

TO P16-22 —— TO J4-A1S

SHIELD GND. FOR WIRE AT T1 —— TO P16-25

- TO P16-A1 —— TO J5-A2

- TO P16-16

- TO P19-7 —— I.O. SOCKET PIN 7D

Figure III-3. Preamplifier, Schematic Diagram

3

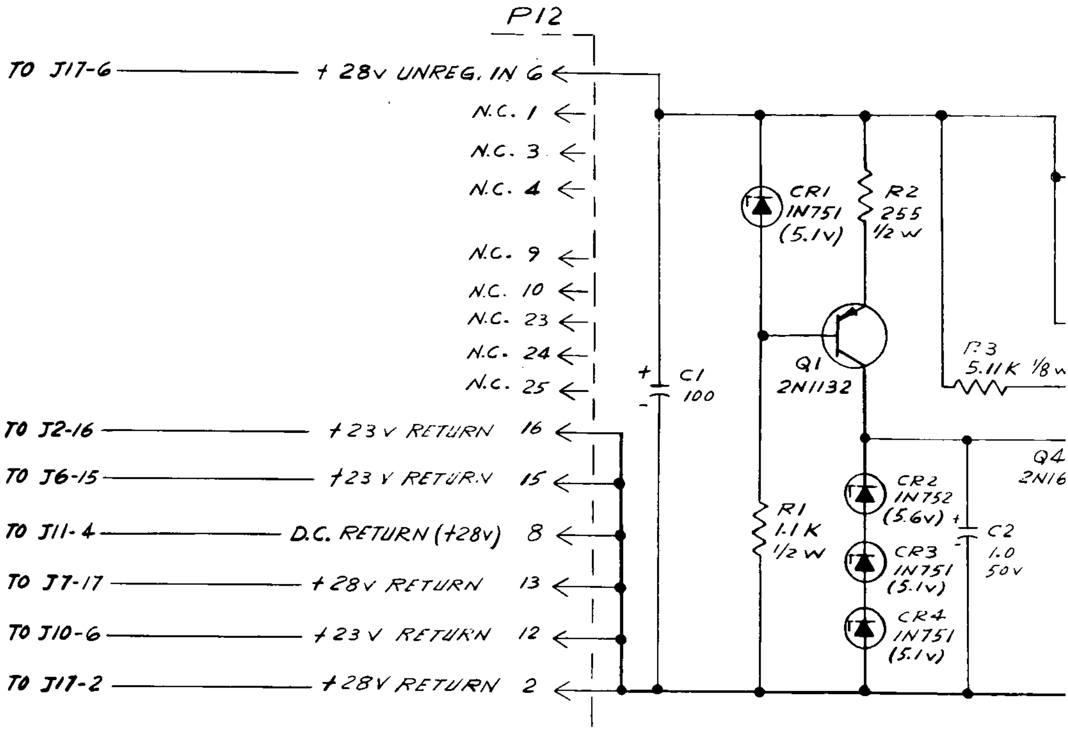

P12
TO J17-6
+28v UNREG. IN 6
N.C. 1
N.C. 3
N.C. 4
N.C. 9
N.C. 10
N.C. 23
N.C. 24
N.C. 25
TO J2-16
+23v RETURN 16
TO J6-15
+23v RETURN 15
TO J11-4
D.C. RETURN (+28v) 8
TO J7-17
+28v RETURN 13
TO J10-6
+23v RETURN 12
TO J17-2
+28V RETURN 2
C1
100
CR1
1N751
(5.1v)
R2
255
1/2 w
Q1
2N1132
R3
5.11K 1/8 w
Q4
R1
1.1K
1/2 w
CR2
1N752
(5.6v)
CR3
1N751
(5.1v)
CR4
1N751
(5.1v)
C2
1.0
50v

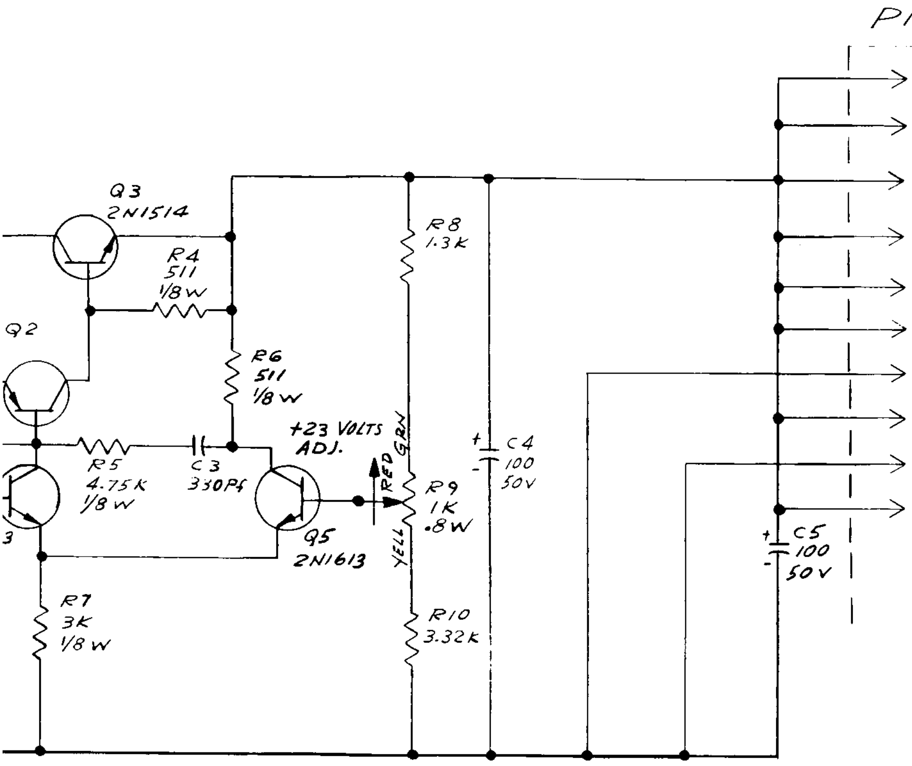
Q3
2N1514
R4
511
1/8 W
Q2
R6
511
1/8 W
+23 VOLTS
ADJ.
RED
GRN
YELL
R5
4.75K
1/8 W
C3
330Pf
Q5
2N1613
R8
1.3K
R9
1K
.8 W
R10
3.32K
C4
100
50V
C5
100
50V
R7
3K
1/8 W

2

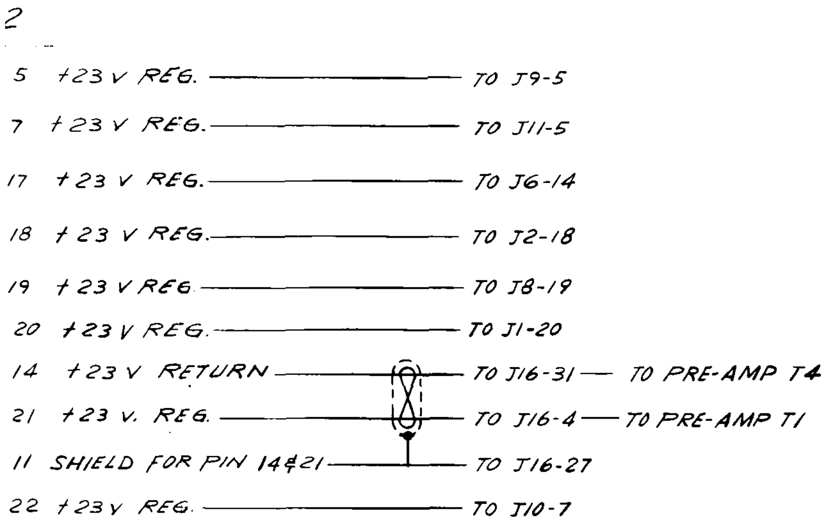

3

Figure III-4. +23V Regulated Power Supply, Schematic Diagram (Circuit Board No. F1P2)

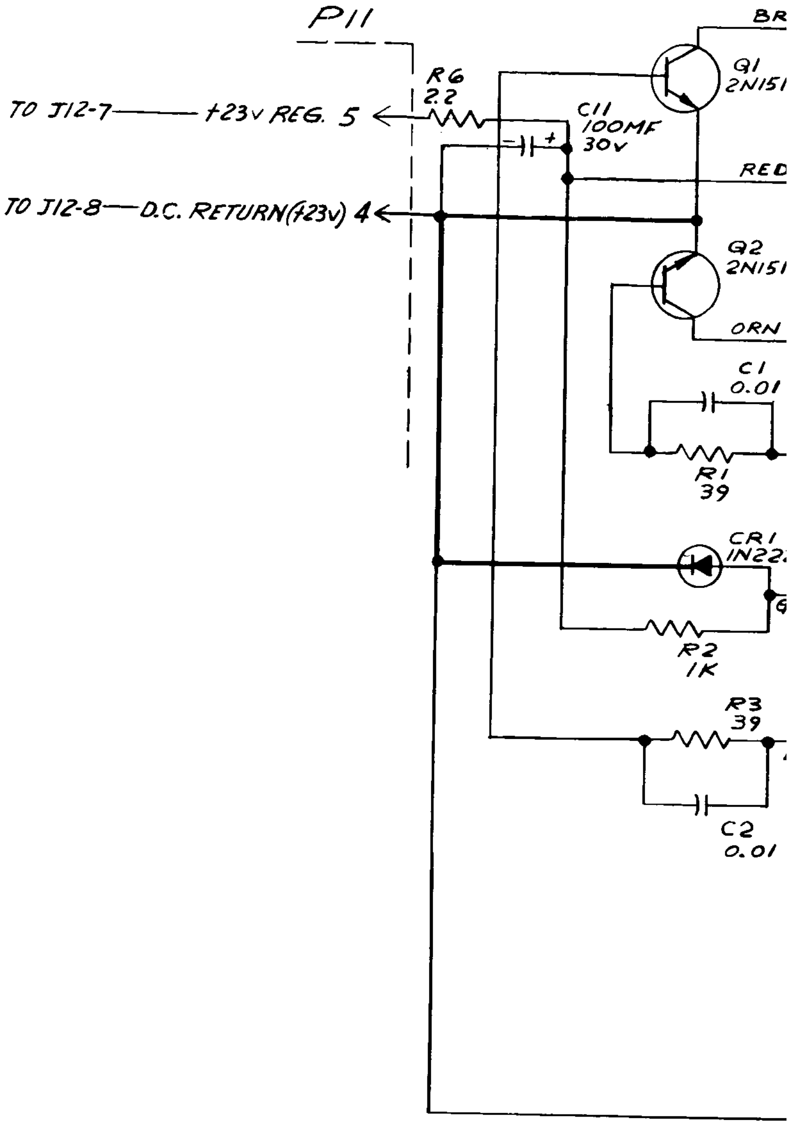
P11
R6
2.2
TO J12-7 — +23V REG. 5
C11
100MF
30V
TO J12-8 — D.C. RETURN(+23V) 4
Q1
Q2
BR
RED
ORN
C1
0.01
R1
39
CR1
R2
1K
R3
39
C2
0.01

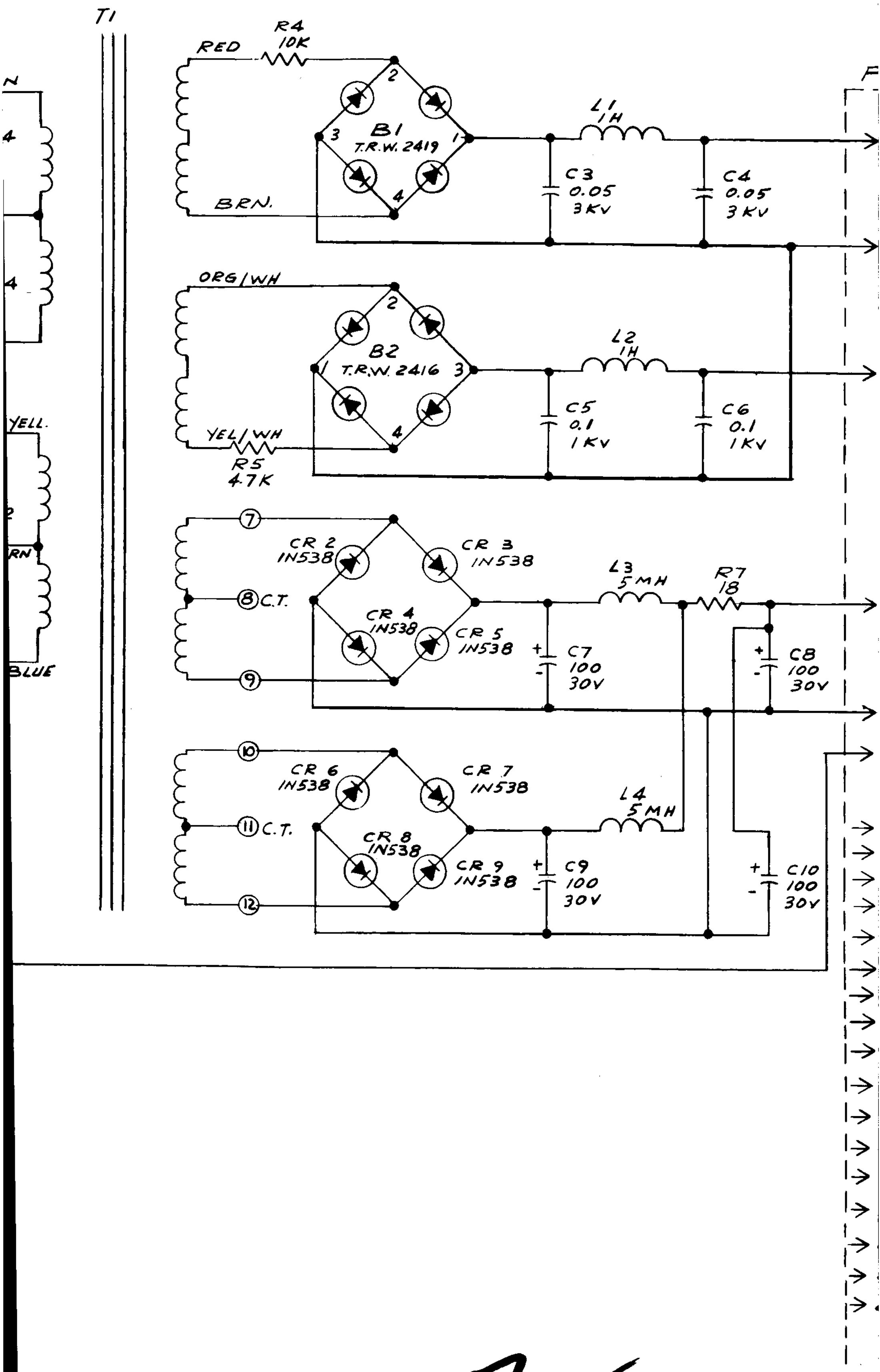

T1
R4
10K
RED
BRN.
B1
T.R.W. 2419
L1
1H
C3
0.05
3KV
C4
0.05
3KV
ORG/WH
B2
T.R.W. 2416
L2
1H
C5
0.1
1KV
C6
0.1
1KV
YEL/WH
R5
4.7K
7
8 C.T.
9
CR 2
1N538
CR 3
1N538
CR 4
1N538
CR 5
1N538
L3
5MH
R7
18
C7
100
30V
C8
100
30V
10
11 C.T.
12
CR 6
1N538
CR 7
1N538
CR 8
1N538
CR 9
1N538
L4
5MH
C9
100
30V
C10
100
30V
YELL.
BLUE

2

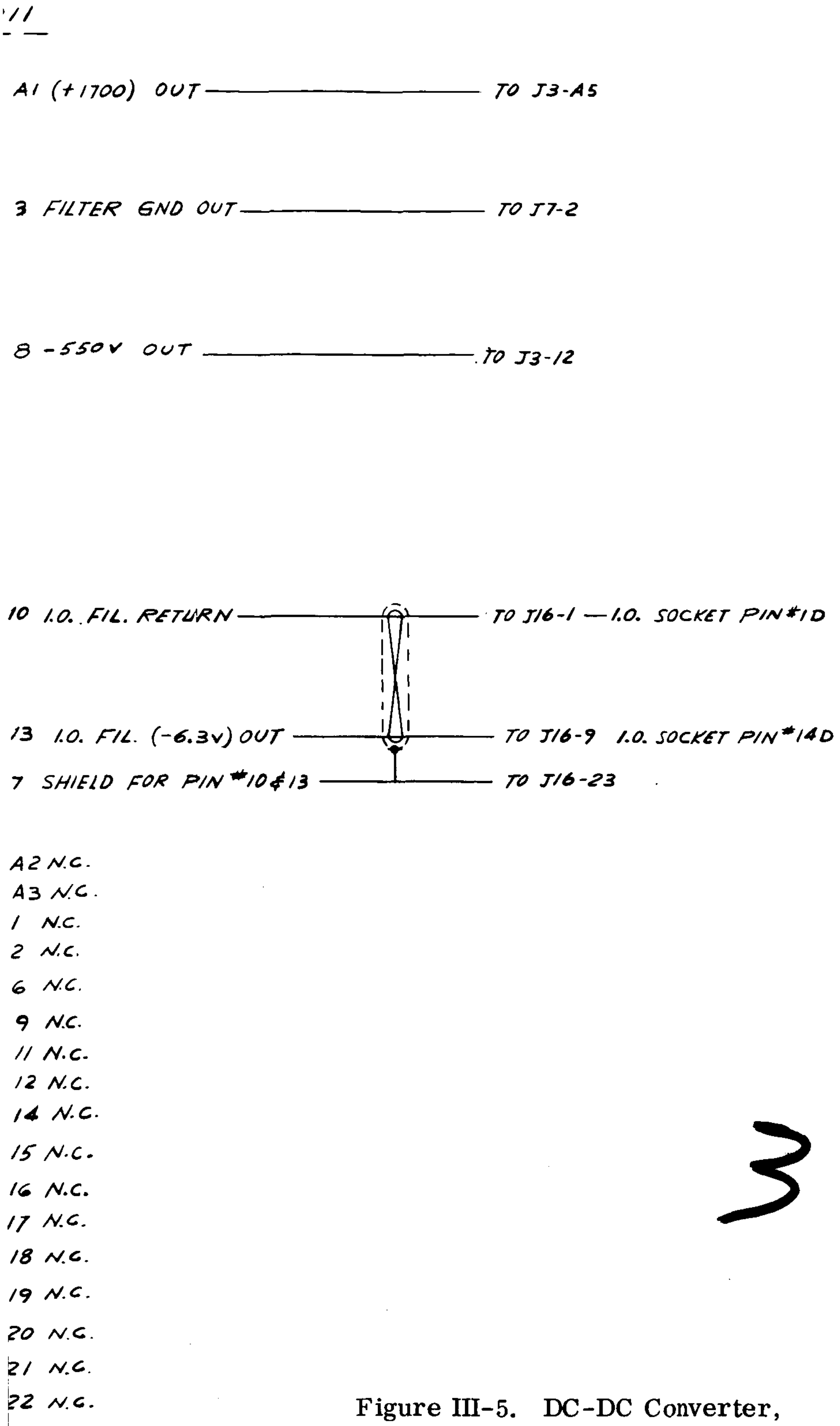

Figure III-5. DC-DC Converter, Schematic Diagram (Circuit Board No. F0P11)

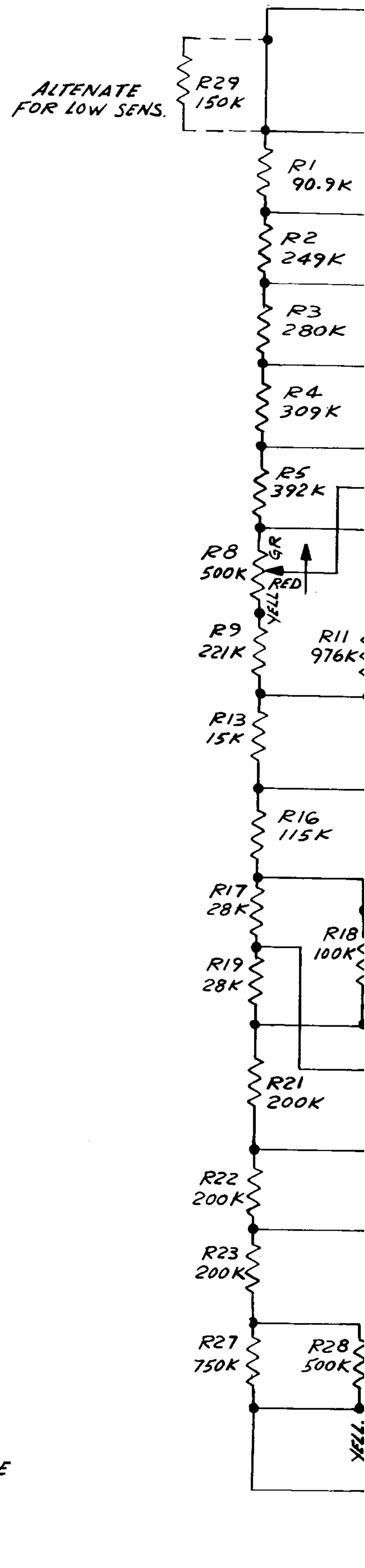

NOTES:

1. VOLTAGES IN PARENTHESES ARE FOR REFERENCE ONLY.

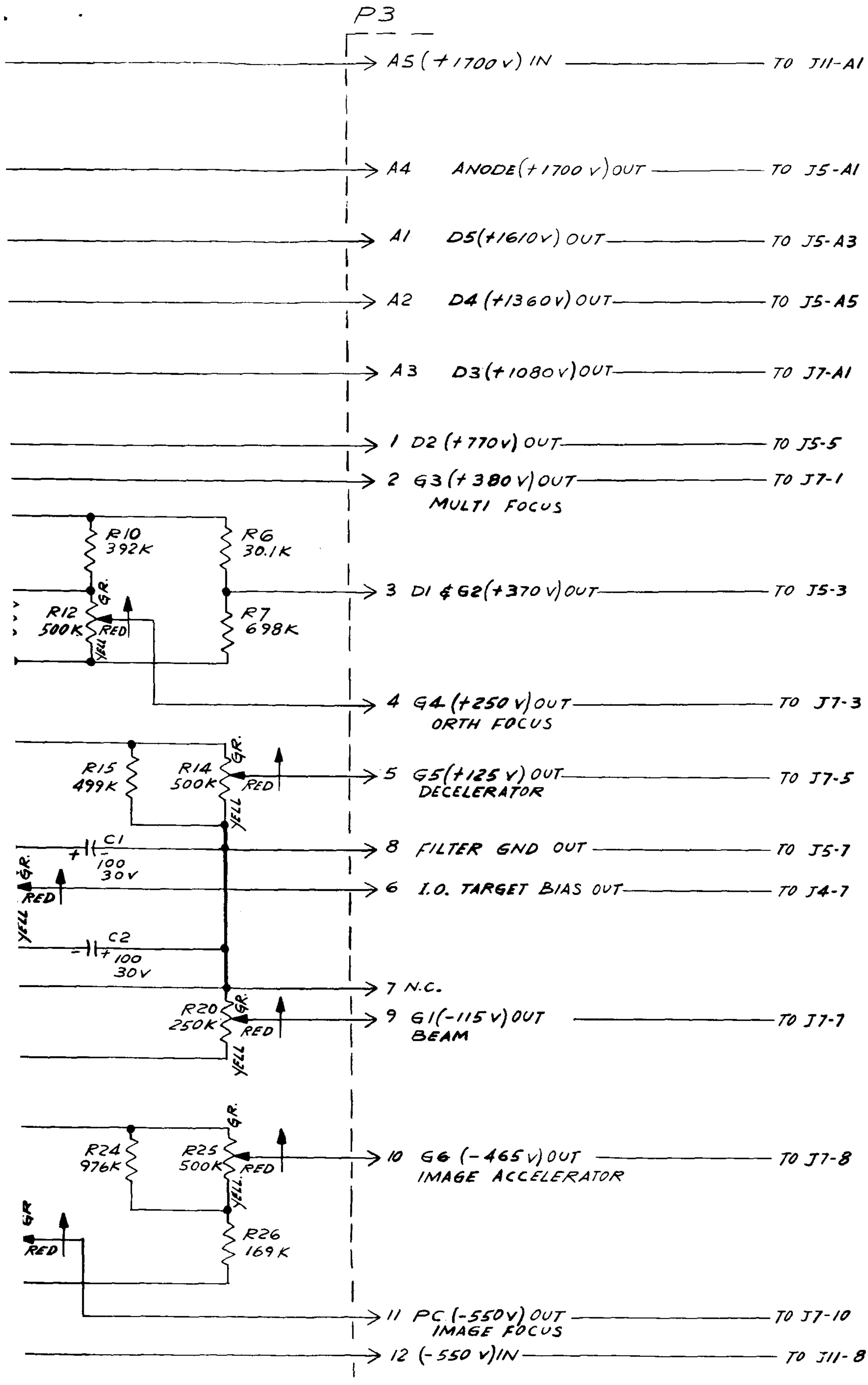
P3
A5 (+1700 v) IN — TO J11-A1
A4 ANODE (+1700 v) OUT — TO J5-A1
A1 D5 (+1610 v) OUT — TO J5-A3
A2 D4 (+1360 v) OUT — TO J5-A5
A3 D3 (+1080 v) OUT — TO J7-A1
1 D2 (+770 v) OUT — TO J5-5
2 G3 (+380 v) OUT — TO J7-1
MULTI FOCUS
R10 392K
R6 30.1K
3 D1 & G2 (+370 v) OUT — TO J5-3
R12 500K
GR.
RED
YELL
R7 698K
4 G4 (+250 v) OUT — TO J7-3
ORTH FOCUS
R15 499K
R14 500K
5 G5 (+125 v) OUT — TO J7-5
DECELERATOR
C1 100 30V
8 FILTER GND OUT — TO J5-7
6 I.O. TARGET BIAS OUT — TO J4-7
C2 100 30V
7 N.C.
R20 250K
9 G1 (-115 v) OUT — TO J7-7
BEAM
R24 976K
R25 500K
10 G6 (-465 v) OUT — TO J7-8
IMAGE ACCELERATOR
R26 169K
11 PC (-550 v) OUT — TO J7-10
IMAGE FOCUS
12 (-550 v) IN — TO J11-8

2

Figure III-6. Bias Bleeder, Schematic Diagram (Circuit Board No. B0P3)

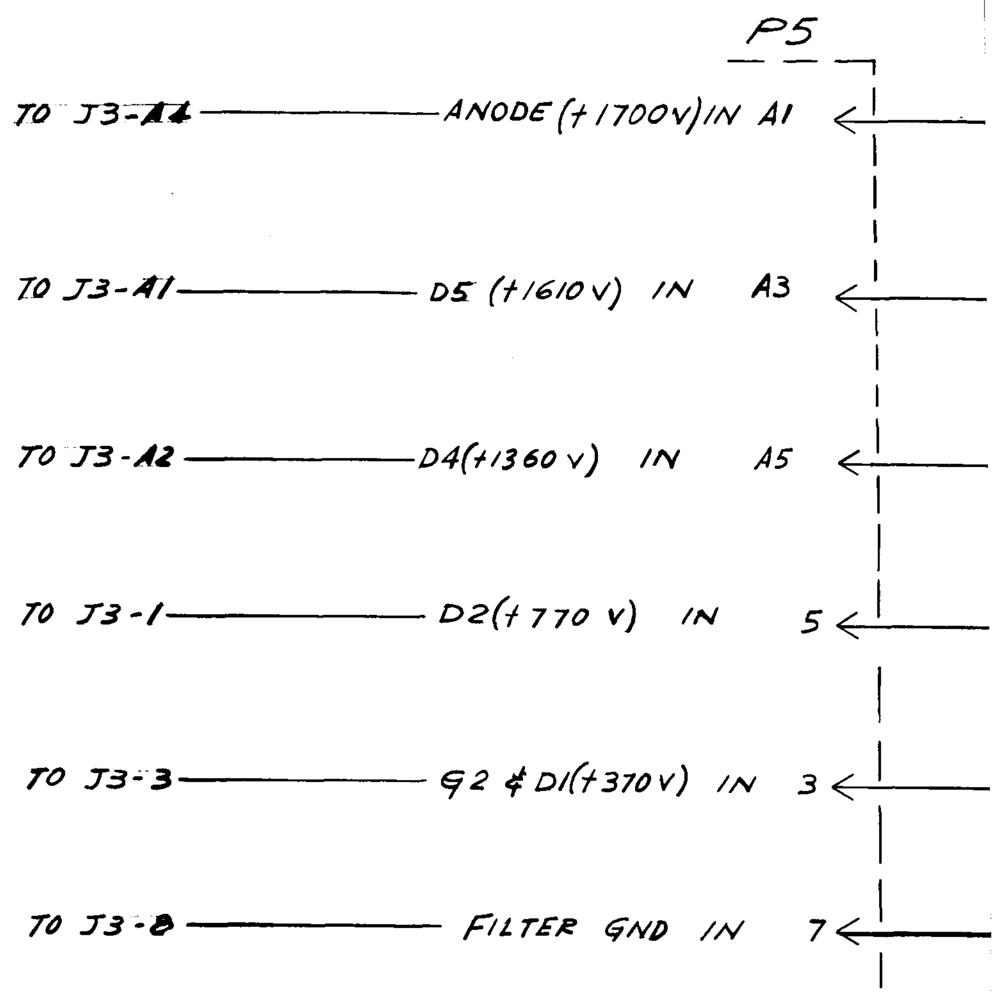

NOTE:

1. VOLTAGES IN PARENTHESES ARE FOR REFERENCE ONLY.

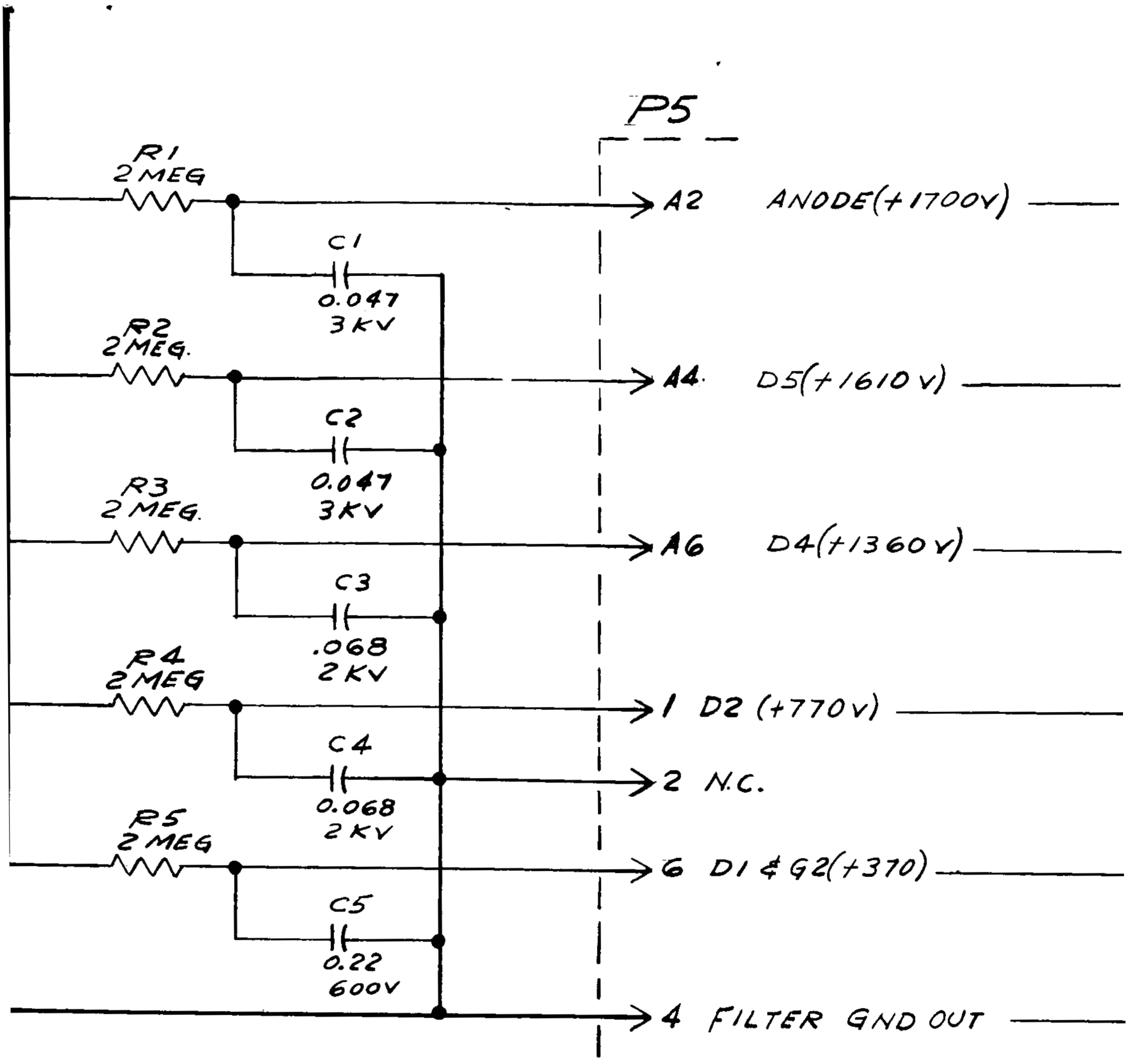
P5
R1
2 MEG
R2
2 MEG.
R3
2 MEG.
R4
2 MEG
R5
2 MEG
C1
0.047
3KV
C2
0.047
3KV
C3
.068
2KV
C4
0.068
2KV
C5
0.22
600V
A2 ANODE(+1700V)
A4 D5(+1610 V)
A6 D4(+1360 V)
1 D2 (+770V)
2 N.C.
6 D1 & G2(+370)
4 FILTER GND OUT

2

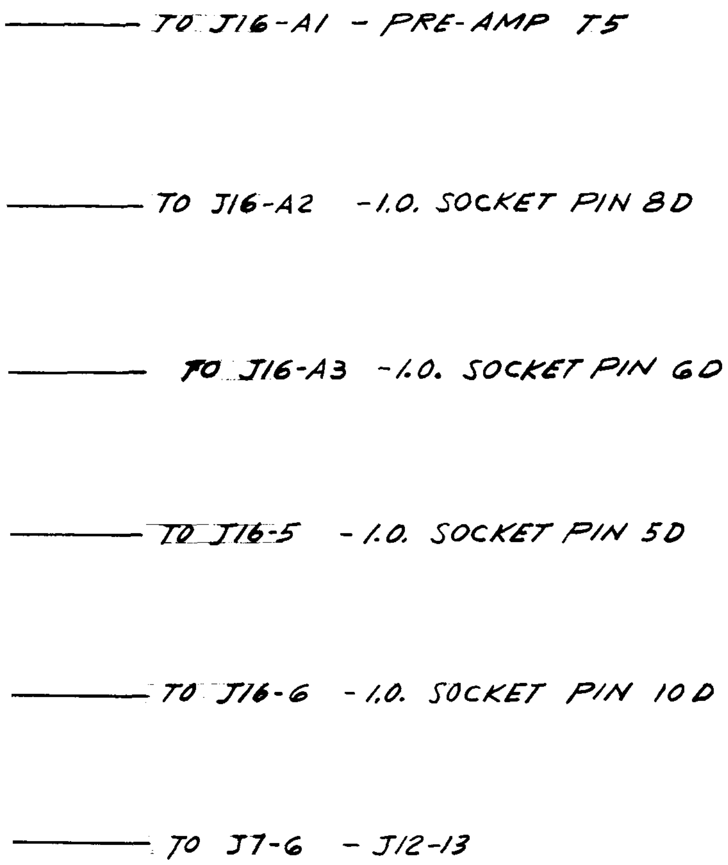

3

Figure III-7. Decoupler No. 1, Schematic Diagram (Circuit Board No. C0P5)

N.C.

TO J3-A3 —— D3(+1080v)IN

TO J3-2 —— G3(+380v) IN

TO J3-4 —— G4 (+250v) IN

TO J3-5 —— G5 (+125v) IN

TO J3-9 —— G1 (-115v) IN

TO J3-10 —— G6 (-465v) IN

TO J3-11 —— P.C. (-550v) IN

TO J12-13 —— FILTER GND OUT

TO J11-3 —— FILTER GND (+1700v & -550v

NOTE:
1. VOLTAGES IN PARENTHESES ARE FOR REFERENCE ONLY.

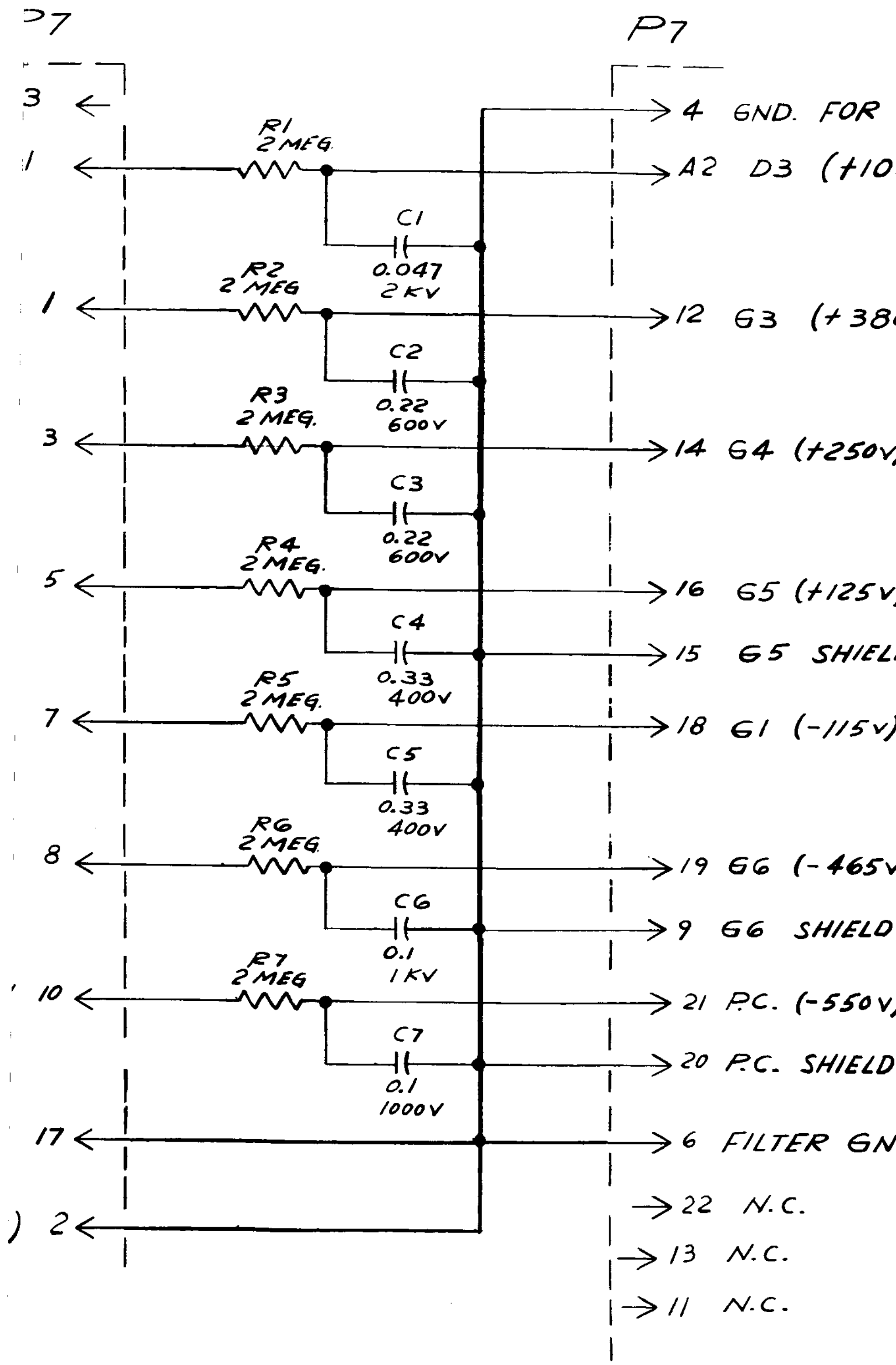
P7
P7
4 GND. FOR
A2 D3 (+10
R1
2 MEG.
C1
0.047
2KV
R2
2 MEG
12 G3 (+38
C2
0.22
600V
R3
2 MEG.
14 G4 (+250V
C3
0.22
600V
R4
2 MEG.
16 G5 (+125V
C4
0.33
400V
15 G5 SHIEL
R5
2 MEG.
18 G1 (-115V)
C5
0.33
400V
R6
2 MEG
19 G6 (-465V
C6
0.1
1KV
9 G6 SHIELD
R7
2 MEG
21 P.C. (-550V
C7
0.1
1000V
20 P.C. SHIELD
6 FILTER GN
22 N.C.
13 N.C.
11 N.C.
3
1
1
3
5
7
8
10
17
2

2

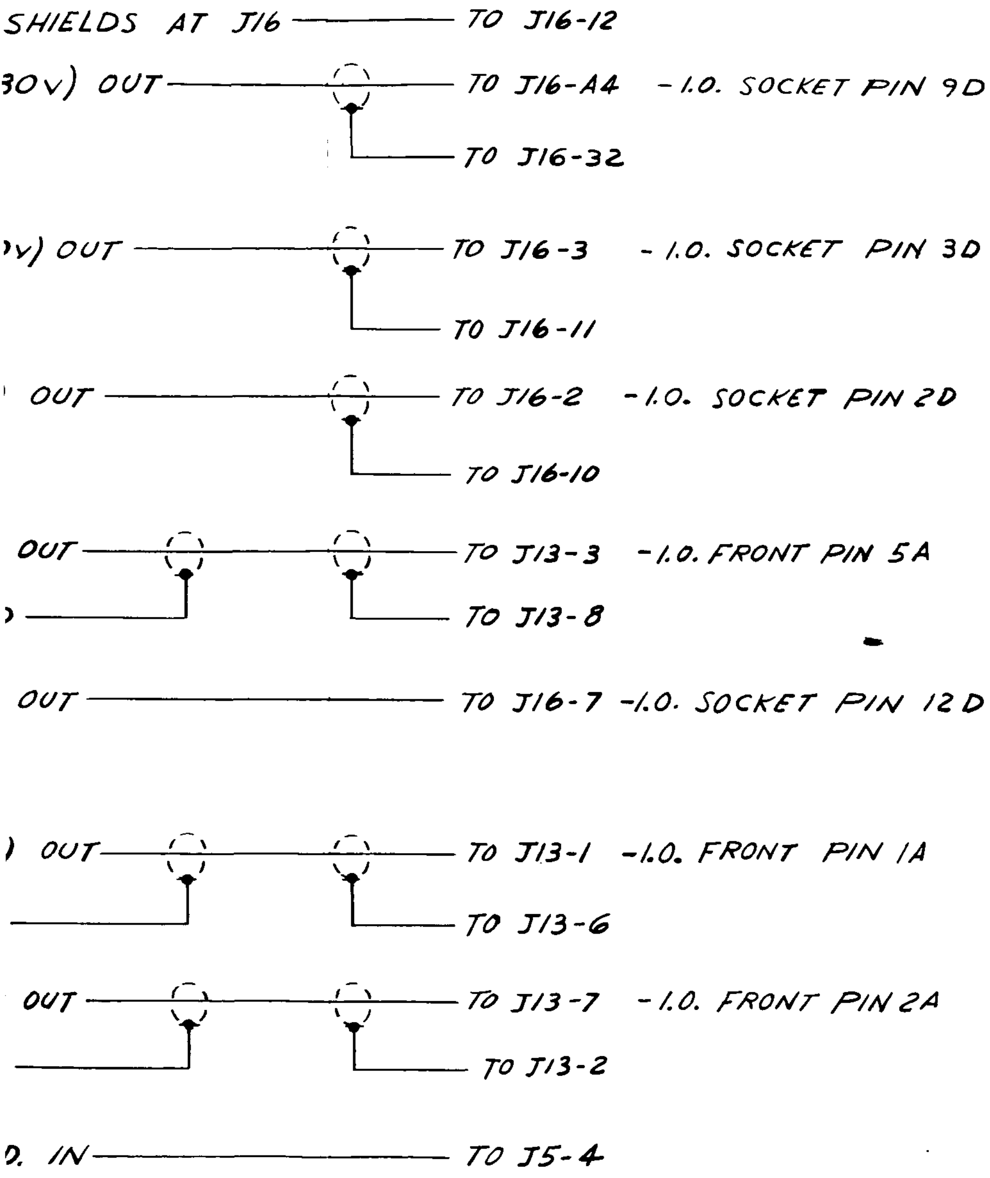

3

Figure III-8. Decoupler No. 2, Schematic Diagram (Circuit Board No. D0P7)

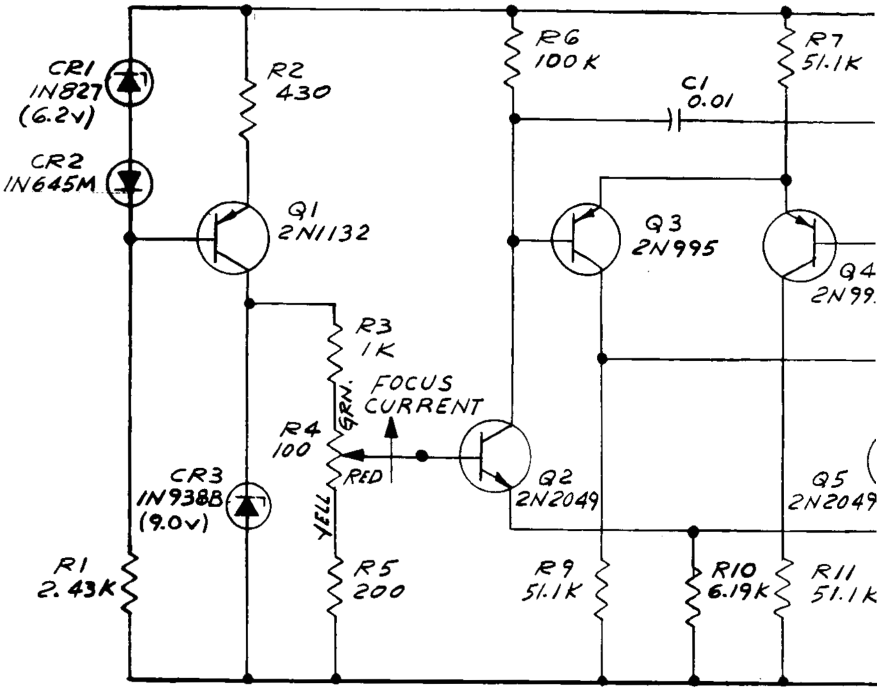
CR1
1N827
(6.2v)
CR2
1N645M
R2
430
Q1
2N1132
R3
1K
FOCUS
CURRENT
R4
100
GRN.
RED
YELL
CR3
1N938B
(9.0v)
R1
2.43K
R5
200
R6
100K
C1
0.01
Q3
2N995
Q2
2N2049
R9
51.1K
R10
6.19K
R7
51.1K
Q5
2N2049
R11

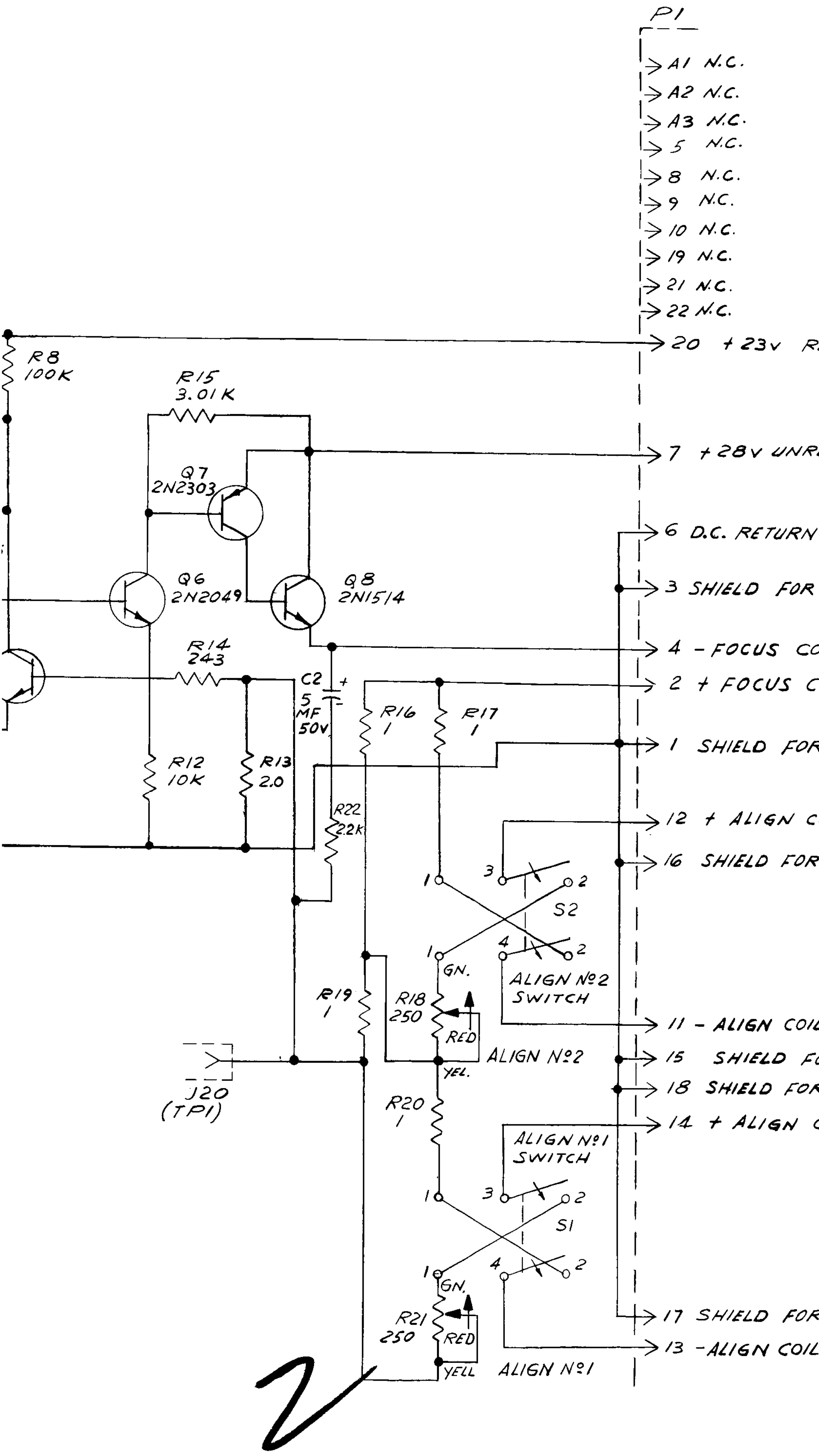

P1
A1 N.C.
A2 N.C.
A3 N.C.
5 N.C.
8 N.C.
9 N.C.
10 N.C.
19 N.C.
21 N.C.
22 N.C.
20 +23V
7 +28V
6 D.C. RETURN
3 SHIELD FOR
4 - FOCUS
2 + FOCUS
1 SHIELD FOR
12 + ALIGN
16 SHIELD FOR
11 - ALIGN COIL
15 SHIELD
18 SHIELD FOR
14 + ALIGN
17 SHIELD FOR
13 -ALIGN COIL
R8 100K
R15 3.01K
Q7 2N2303
Q6 2N2049
Q8 2N1514
R14 243
C2 5 MF 50V
R16 1
R17 1
R12 10K
R13 2.0
R22 2.2K
S2
ALIGN Nº2 SWITCH
R19 1
R18 250
GN.
RED
YEL.
ALIGN Nº2
J20 (TP1)
R20 1
ALIGN Nº1 SWITCH
S1
R21 250
GN.
RED
YELL
ALIGN Nº1
2

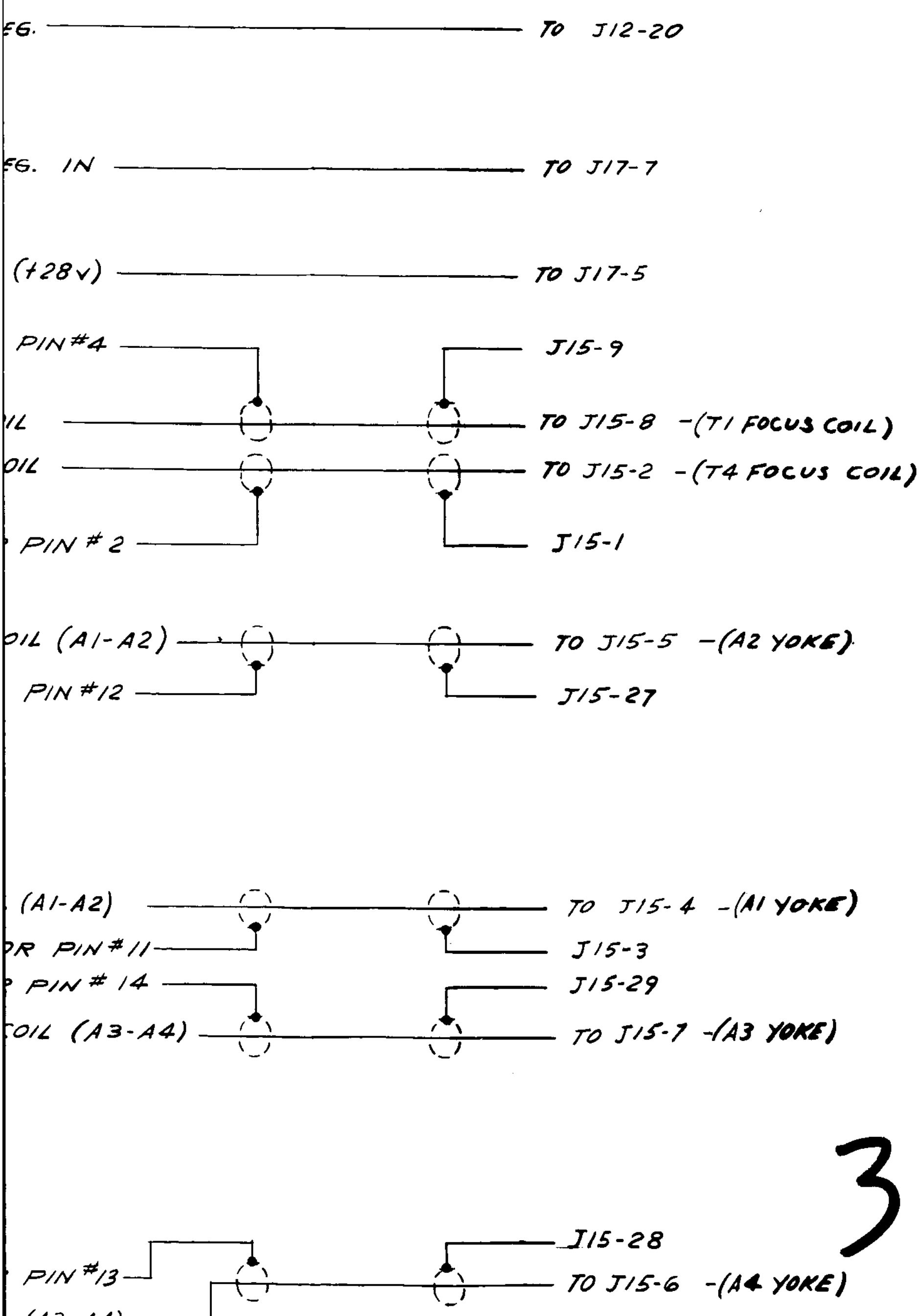

Figure III-9. Focus Current Regulator, Schematic Diagram (Circuit Board No. A0P1)

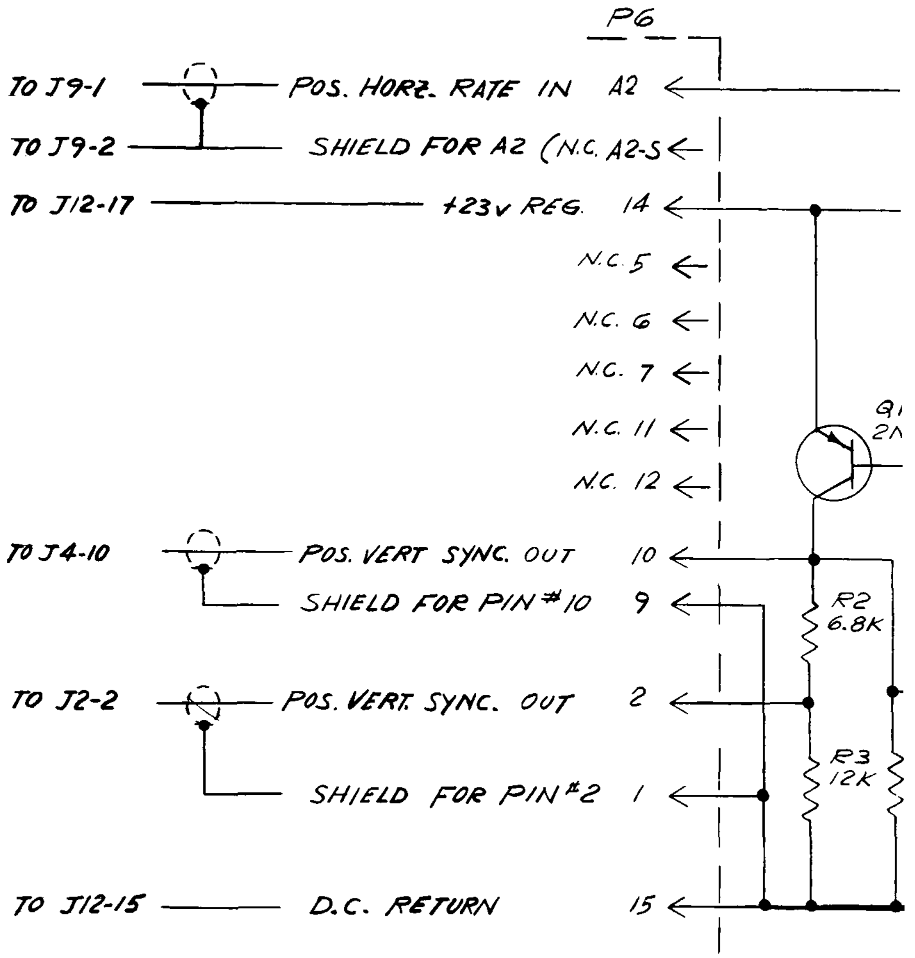
P6
TO J9-1
POS. HORZ. RATE IN
A2
TO J9-2
SHIELD FOR A2 (N.C. A2-S
TO J12-17
+23v REG.
14
N.C. 5
N.C. 6
N.C. 7
N.C. 11
N.C. 12
TO J4-10
POS. VERT SYNC. OUT
10
SHIELD FOR PIN #10
9
R2
6.8K
TO J2-2
POS. VERT. SYNC. OUT
2
R3
12K
SHIELD FOR PIN #2
1
TO J12-15
D.C. RETURN
15

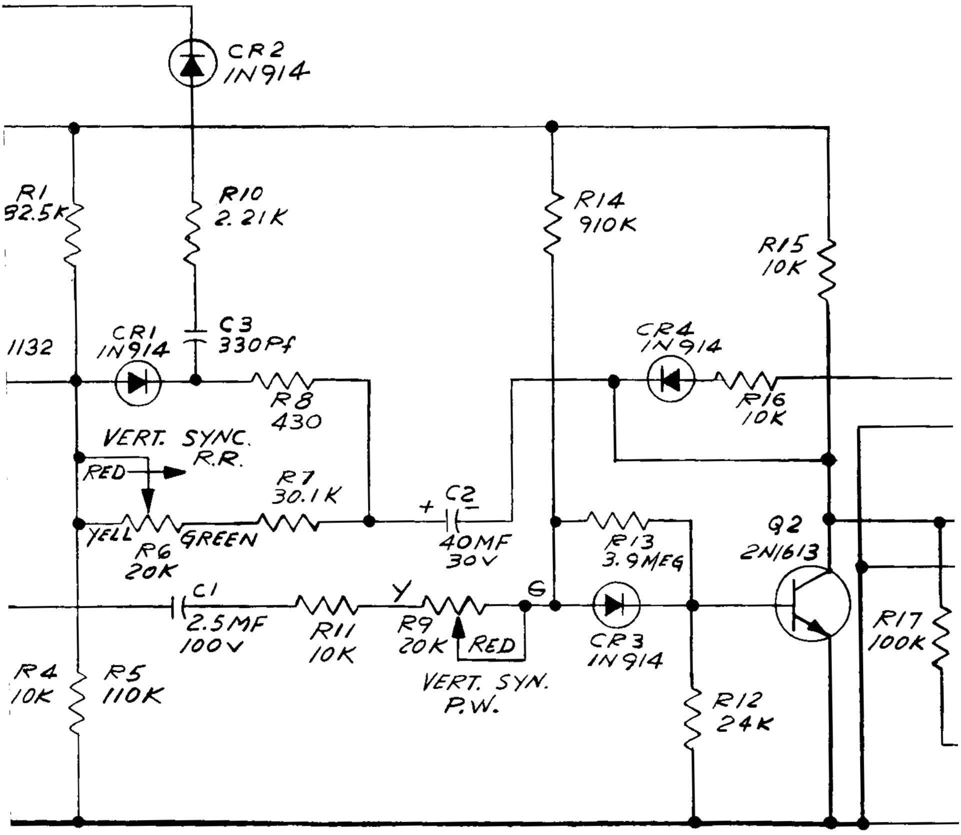
CR2
1N914
R1
32.5K
R10
2.21K
R14
910K
R15
10K
1132
CR1
1N914
C3
330Pf
CR4
1N914
R8
430
R16
10K
VERT. SYNC.
R.R.
RED
R7
30.1K
+ C2 -
Q2
2N1613
YELL
R6
20K
GREEN
40MF
30V
R13
3.9MEG
C1
2.5MF
100V
R11
10K
Y
R9
20K
RED
G
CR3
1N914
R17
100K
R4
10K
R5
110K
VERT. SYN.
P.W.
R12
24K

2

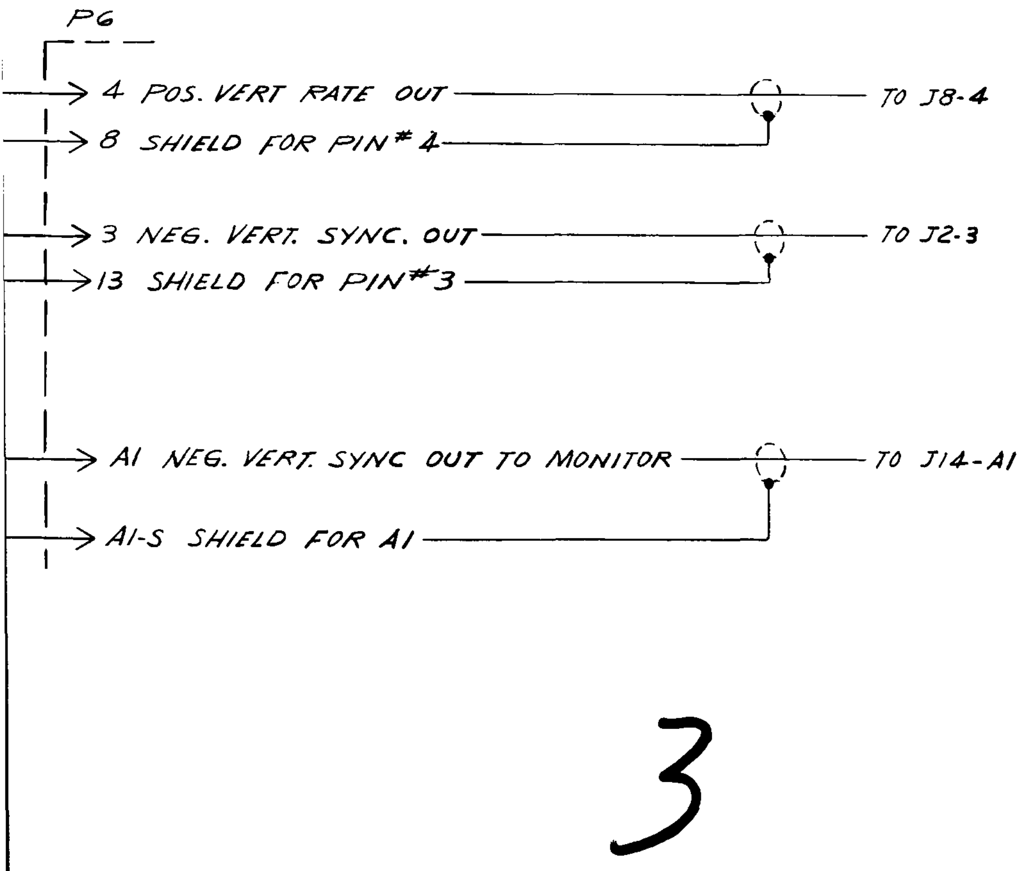

Figure III-10. Vertical Rate Generator, Schematic Diagram (Circuit Board No. C1P6)

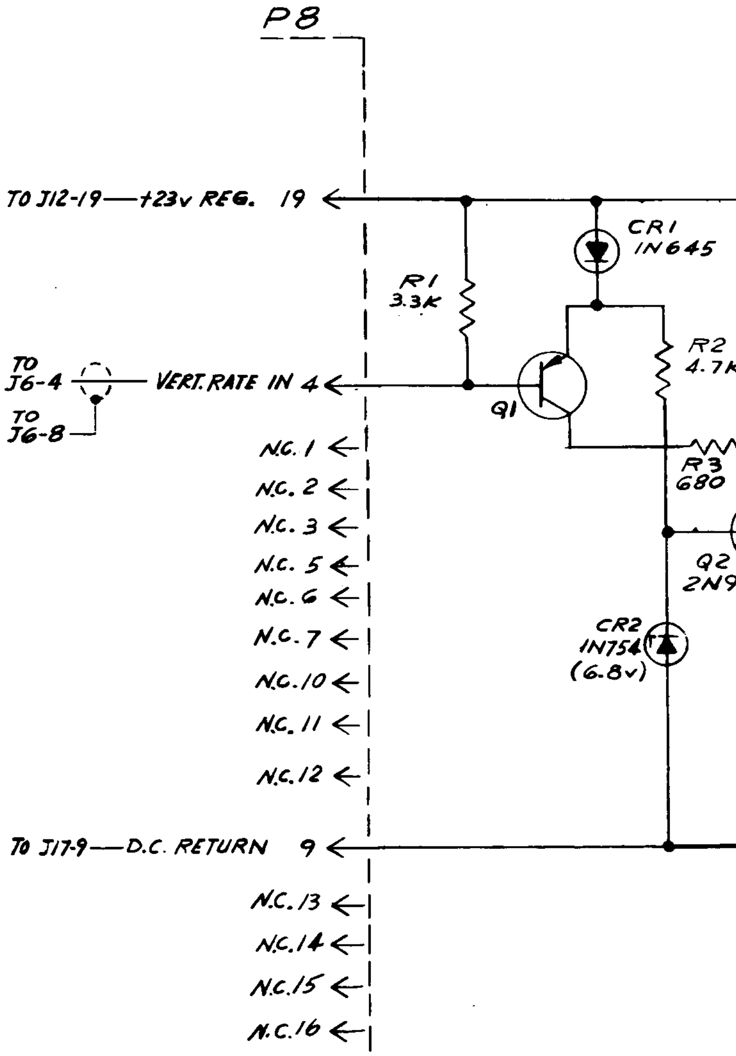

P8
TO J12-19 — +23v REG. 19
CR1
1N645
R1
3.3K
R2
4.7K
TO
J6-4
TO
J6-8
VERT. RATE IN 4
Q1
N.C. 1
N.C. 2
N.C. 3
N.C. 5
N.C. 6
N.C. 7
N.C. 10
N.C. 11
N.C. 12
R3
680
Q2
CR2
1N754
(6.8v)
TO J17-9 — D.C. RETURN 9
N.C. 13
N.C. 14
N.C. 15
N.C. 16

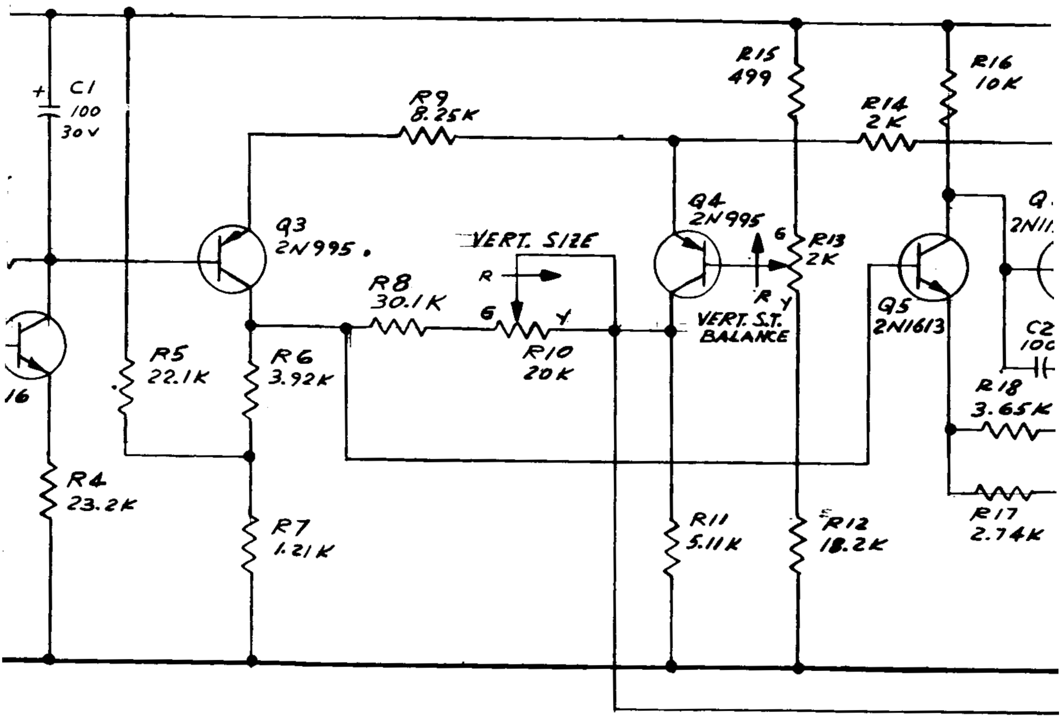
C1
100
30v
R9
8.25K
R15
499
R16
10K
R14
2K
Q3
2N995
Q4
2N995
VERT. SIZE
R
G
Y
R8
30.1K
R10
20K
R13
2K
VERT. S.T. BALANCE
Q5
2N1613
R5
22.1K
R6
3.92K
R4
23.2K
R7
1.21K
R11
5.11K
R12
18.2K
R18
3.65K
R17
2.74K

2

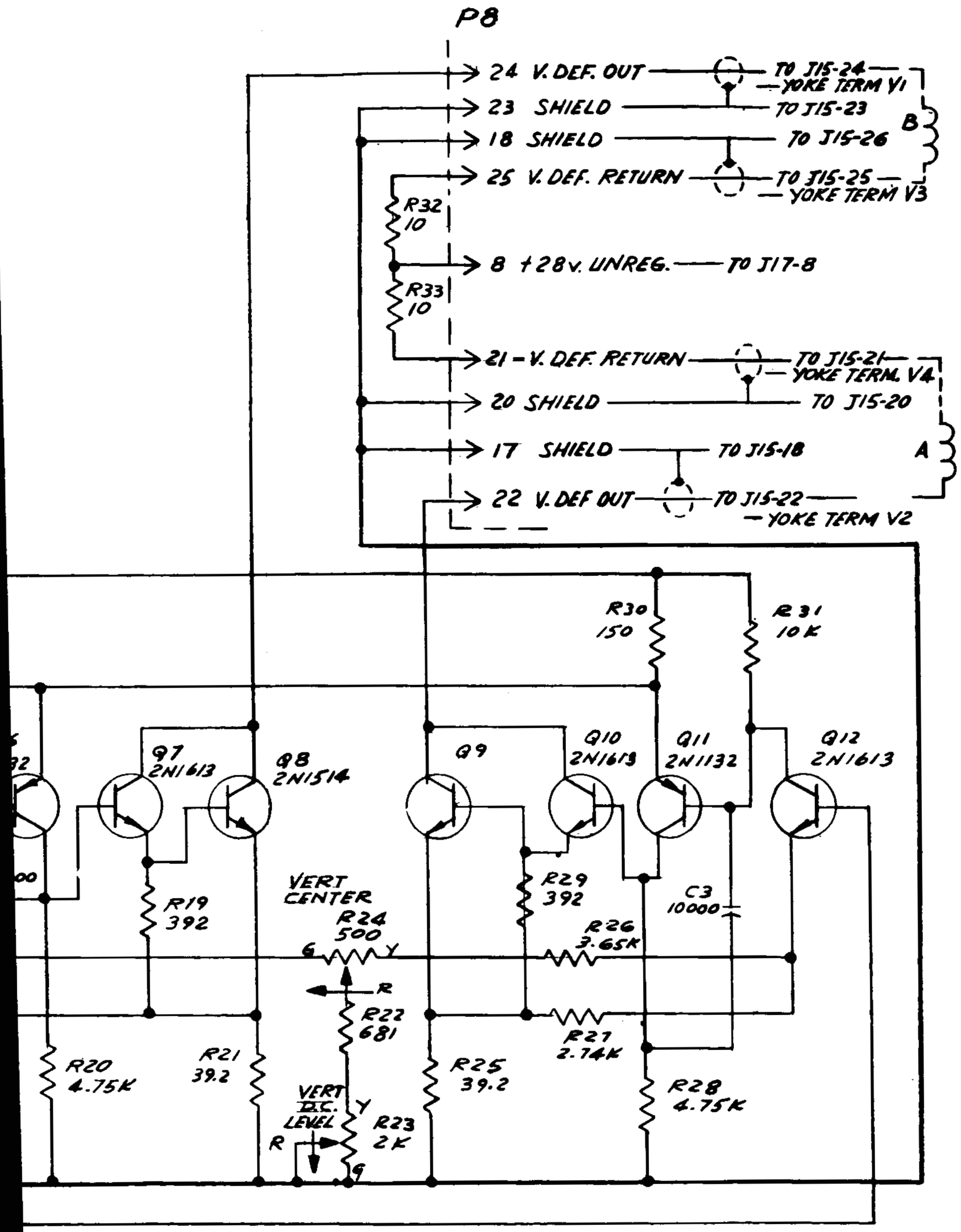

Figure III-11. Vertical Sawtooth Generator & Deflection Amplifier, Schematic Diagram (Circuit Board No. D1P8)

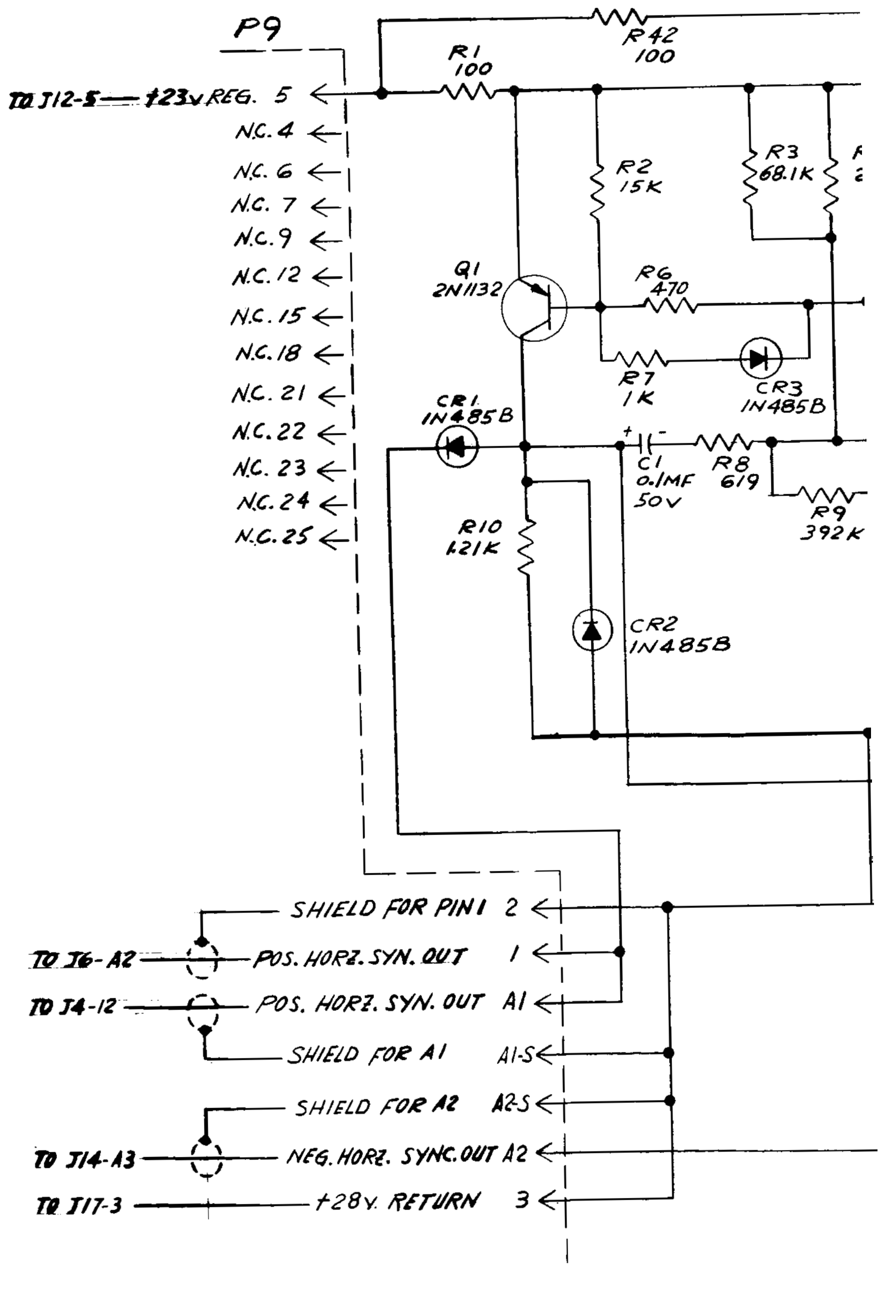
P9
TO J12-5 — +23V REG. 5
N.C. 4
N.C. 6
N.C. 7
N.C. 9
N.C. 12
N.C. 15
N.C. 18
N.C. 21
N.C. 22
N.C. 23
N.C. 24
N.C. 25
R42 100
R1 100
R2 15K
R3 68.1K
Q1 2N1132
R6 470
R7 1K
CR3 1N485B
CR1 1N485B
C1 0.1MF 50V
R8 619
R9 392K
R10 1.21K
CR2 1N485B
SHIELD FOR PIN 1 2
TO J6-A2 POS. HORZ. SYN. OUT 1
TO J4-12 POS. HORZ. SYN. OUT A1
SHIELD FOR A1 A1-S
SHIELD FOR A2 A2-S
TO J14-A3 NEG. HORZ. SYNC. OUT A2
TO J17-3 +28V. RETURN 3

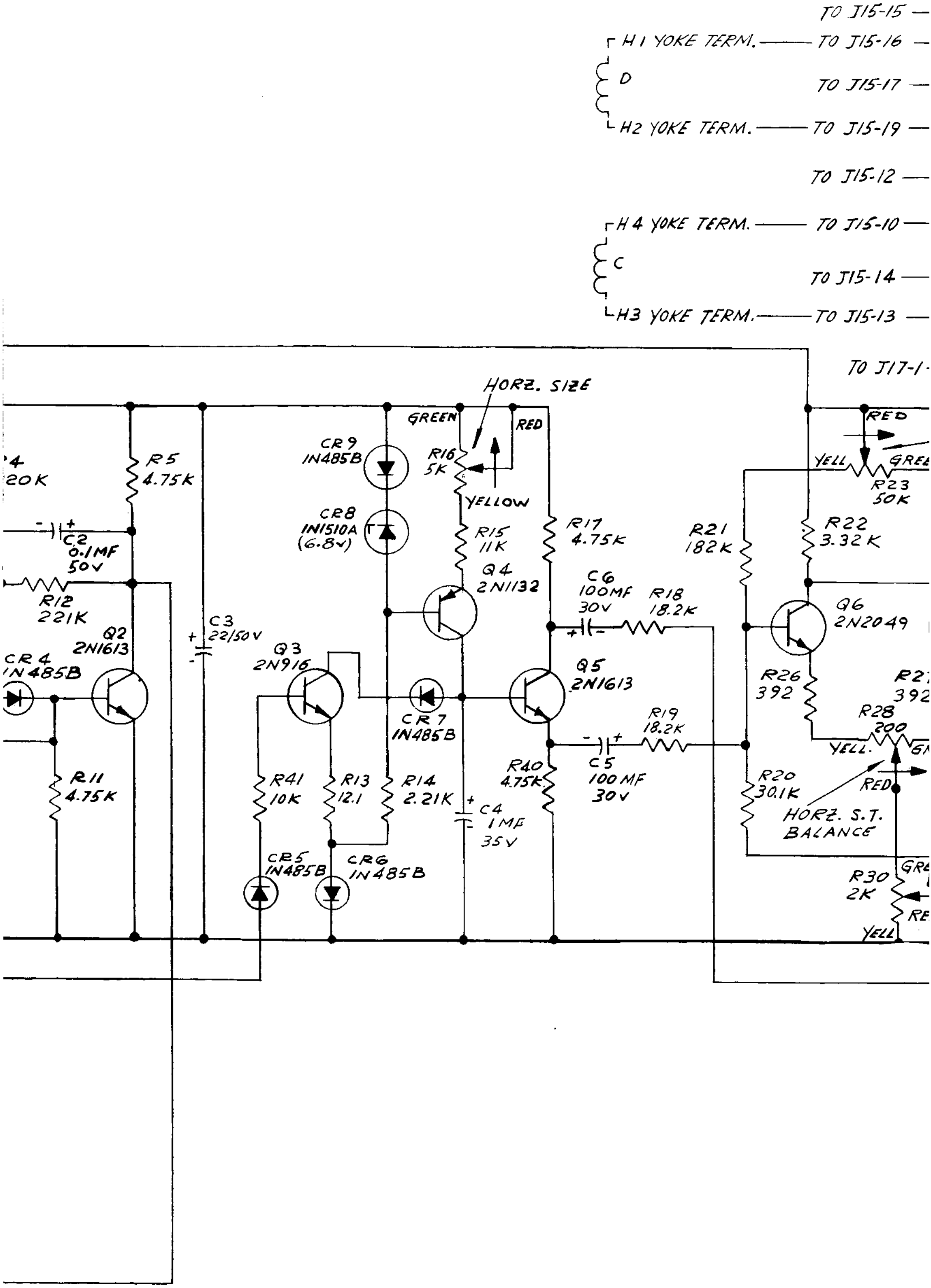
TO J15-15
H1 YOKE TERM.
TO J15-16
D
TO J15-17
H2 YOKE TERM.
TO J15-19
TO J15-12
H4 YOKE TERM.
TO J15-10
C
TO J15-14
H3 YOKE TERM.
TO J15-13
TO J17-1
HORZ. SIZE
GREEN
RED
YELLOW
R5 4.75K
C2 0.1MF 50V
R12 221K
Q2 2N1613
CR4 1N485B
R11 4.75K
C3 22/50V
CR9 1N485B
CR8 1N1510A (6.8V)
R16 5K
R15 11K
Q4 2N1132
R17 4.75K
Q3 2N916
CR7 1N485B
Q5 2N1613
R41 10K
R13 12.1
R14 2.21K
C4 1MF 35V
CR5 1N485B
CR6 1N485B
R40 4.75K
C6 100MF 30V
R18 18.2K
C5 100MF 30V
R19 18.2K
R21 182K
R22 3.32K
R23 50K
Q6 2N2049
R26 392
R28 200
R20 30.1K
HORZ. S.T. BALANCE
R30 2K
YELL

2

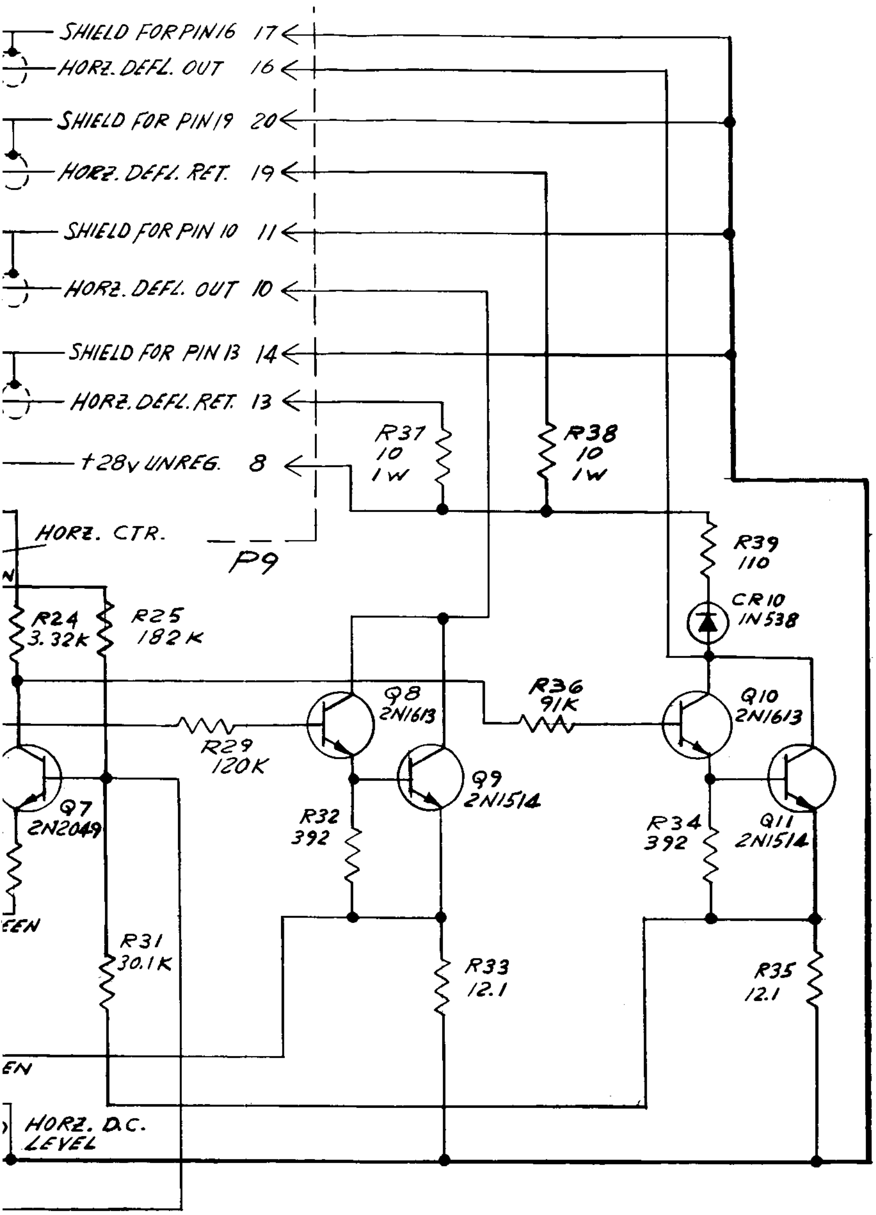

Figure III-12. Horizontal Rate Generator, Sawtooth Generator, & Deflection Amplifier, Schematic Diagram (Circuit Board No. E0P9)

3

REFERENCE- MECHANICAL

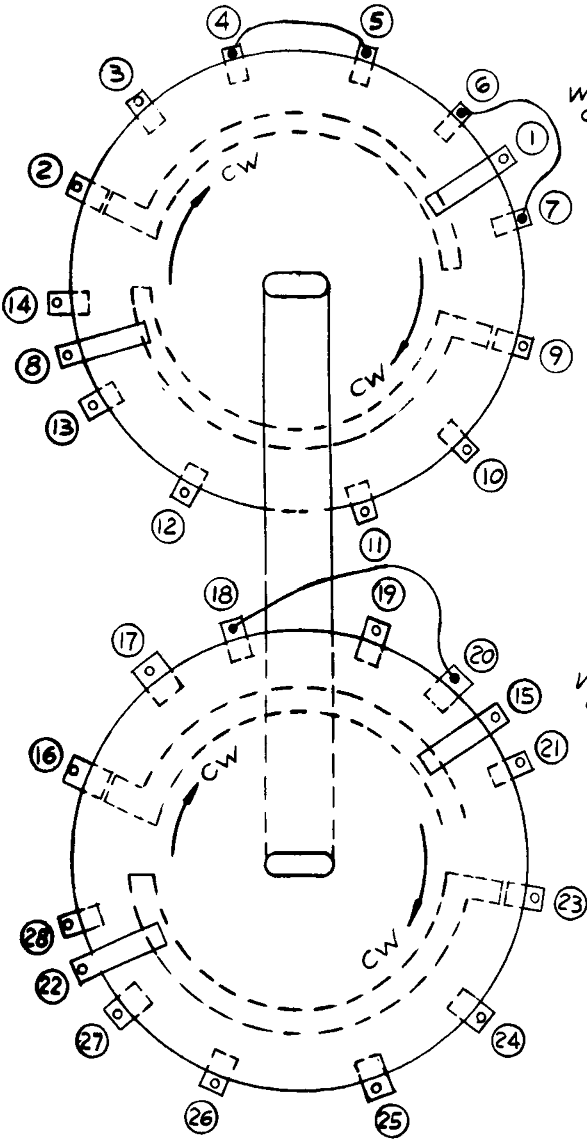

SWITCH VIEWED FROM FRONT (KNOB

PROGRAMMER SWITC

FIG.- 1

UTLINE

DECK-1

PER SHOWN IN FULL
CW POSITION

DECK-2

IPER SHOWN IN FULL
CW POSITION

ND OF SHAFT)

H

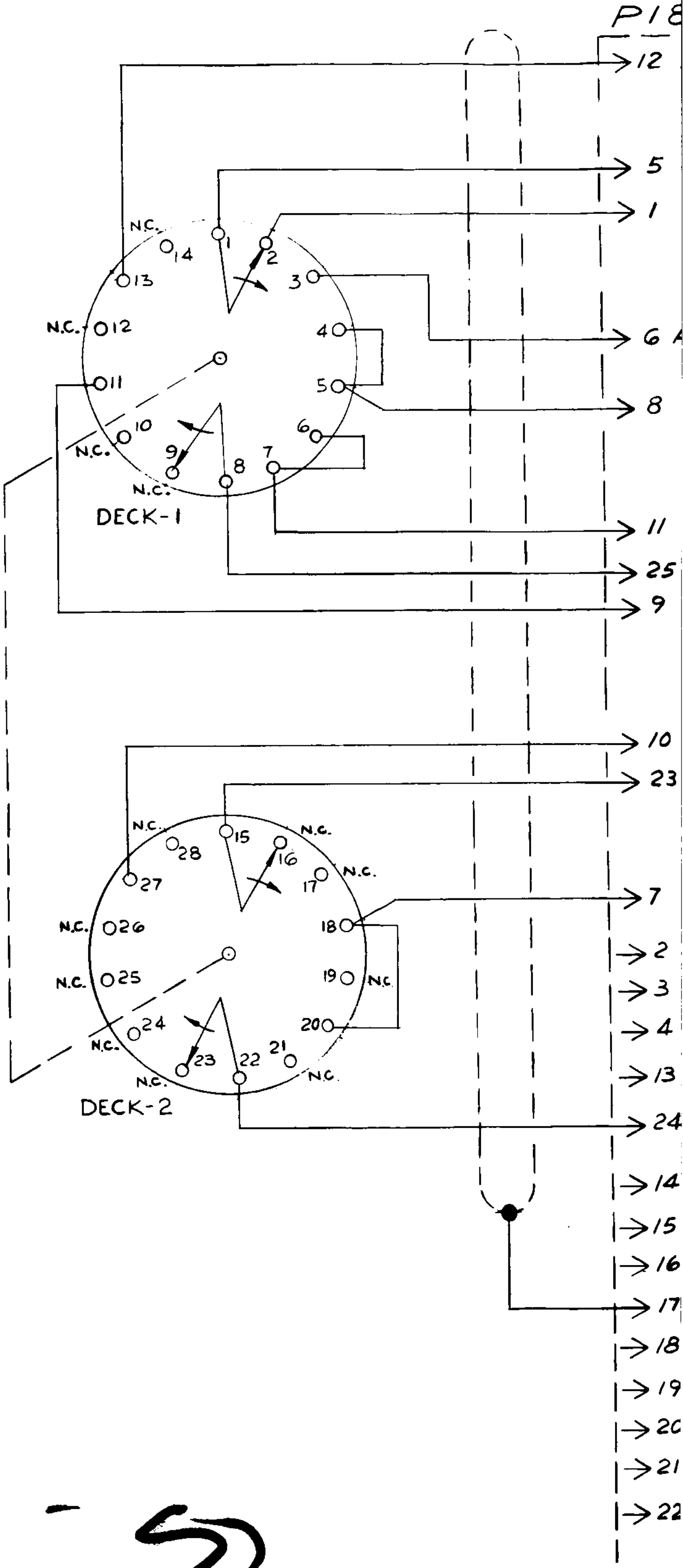

52

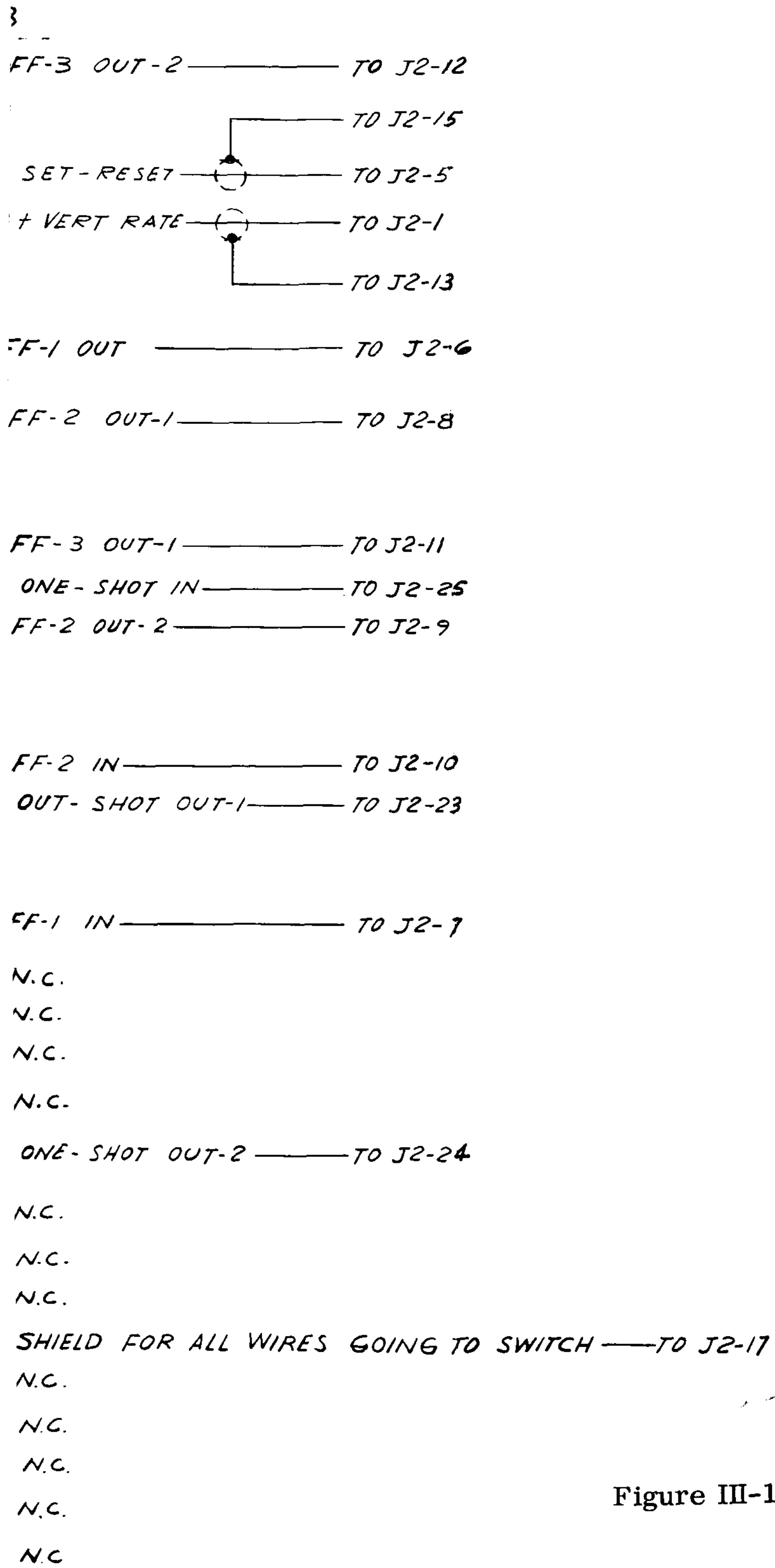

3

Figure III-13. Integration Selector Switch, Schematic Diagram

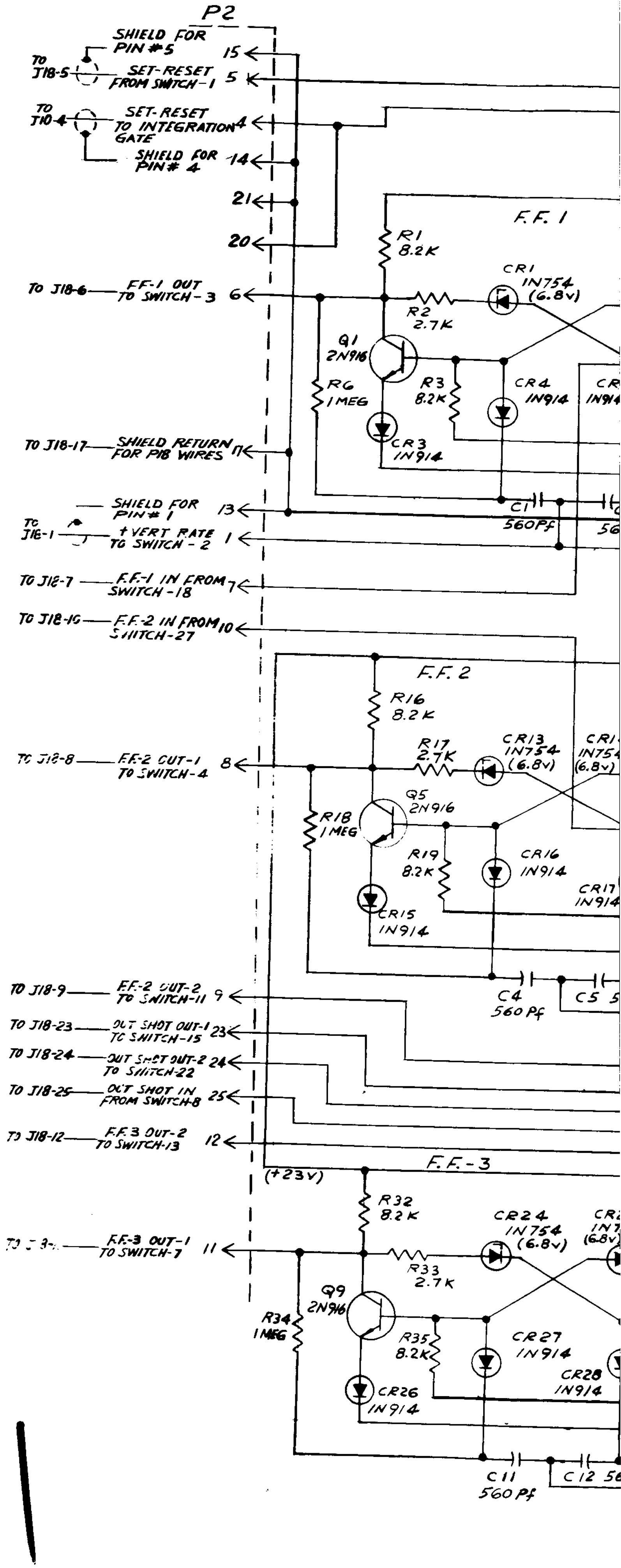

P2
SHIELD FOR PIN #5
TO J18-5
SET-RESET FROM SWITCH-1
TO J10-4
SET-RESET TO INTEGRATION GATE
SHIELD FOR PIN # 4
F.F. 1
R1 8.2K
CR1 1N754 (6.8v)
TO J18-6
FF-1 OUT TO SWITCH-3
R2 2.7K
Q1 2N916
R6 1MEG
R3 8.2K
CR4 1N914
CR3 1N914
TO J18-17
SHIELD RETURN FOR P18 WIRES
SHIELD FOR PIN # 1
C1 560Pf
+VERT RATE TO SWITCH-2
TO J18-7
F.F.-1 IN FROM SWITCH-18
TO J18-10
F.F.-2 IN FROM SWITCH-27
F.F. 2
R16 8.2K
R17 2.7K
CR13 1N754 (6.8v)
TO J18-8
F.F.-2 OUT-1 TO SWITCH-4
Q5 2N916
R18 1MEG
R19 8.2K
CR16 1N914
CR15 1N914
TO J18-9
F.F.-2 OUT-2 TO SWITCH-11
C4 560 Pf
TO J18-23
OUT SHOT OUT-1 TO SWITCH-15
TO J18-24
OUT SHOT OUT-2 TO SWITCH-22
TO J18-25
OUT SHOT IN FROM SWITCH-8
TO J18-12
F.F.3 OUT-2 TO SWITCH-13
F.F.-3
(+23V)
R32 8.2K
CR24 1N754 (6.8v)
F.F.-3 OUT-1 TO SWITCH-7
R33 2.7K
Q9 2N916
R34 1MEG
R35 8.2K
CR27 1N914
CR28 1N914
CR26 1N914
C11 560Pf

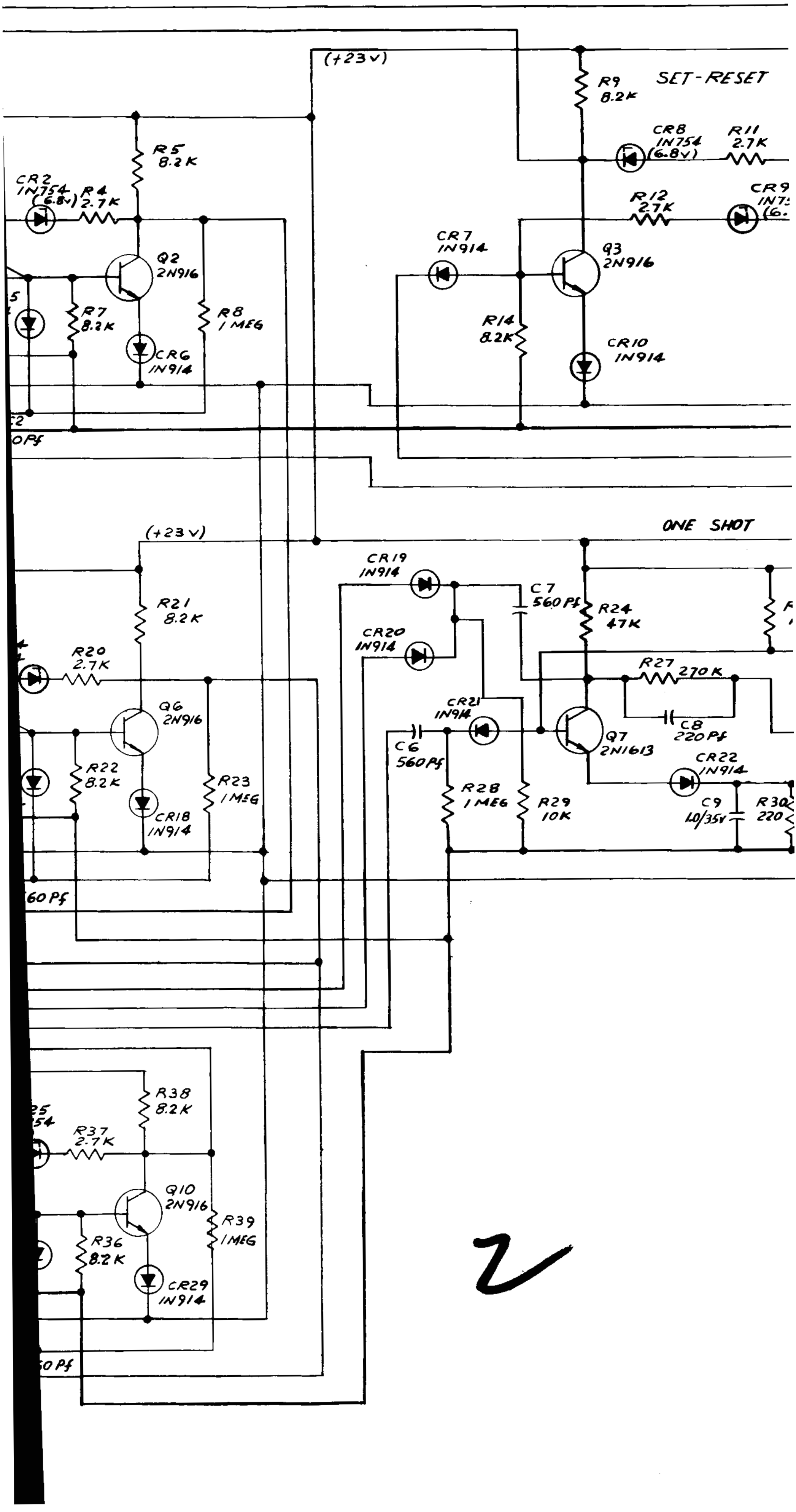

(+23V)
R9 8.2K
SET-RESET
CR8 1N754 (6.8V)
R11 2.7K
R5 8.2K
CR2 1N754 (6.8V)
R4 2.7K
R12 2.7K
CR7 1N914
Q2 2N916
Q3 2N916
R7 8.2K
R8 1MEG
R14 8.2K
CR6 1N914
CR10 1N914
(+23V)
ONE SHOT
CR19 1N914
C7 560Pf
R24 47K
R21 8.2K
CR20 1N914
R20 2.7K
R27 270K
Q6 2N916
CR21 1N914
C8 220Pf
C6 560Pf
Q7 2N1613
CR22 1N914
R22 8.2K
R23 1MEG
R28 1MEG
R29 10K
C9 1.0/35V
R30 220
CR18 1N914
R38 8.2K
R37 2.7K
Q10 2N916
R39 1MEG
R36 8.2K
CR29 1N914
2

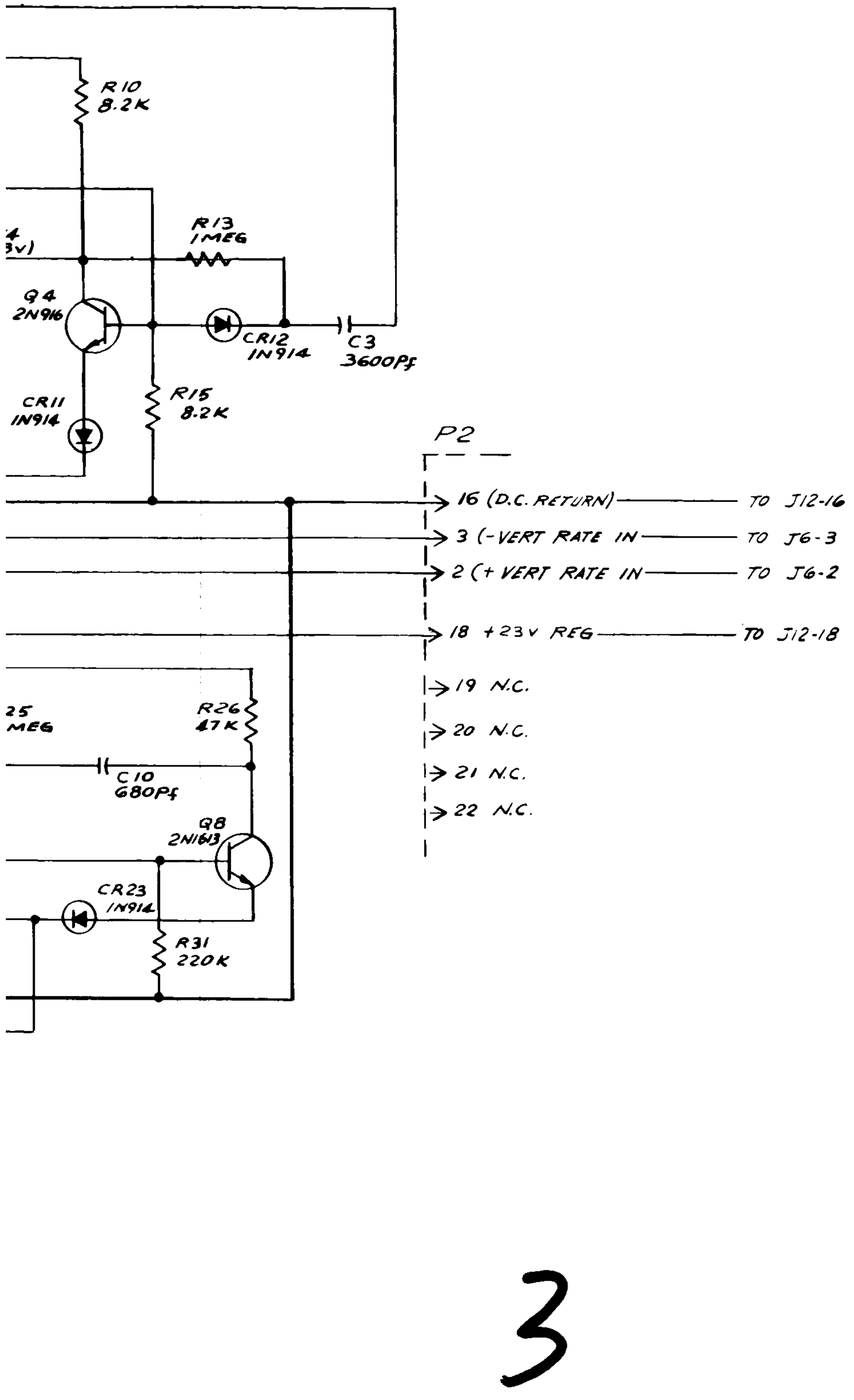

Figure III-14. Programmer, Schematic Diagram (Circuit Board No. A1P2)

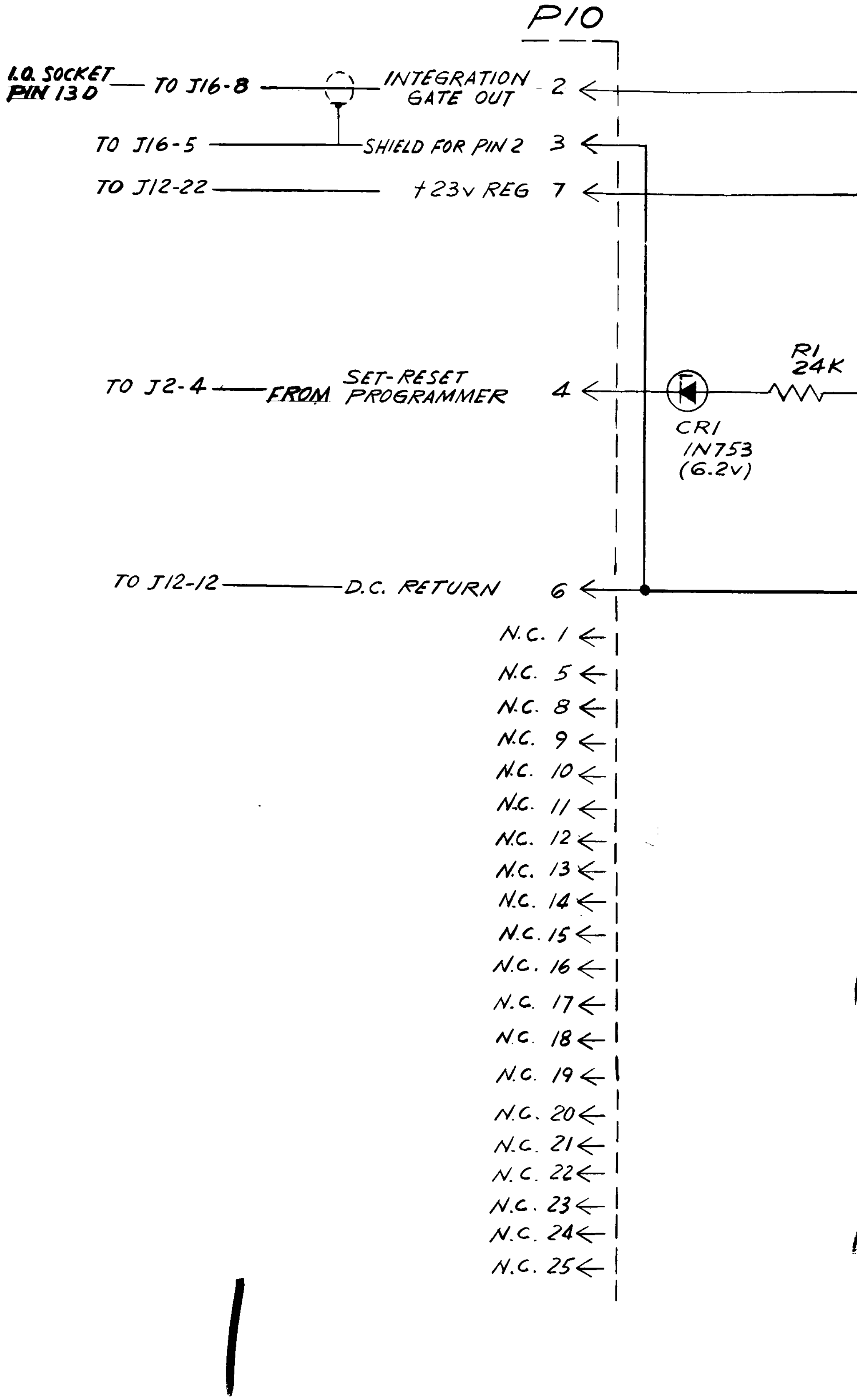
P10
I.O. SOCKET PIN 13 D
TO J16-8
INTEGRATION GATE OUT
2
TO J16-5
SHIELD FOR PIN 2
3
TO J12-22
+23v REG
7
TO J2-4
FROM
SET-RESET PROGRAMMER
4
R1 24K
CR1 1N753 (6.2v)
TO J12-12
D.C. RETURN
6
N.C. 1
N.C. 5
N.C. 8
N.C. 9
N.C. 10
N.C. 11
N.C. 12
N.C. 13
N.C. 14
N.C. 15
N.C. 16
N.C. 17
N.C. 18
N.C. 19
N.C. 20
N.C. 21
N.C. 22
N.C. 23
N.C. 24
N.C. 25

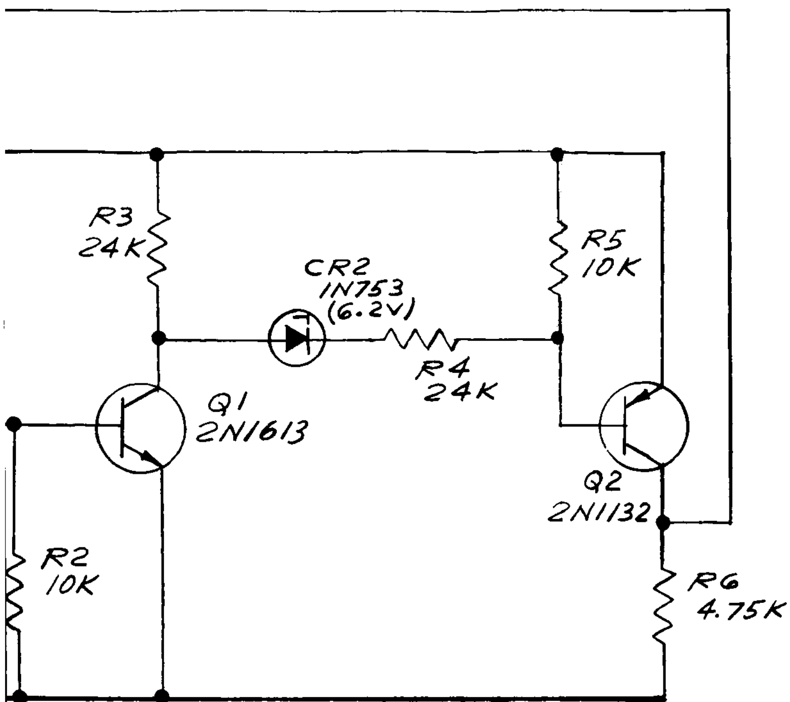

Figure III-15. Integration Gate, Schematic Diagram (Circuit Board No. E1P10)

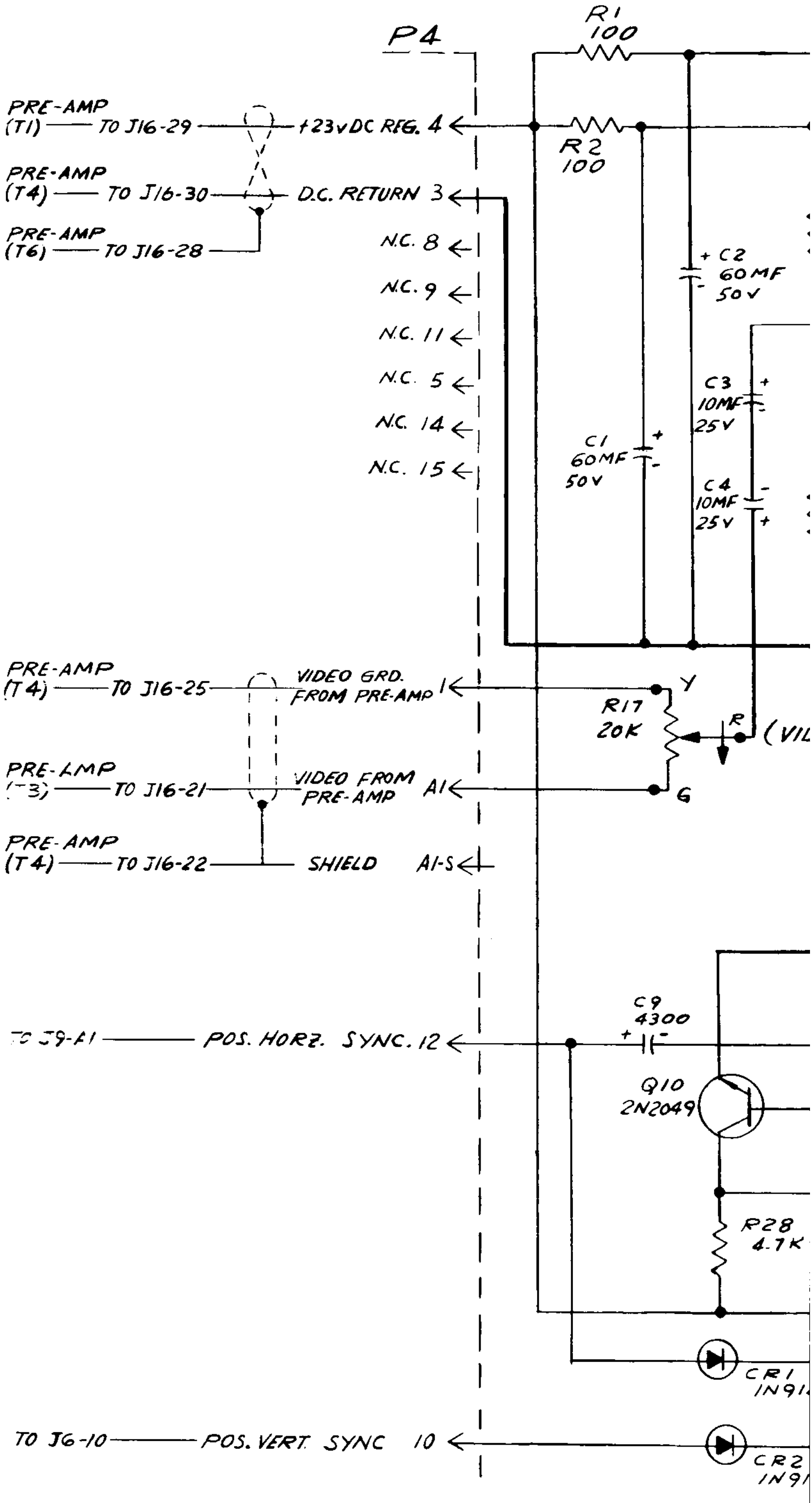
P4
R1
100
R2
100
PRE-AMP
(T1) TO J16-29
+23vDC REG. 4
PRE-AMP
(T4) TO J16-30
D.C. RETURN 3
PRE-AMP
(T6) TO J16-28
N.C. 8
N.C. 9
N.C. 11
N.C. 5
N.C. 14
N.C. 15
C2
60MF
50V
C3
10MF
25V
C1
60MF
50V
C4
10MF
25V
PRE-AMP
(T4) TO J16-25
VIDEO GRD.
FROM PRE-AMP 1
R17
20K
Y
R
G
(VIL
PRE-AMP
TO J16-21
VIDEO FROM
PRE-AMP A1
PRE-AMP
(T4) TO J16-22
SHIELD
A1-S
C9
4300
POS. HORZ. SYNC. 12
Q10
2N2049
R28
4.7K
CR1
1N91
TO J6-10
POS. VERT. SYNC 10
CR2
1N91

1

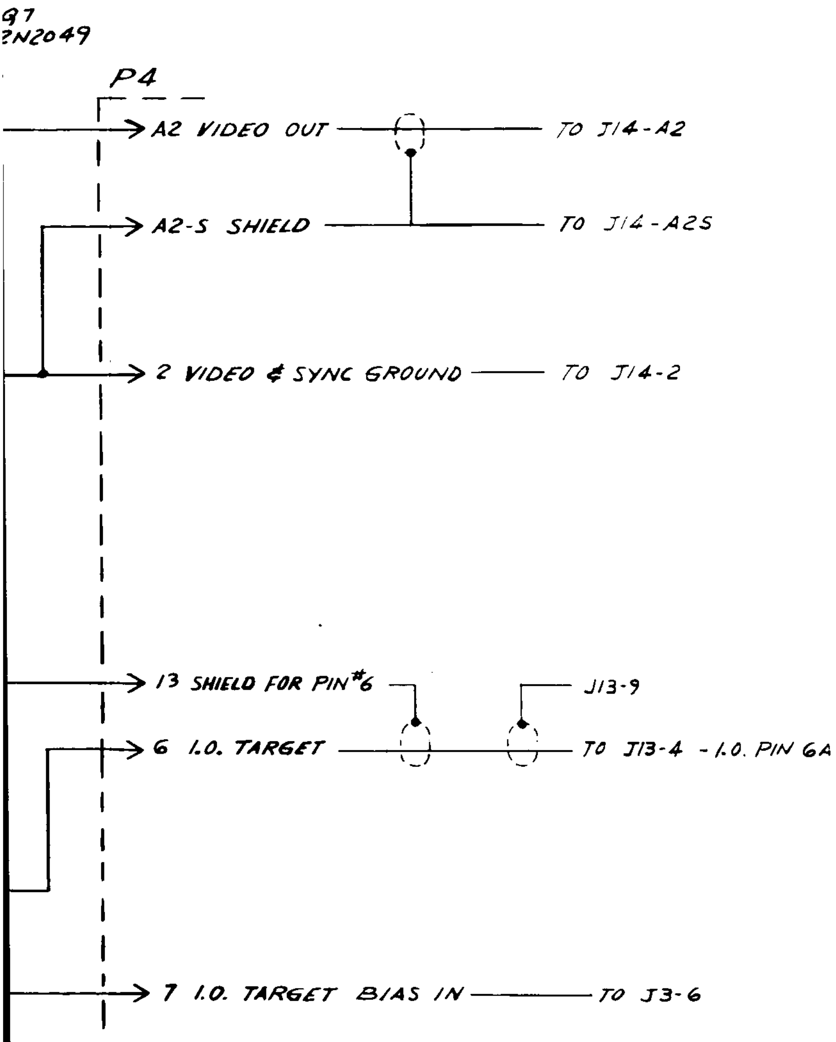

3

Figure III-16. Video Amplifier & Target Blanking, Schematic Diagram (Circuit Board No. B1P4)

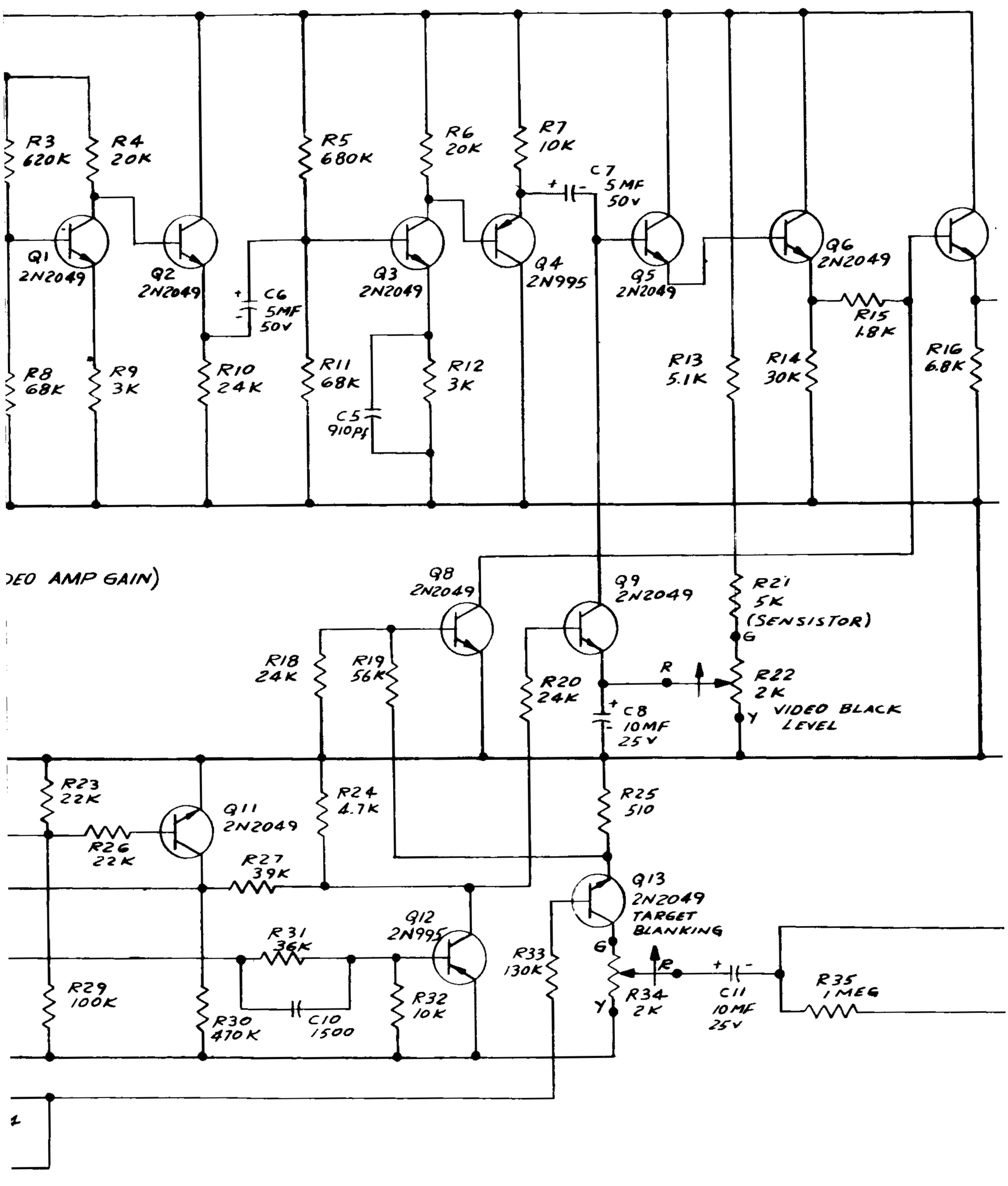
R3
620K
R4
20K
R5
680K
R6
20K
R7
10K
C7
5 MF
50v
Q1
2N2049
Q2
2N2049
Q3
2N2049
Q4
2N995
Q5
2N2049
Q6
2N2049
C6
5MF
50v
R15
1.8K
R8
68K
R9
3K
R10
24K
R11
68K
R12
3K
R13
5.1K
R14
30K
R16
6.8K
C5
910pf
DEO AMP GAIN)
Q8
2N2049
Q9
2N2049
R21
5K
(SENSISTOR)
R18
24K
R19
56K
R20
24K
R22
2K
C8
10MF
25v
VIDEO BLACK
LEVEL
R23
22K
R24
4.7K
R25
510
Q11
2N2049
R26
22K
R27
39K
Q13
2N2049
TARGET
BLANKING
Q12
2N995
R31
36K
R33
130K
R34
2K
C11
10MF
25v
R35
1 MEG
R29
100K
R30
470K
C10
1500
R32
10K
1
4

SECTION IV

ENVIRONMENTAL CONSIDERATIONS

A. GENERAL

The performance of the Javelin rocket launch vehicle was studied to establish environmental launch-condition criteria for the design of the television camera system for the TIGRIS flight model. Although the present contract does not require ruggedization of the camera system to meet any environmental conditions, it does require that the preprototype be of such a design that in a follow-up program, a space-qualified system could be produced with minimum redesign.

A review of the Javelin rocket performance specifications, listed in Tables IV-1 through IV-3 indicated that the camera-system flight-type hardware should be designed as a rigid structure that would allow external vibration isolators if required.

After this study was completed, it was suggested that the new Aero-Bee rocket might be used. The Aero-Bee would reduce the stress levels below those herein considered.

B. ENVIRONMENTAL DESIGN CRITERIA

The following design criteria were established after an analysis of the Javelin rocket environmental test conditions. Note that these values are not applicable to the preprototype model, but are indicative of the requirements for the follow-on prototype model.

1. Acceleration

The expected stress to be exerted on a flight model in the thrust direction is 45 g for a period of one minute. A prototype model would be tested at 50 g for three minutes.

2. Shock

The expected shock stress is expected to be a 206 g peak amplitude 6 millisecond duration sawtooth along the thrust axes and a 66 g peak amplitude 6 millisecond duration sawtooth along the lateral axis.

3. Sinusoidal Vibration

As indicated in Table IV-1, the maximum stress due to sinusoidal vibrations for a flight model is expected to be 14g along the thrust axis and 2.8 g along the lateral axis in the frequency range of 150 to 250 cps. A qualification

TABLE IV-1. SINUSOIDAL VIBRATION TEST REQUIREMENTS

Axis	Frequency Range (cps)	Platform Interface Level (g 0 to peak)		Camera Level (g 0 to peak)		Duration Minute	
		Qualification	Flight	Qualification	Flight	Qualification	Flight
Thrust	10-50	2.3	1.5	2.5	1.6	1.6	4 octaves
	50-150	10.7	7	12.8	8.4	1.6	per minute
	150-250	10.7	7	21.4	14	1.6	2.06
	250-500	10.7	7	6.1	4	1.6	total
	500-2000	21	14	3.1	2.1	1.0	
	2000-3000	54	36	3.8	2.5	0.26	
	3000-5000	21	-	1.3	-	0.34	
Lateral	5-50	0.9	0.6	0.9	0.6	1.6	4 octaves
	50-150	2.1	1.4	2.5	1.7	1.6	per minute
	150-250	2.1	1.4	4.2	2.8	1.6	2.06
	250-500	2.1	1.4	1.2	0.8	1.6	total
	500-2000	4.2	2.8	0.6	0.4	1.0	
	2000-3000	17	11	1.2	0.8	1.0	
	3000-5000	17	-	1.2	-	0.6	

prototype model would be subjected to 21.4g stress along the thrust axis and 4.2g stress along the lateral axis.

As indicated in Table IV-2, during combustion dwell time (approximately a duration of 0.25 second), the stress is expected to be 8.4g along the thrust axis and 1.4g along the lateral axis. A qualification prototype model would be tested at 12.9g and 2.5g respectively in the frequency range of 550 to 650 cps.

4. Random Vibration

The stress due to random vibrations is expected to be 6.0g rms along the thrust axis and 2.56g rms along the lateral axis. A qualification prototype model would be tested at 8.5g rms and 3.6g rms respectively. Refer to Table IV-3 for the random vibration expected throughout the frequency range of 5 cps to 2000 cps.

5. Thermal Vacuum

The ambient temperature is expected to be between $-6^{o}C$ and $+35^{o}C$ at vacuum conditions. A qualification prototype model would be tested at $-16^{o}C$ and $+45^{o}C$ at 10^{-5} mm Hg pressure.

TABLE IV-2. COMBUSTION RESONANCE DWELL VIBRATION TEST REQUIREMENTS

Axis	Frequency Range (cps)	Duration (Minutes)		Platform Acceleration (g 0 to peak)		Camera Acceleration (g 0 to peak)	
		Qualification	Flight	Qualification	Flight	Qualification	Flight
Thrust	550-650	0.5	0.25	86	56	12.9	8.4
Lateral	550-650	0.5	0.25	15	9.5	2.5	1.4

TABLE IV-3. RANDOM VIBRATION TEST REQUIREMENTS

Axis	Frequency Range (cps)	Platform PSD Level (g/cps)		Camera PSD Level (g/cps)		Platform Acceleration (g rms)		Camera Acceleration (g rms)	
		Qualification	Flight	Qualification	Flight	Qualification	Flight	Qualification	Flight
Thrust	5-200	0.12	–	–	–	4.8	–	–	–
	10-200	–	0.06	–	–	–	3.38	–	–
	10-50	–	–	0.12	0.06	–	–	2.2	1.55
	50-100	–	–	6db/oct increase	6db/oct increase	–	–	3.8	2.65
	100-250	–	–	0.48	0.24	–	–	8.5	6.0
	200-400	12db/oct roll off	10.8db/oct roll off	–	–	2.9	1.96	–	–
	250-600	–	–	13.4db/oct roll off	13.4db/oct roll off	–	–	6.8	4.06
	400-2000	0.01	0.005	–	–	4.0	2.84	–	–
	600-2000	–	–	0.01	0.005	–	–	3.7	2.64
Lateral	5-25	0.6	–	0.6	–	3.5	–	3.0	–
	10-25	–	0.3	–	0.3	–	2.12	–	2.12
	25-100	12db/oct roll off	9db/oct roll off	–	–	1.91	1.75	–	–
	25-200	–	–	12db/oct roll off	6db/oct roll off	–	–	3.6	2.56
	100-2000	0.01	0.005	–	–	4.4	3.08	–	–
	200-2000	–	–	–	0.005	–	–	–	3.0

SECTION V

LABORATORY TESTS

A. GENERAL

A series of laboratory acceptance tests for the TIGRIS preprototype camera were conducted on September 17, 1964 in accordance with the contractual requirements for demonstration of the camera's performance capability. The tests included a demonstration of the linear increase in information capability with integration, signal-to-noise ratio measurements, horizontal resolution measurements, and grey step measurements.

B. LABORATORY TEST EQUIPMENT

1. General

In order to conduct the laboratory performance tests on the camera system, a calibrated light box was designed and fabricated and a Conrac Type T100 Monitor was purchased and modified.

2. Calibrated Light Box

A 5-foot by 1.5-foot by 17-inch calibrated light box was fabricated to provide an illumination test pattern. The pattern is generated by the light box and a suitable transparency, such as a RETMA chart. This chart shows various aspects of camera performance, including both resolution and grey-scale response. The light box consists of lamps, filter disk, aperture disk, two diffusers, test slide holder, and a provision for mounting the TIGRIS camera. Power for the lamps is supplied by a regulated d-c power supply. The lamp output is monitored with a photocell and a milliammeter.

The light box was calibrated by using a Pritchard Photometer Model No. 147 Spectrophotometer. The photometer was calibrated using a National Bureau of Standards No. 7041 calibrated light source and opal. The light emanating from a test slide illuminated by the largest aperture existing in the light box was measured by the photometer. The procedure was repeated for several successive apertures until the meter readings fell below the threshold sensitivity of the photometer. In each case the light level measured was approximately one half that of the light level measured with the next larger aperture. This was anticipated since each hole on the aperture wheel has an area equal to the reciprocal of the cube root of 10 ($10^{-1/3} = 0.46415$) of the next larger aperture hole. The scene surface brightness readings taken with the photometer are compared in Figure V-1 with calculated values based on the aperture area. The lower light level readings were interpolated assuming that they lay on the same curve as the other readings.

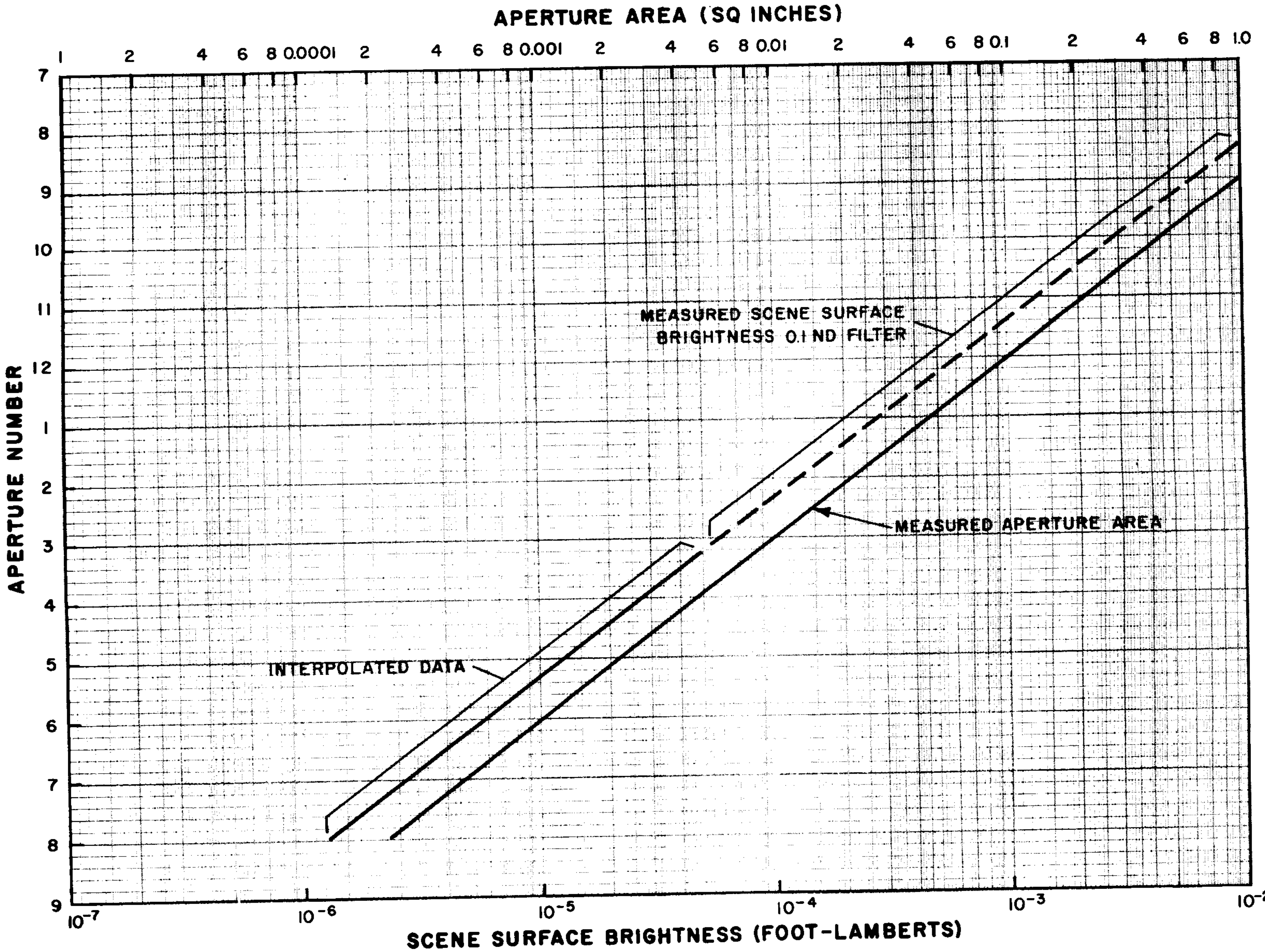

Figure V-1. Scene Surface Brightness

The scene surface brightness (B_s) for the largest aperture was established using the calibrated photocell. The calculated value of scene surface brightness for a smaller aperture is then the product of the ratio of the given aperture area to the largest aperture and the brightness for the largest aperture. The photocathode illumination (I_{pc}) is then determined using the following equation:

$$I_{pc} = \frac{I_s T}{4f^2 (1 + m)^2}$$

where

I_{pc} is the photocathode illumination in foot candles

I_s is the scene brightness in foot lamberts

T is the lens efficiency, which is assumed to be 0.85

f is the lens aperture number, which is f/2.8

m is the scene to photocathode magnification, which is 0.171

Further verification is achieved by comparing the reduction in light output through a 0.333 density filter with the reduction in light output due to the next smallest aperture. Table V-1 summarizes the calculated and measured values of the light box calibration.

3. Monitor

A Conrac Type T100 monitor was purchased and modifications were incorporated in the unit to enable it to fulfill the following test requirements.

a. Input power: 115 v, 60 cps, 110 watts

b. Scanning standards: horizontal - 250 cps, driven
vertical - 2 second, driven

c. Video: d-c coupled, black negative
peak white: 0 volts, black: - 1 volt
impedance: 20 Kohms
frequency response: dc to 200 kc ± 1 db
linearity: less than 5% distortion in a ten-equal-step linearity signal

d. Cathode ray tube: 5 inch diameter, flat face, long persistance

TABLE V-1. LIGHT BOX CALIBRATION

Aperture Number	Jig Bore Diameter ± 0.0002 in. (In.)	Theoretical Area After Black Anodize (In^2)	Measured Area Optical Comparator (In^2)	Calibration Data Step "0" on Gray Scale; 0.1 ND Filter			
				Scene Surface Brightness Measured (ft. lamberts) A	Photocathode Illumination Calculated From "A" (ft. candles) B	Scene Surface Brightness Calculated From Measured Aperture Area (ft. lamberts) C	Photocathode Illumination Calculated From "C" D
9	1.129	1.00	1.003	5.9×10^{-3}	1.2×10^{-4}	5.95×10^{-3}*	1.2×10^{-4}
10	0.768	0.4642	0.460	2.95×10^{-3}	6×10^{-5}	2.74×10^{-3}	5.4×10^{-5}
11	0.524	0.215	0.217	1.45×10^{-3}	2.85×10^{-5}	1.29×10^{-3}	2.5×10^{-5}
12	0.358	0.100	0.100	5.5×10^{-4}	1.1×10^{-5}	5.94×10^{-4}	1.2×10^{-5}
1	0.244	0.4642	0.0464	3.1×10^{-4}	6.2×10^{-6}	2.76×10^{-4}	5.6×10^{-6}
2	0.167	0.0215	0.0230	1.4×10^{-4}	2.85×10^{-6}	1.37×10^{-4}	2.75×10^{-6}
3	0.114	0.010	0.0105	5×10^{-5}	1×10^{-6}	6.25×10^{-5}	1.25×10^{-6}
4	0.0775	0.004642	0.00482	2.3×10^{-5}	4.6×10^{-7}	2.88×10^{-5}	6.0×10^{-7}
5	0.0532	0.00215	0.00235	1.06×10^{-5}	2.12×10^{-7}	1.41×10^{-5}	2.8×10^{-7}
6	0.0366	0.001	0.0011	5×10^{-6}	1×10^{-7}	6.6×10^{-6}	1.3×10^{-7}
7	0.0252	0.000464	0.004	2.3×10^{-6}	4.6×10^{-8}	2.34×10^{-6}	4.3×10^{-8}
8	0.0175	0.000215	0.000228	1.06×10^{-6}	2.12×10^{-8}	1.33×10^{-6}	2.65×10^{-8}

* *Measured reference starting point.*

C. ENGINEERING SYSTEM TESTS

1. System Measurements

The camera system was adjusted to conform to the following operational specifications before any system measurements were performed.

(1) Vertical Period: 2.0 sec ± 0.1 sec
(2) Horizontal Repetition Rate: 250 cps ± 12.5 cps
(3) Aspect Ratio: Square, 1/1
(4) Black Level: 1.25 V
(5) Sync Tips: 0 V
(6) Peak White Video: 4 V for 2×10^{-5} ft.-candle sec.
(7) Horizontal Retrace: 240 μsec ± 12 μsec
(8) Vertical Retrace: 100 msec ± 5 msec

The following measurements were performed prior to the acceptance tests (integration gate derived from vertical period).

a. Integration Time

Position	Integration Gate Duration
1	2.0 sec ± 0.1 sec
2	4.0 sec × 0.2 sec
3	6.0 sec × 0.3 sec
4	8.0 sec × 0.4 sec
5	10.0 sec ± 0.5 sec
6	16.0 sec ± 0.8 sec

b. Power Input: 50.4 watts (28 V at 1.8a)

c. Vertical Deflection Linearity: ± 5% from best fitting straight line

d. Horizontal Deflection Linearity: ± 5% from best fitting straight line

e. Horizontal Resolution: 570 lines for infinite contrast test chart and 2×10^{-5} ft.-candles sec,
250 lines at 10^{-6} ft.-candle sec

The resolution measurements were made using an oscilloscope "A" trace.

f. Signal/Noise Ratio $\frac{\text{Peak Signal}}{\text{RMS Noise}}$: 28 db measured at 2×10^{-5} ft.-candle-sec. photocathode illumination

g. Video Bandwidth: 65 Kc to -3db point

h. Grey Step: Ten steps. measured with highlight of 1×10^{-5} ft.-candle on photocathode thru least dense neutral density filter. Each step increases in density by a factor of 0.1.

2. Integration Performance

a. General

The transfer characteristics for the GE Z7806 LHP image orthicon at an integration time of two seconds and ten seconds are shown in Figure V-2. It can be seen that the signal increases nearly linearly with integration time below the saturation "knee" of the transfer curve. The camera sensitivity characteristic which was measured as a function of integration time at 2.7×10^{-7} foot-candles is shown in Figure V-3.

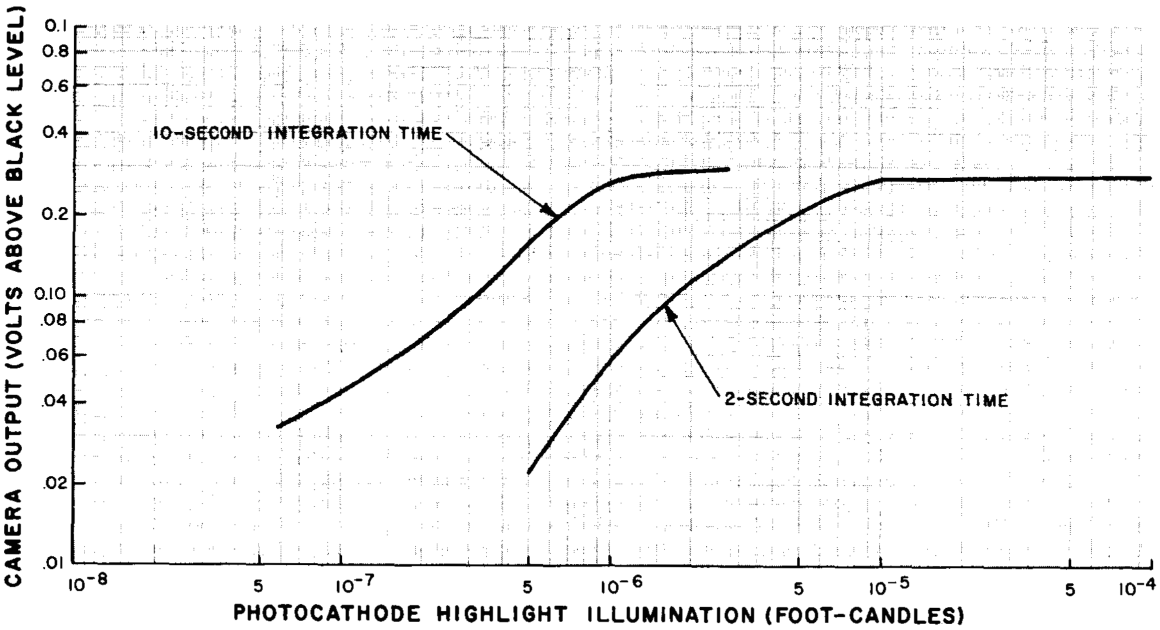

Figure V-2. Transfer Characteristics of Camera System

During the tests to illustrate the integration performance of the camera, an image retention phenomena was observed. Approximately 20 or 30 seconds after the image orthicon was exposed and allowed to readout the signal, an inverse image of the original exposure was seen to appear on the monitor. The phenomena was observed to appear during the performance of a normal exposure and readout cycle - (1) the image orthicon is exposed with the beam off, (2) the illumination is removed, the beam turned on, and the tube is allowed to scan, (3) the signal is readout during the first scan, and (4) there is a negligible amount of signal readout during the second or succeeding scans until approximately 20 or 30 seconds have elapsed. At that time an image appears which is the inverse of the original exposure. The video signal as seen on the scope is difficult to distinguish from the noise, but the image is plainly visable on the monitor. The image described disappears completely 60 seconds after exposure. The above was noted even when the exposure was kept below the knee of the image orthicon sensitivity curve.

When the exposure is increased, the after-image becomes more severe. At a light-level equivalent to the knee of the sensitivity curve, a different kind of after-image appears. Whenever there is a sharp black to white or white-to-black transition in the original scene, a sharp bright white line appears in the after-image. As the exposure is increased the time it takes the after-image to fade out also increases.

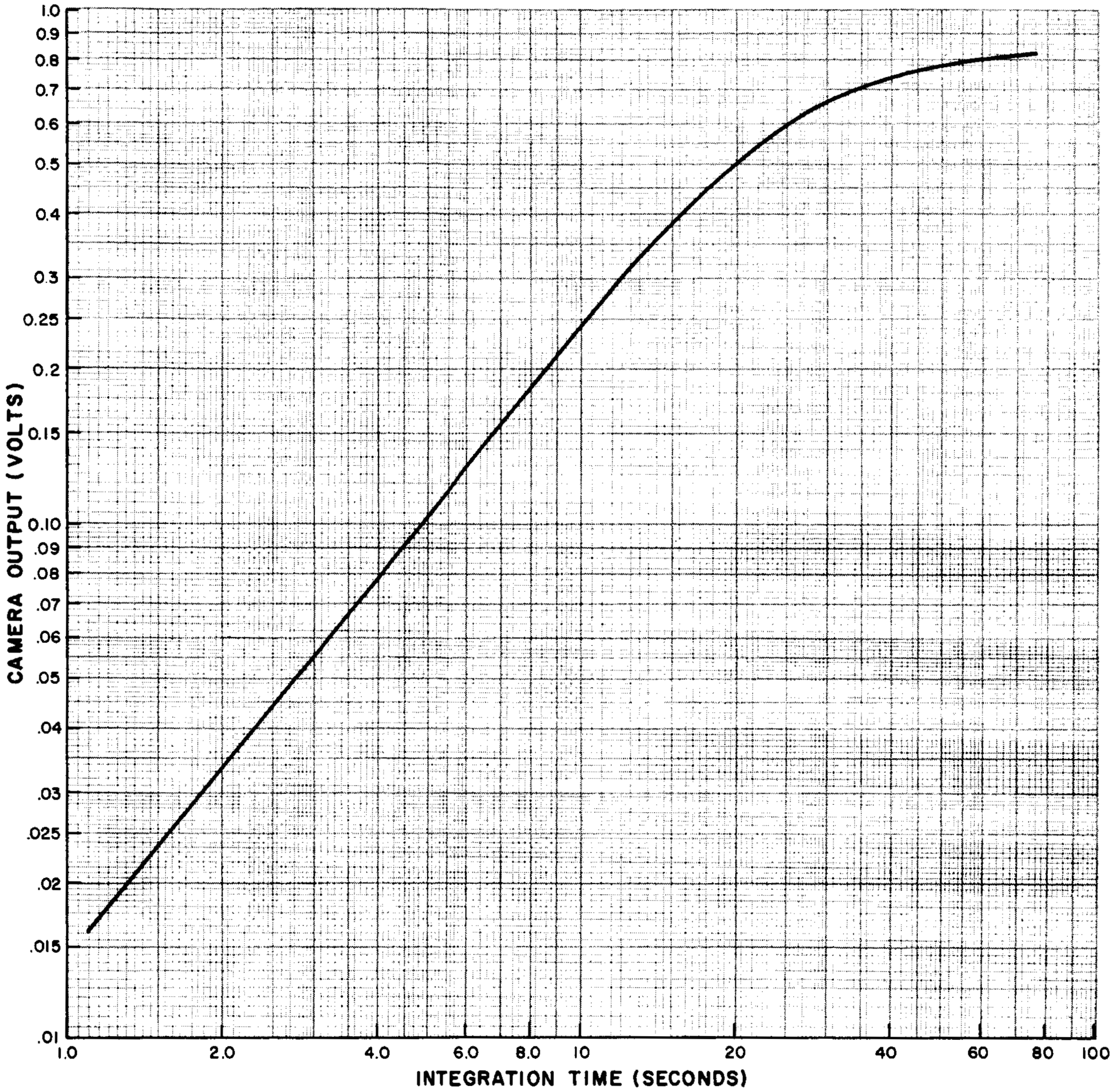

Figure V-3. Sensitivity of Camera System Versus Integration Time

Allowing the tube to integrate (beam turned off and lens capped) increases the signal level of the after-image. Scanning continuously for two-second intervals prevents this phenomena from appearing at all; or at worst, reduces it considerably, due apparently to elimination of the integration or build-up time.

Table V-2 summarizes the image retention results discussed.

TABLE V-2. IMAGE RETENTION PHENOMENA DATA

Photocathode Illumination (foot-candles) Exposure For Two Seconds	Time After Exposure For Negative After-Image To Appear		Time After Exposure For the Disappearance Of Negative After-Image		Time After Exposure For The White Edges To Appear	
	With Continuous Scanning Beam: ON all the time	With One 2-Second Scan Every 10 Seconds Beam: 2 seconds ON 8 seconds OFF	With Continuous Scanning	With One 2-Second Scan Every 10 Seconds	With Continuous Scanning	With One 2-Second Scan Every 10 Seconds
5.8×10^{-8}	none	none	—	—	none	none
1.0×10^{-7}	none	none	—	—	none	none
2.7×10^{-7}	none	none	—	—	none	none
5.8×10^{-7}	none	none	—	—	none	none
1.2×10^{-6}	none	30 sec.	—	60 sec.	none	none
2.7×10^{-6}	none	30 sec.	—	70 sec.	none	none
5.8×10^{-6} See Note 1	slight	approx. 30 sec.	—	90 sec.	none	40 sec.
1.1×10^{-5}	approx. 30 sec.	approx. 30 sec.	60 sec.	120 sec.	20 sec.	40 sec.
2.5×10^{-5}	approx. 30 sec.	approx. 30 sec.	70 sec.	160 sec.	20 sec.	40 sec.
5.4×10^{-5}	approx. 30 sec.	approx. 30 sec.	120 sec.	280 sec.	20 sec.	40 sec.
1.1×10^{-4}	approx. 30 sec.	approx. 30 sec.	180 sec.	330 sec.	22 sec.	40 sec.
2.6×10^{-4}	approx. 30 sec.	approx. 30 sec.	200 sec.	330 sec.	20 sec.	40 sec.

Note 1. The knee of the image orthicon transfer curve (Figure V-2) occurs at about this level of photocathode illumination.

The tests mentioned were made with test patterns that had black and white areas which were relatively large and had sharp black-to-white transitions. In flight or field use, this type of scene is not anticipated. However, the use of an electronic or mechanical shutter might lead to some improvement.

D. ACCEPTANCE TESTS

1. Demonstration of the Linear Increase in Information Capability With Increase in Integration Time

By increasing integration time for a given light level more charge is accumulated on the image orthicon target with a resulting increase in modulation of the beam. Ideally, the signal should increase linearly with integration time, but the finite conductivity of the target allows the charge distribution to spread which results in a degradation of the signal. The purpose of this test was to determine the effect of this lateral charge spread on the video amplitude. Electronic adjustments were avoided in the test by decreasing the light level by approximately a factor 1/2 for each doubling of the integration time. Since the light levels could not be exactly halved, the video amplitude measurement had to be corrected for linear increase in information capability with integration. The video amplitude is measured peak to peak on an oscilloscope. The test pattern used in the test was a bar chart of infinite contrast which is the same one used for resolution studies. The test data accumulated (Table V-3) is based upon the calibration of the light box described in Paragraph V-B2, the use of the measured value of scene brightness obtained from wheel aperture position No. 9 (5.95×10^{-3} foot lamberts) as a reference point, and the measured aperture areas of the other aperture positions to calculate the respective photocathode illumination levels for each successive aperture position.

TABLE V-3. INFORMATION CAPABILITY VERSUS INTEGRATION TIME

Aperture Position	Integration Time (sec)	Photocathode Light Level (ft - candles)	Video Amplitude (volts p-p)	Corrected Video Amplitude (volts p-p)
3	2	1.25×10^{-6}	0.9	0.9
4	4	6.0×10^{-7}	0.85	0.89
5	8	2.8×10^{-7}	0.75	0.84
6	16	1.3×10^{-7}	0.7	0.84

An absolutely linear increase in information with integration time would be represented by a constant video amplitude. As indicated by the data in Table V-3, there is about a 7-percent variation in the video amplitude; this is within the error of the light box calibration. The integration characteristic is therefore almost linear up to 16-seconds integration time, which meets the contract requirement.

2. Signal-to-Noise Ratio Measurement

The image orthicon beam was set to just discharge the highlights of the bar chart test pattern with an illumination of 1.2×10^{-5} foot-candles on the photocathode. The illumination level was attained by setting the aperture wheel to position No. 12. The repetitive scan mode (2-second integration time) was used. Under these scan conditions, the light was removed from the camera, and the average peak-to-peak noise was measured at the output of the video amplifier on an oscilloscope. The light was then reapplied and the peak-to-peak signal was measured across a white-to-black transition on the chart on the oscilloscope with all adjustments remaining identical to those set for the noise measurements. The following ratio was obtained:

$$\frac{\text{Peak-to-Peak Signal}}{\text{Peak-to-Peak Noise}} = \frac{3.5}{1}$$

The formula used for calculating the signal-to-noise ratio in decibels is:

$$\frac{S}{N} = 20 \log \frac{\text{Peak-to-Peak Signal}}{\text{RMS Noise}}$$

where:

$$\text{RMS Noise Voltage} = \frac{\text{Peak-to-Peak Noise Voltage}}{6}$$

Application of the above formulae to the measured ratio yields

$$\frac{S}{N} = 26.4 \text{ db}$$

which exceeds the contract specification of 20 db by 6.4 db.

3. Horizontal Resolution Measurements

This test was conducted with the infinite contrast bar chart as the test pattern, where vertical lines or bars were arranged in groups. Two adjacent groups of lines were separated from one another by wider spacing than appeared in either of the two groups. The density of the lines expressed as the number of lines per total horizontal picture width varied from a minimum of about 100 to a maximum of over 600. The beam current of the image orthicon tube was set to just discharge the highlights of the test pattern focused on the photocathode using the 2-second repetitive scan mode. The illumination level is set by the aperture wheel position. The output of the video amplifier is observed on an oscilloscope. A monitor picture of the video output is also obtained for comparative purposes.

The resolution for each light level was then determined by noting the last group of lines in the direction of increasing line density which were resolved in the oscilloscope trace of the video signal. Response limit is obtained when the peak-to-peak signal equals the noise. Since the minimum integration time of the system is 2 seconds, the contract specification for a one-second integration time for specified light levels was compensated for by approximately halving these specific light levels. Table V-4 lists the contract requirements and the demonstrated capabilities of the system. As indicated by Table V-4, the system exceeds the contract resolution specifications.

TABLE V-4. HORIZONTAL RESOLUTION MEASUREMENTS

Aperture Wheel Position	Highlight Energy Per Unit Area of Photocathode		Resolution	
	Contract Spec. (ft.-c-sec.)	Actual Calibration (ft.-c-sec.)	Contract Spec. (lines)	Demonstrated (lines)
12	1×10^{-5}	1.1×10^{-5}	500	550
5	5×10^{-7}	5.0×10^{-7}	200	225

4. Grey Step Measurements

The test pattern used for this test consisted of 11 steps of 0.1-neutral-density per-step filters. The contrasts between adjacent steps in the series is 0.26. With the light level set for 5.6×10^{-6} foot-candles illumination on the photocathode, about 9 steps could be detected on the monitor screen. This determination was based on actual brightness differences between steps, as an attempt was made to eliminate the influence of the lines between adjacent steps which were evident on the monitor. Examination of the test-chart indicated that these lines may have been caused by scattered light from the edges of the film strips used for the neutral density steps.

The contract is somewhat vague as far as the grey step specification is concerned. Although the contract specifies that ten steps be discernible, whether these steps be taken above a given light or below is not specified. The test was conducted such that the steps were taken below a 5.6×10^{-6} foot-candle photocathode illumination with the result that 9 distinct steps were discernible. Had this illumination been placed in the middle or near the most dense end of the grey scale there would have been no difficulty in displaying 10 grey steps.

The attached pages should be substituted for the same-numbered pages in your present copy of the TIGRIS Final Engineering Report. The pages that are removed from the report should be destroyed.

CONTRACT NO. NASw-823

TIGRIS (TELEVISED IMAGES OF GASEOUS REGIONS IN INTERPLANETARY SPACE) TELEVISION CAMERA SYSTEM

FINAL ENGINEERING REPORT

Prepared for the

NATIONAL AERONAUTICS AND
SPACE ADMINISTRATION
WASHINGTON, D. C.

By the

ASTRO-ELECTRONICS DIVISION
DEFENSE ELECTRONIC PRODUCTS
RADIO CORPORATION OF AMERICA
PRINCETON, NEW JERSEY

AED R-2583

Issued: January 15, 1965
Change Page (pp IV-1) Issued: February 5, 1965

SECTION IV

ENVIRONMENTAL CONSIDERATIONS

A. GENERAL

The performance of the Javelin rocket launch vehicle was studied to establish environmental launch-condition criteria for the design of the television camera system for the TIGRIS flight model. Although the present contract does not require ruggedization of the camera system to meet any environmental conditions, it does require that the preprototype be of such a design that in a follow-up program, a space-qualified system could be produced with minimum redesign.

A review of the Javelin rocket performance specifications, listed in Tables IV-1 through IV-3 indicated that the camera-system flight-type hardware should be designed as a rigid structure that would allow external vibration isolators if required.

After this study was completed, it was suggested that the new Aero-Bee rocket might be used. The Aero-Bee would reduce the stress levels below those herein considered.

B. ENVIRONMENTAL DESIGN CRITERIA

The following design criteria were established after an analysis of the Javelin rocket environmental test conditions. Note that these values are not applicable to the preprototype model, but are indicative of the requirements for the follow-on prototype model.

1. Acceleration

The expected stress to be exerted on a flight model in the thrust direction is 45g for a period of one minute. A prototype model would be tested at 50g for three minutes.

2. Shock

The expected shock stress is expected to be a 20 g* peak amplitude 6 millisecond duration sawtooth along the thrust axes and a 6 g* peak amplitude 6 millisecond duration sawtooth along the lateral axis.

3. Sinusoidal Vibration

As indicated in Table IV-1, the maximum stress due to sinusoidal vibrations for a flight model is expected to be 14g along the thrust axis and 2.8g along the lateral axis in the frequency range of 150 to 250 cps. A qualification

* Changed: February 5, 1965

TABLE IV-1. SINUSOIDAL VIBRATION TEST REQUIREMENTS

Axis	Frequency Range (cps)	Platform Interface Level (g 0 to peak)		Camera Level (g 0 to peak)		Duration Minute	
		Qualification	Flight	Qualification	Flight	Qualification	Flight
Thrust	10-50	2.3	1.5	2.5	1.6	1.6	4 octaves
	50-150	10.7	7	12.8	8.4	1.6	per minute
	150-250	10.7	7	21.4	14	1.6	2.06
	250-500	10.7	7	6.1	4	1.6	total
	500-2000	21	14	3.1	2.1	1.0	
	2000-3000	54	36	3.8	2.5	0.26	
	3000-5000	21	-	1.3	-	0.34	
Lateral	5-50	0.9	0.6	0.9	0.6	1.6	4 octaves
	50-150	2.1	1.4	2.5	1.7	1.6	per minute
	150-250	2.1	1.4	4.2	2.8	1.6	2.06
	250-500	2.1	1.4	1.2	0.8	1.6	total
	500-2000	4.2	2.8	0.6	0.4	1.0	
	2000-3000	17	11	1.2	0.8	1.0	
	3000-5000	17	-	1.2	-	0.6	

prototype model would be subjected to 21.4g stress along the thrust axis and 4.2g stress along the lateral axis.

As indicated in Table IV-2, during combustion dwell time (approximately a duration of 0.25 second), the stress is expected to be 8.4g along the thrust axis and 1.4g along the lateral axis. A qualification prototype model would be tested at 12.9g and 2.5g respectively in the frequency range of 550 to 650 cps.

4. Random Vibration

The stress due to random vibrations is expected to be 6.0g rms along the thrust axis and 2.56 g rms along the lateral axis. A qualification prototype model would be tested at 8.5g rms and 3.6g rms respectively. Refer to Table IV-3 for the random vibration expected throughout the frequency range of 5 cps to 2000 cps.

5. Thermal Vacuum

The ambient temperature is expected to be between $-6^{o}C$ and $+35^{o}C$ at vacuum conditions. A qualification prototype model would be tested at $-16^{o}C$ and $+45^{o}C$ at 10^{-5} mm Hg pressure.